

## ABSTRACT

LIU, ZEYU. On Routing and Wavelength Assignment in WDM Networks. (Under the direction of Dr. George Rouskas.)

With the help of advanced technology, WDM networks nowadays can support up to more than 100 wavelength on a single fiber. This feature brings new challenges to routing and wavelength assignment (RWA) problem, which is a NP-hard problem. There are three existing categories of integer linear programming (ILP) formulations to solve this problem optimally, namely, link-based, path-based and maximal independent set (MIS)-based formulations. All of the these experience bottlenecks of either wavelength symmetry problem or enormous problem size, which limits their scalability to very small networks. In this dissertation, we study the RWA problem in depth and greatly improve all three existing ILP formulations.

For ring networks, we propose a new, exact ILP formulation that decomposes the path set recursively into several partitions and represents the original MIS with smaller MIS calculated in these partitions. As a result, this MIS decomposition formulation decreases the number of decision variables to a large extent, without sacrificing the benefit of MIS-based formulation. By our simulation analysis, compared with the existing formulations, the new MIS decomposition formulation gains a more-than-3-orders-of-magnitude decrease in running time. Typically, this new formulation based on MIS ILPs could solve any existing WDM ring networks with any number of wavelengths in just a few seconds.

In mesh networks, we introduce the concept of a symmetric RWA solution and develop a new, fast path-based formulation for obtaining such solutions. Experimental study indicates that the approach improves the performance of the original path-based formulation by 2 orders of magnitude in terms of running time. With this new proposed formulation, we can solve mesh topologies representative of backbone and regional networks. The scalability of this approach makes it possible to characterize the performance of heuristics for the RWA problem and our experimental study shows that solutions obtained by the proposed approach are 20% – 60% better than those obtained by heuristics.

As link-based formulation has a natural advantage over path-based and MIS-based formulation in terms of optimality in mesh networks, we propose a new, fast, link-based formulation with wise link selection algorithms. This new approach reduces the problem size by pruning the redundant link decision variables. The formulation scales well to mesh topologies representative of backbone and regional networks. Simulation results show that it decreases the running time by 2 orders of magnitude while providing better-quality solutions than path-based and MIS-based formulation. More importantly, this approach is applicable not only to the link-based formulation for the RWA problem, but also to ILP formulations for any problems formulated

as ILPs that use multicommodity flow equations as their core constraints.

Additionally, we extend our study to traffic grooming, a network design problem that includes RWA as a subproblem. We present a scalable formulation for the traffic grooming problem in WDM ring networks, incorporating the fast MIS decomposition formulation to the RWA subproblem. Our experimental study indicates that the new formulation results in an improvement of up to 2 orders of magnitude in running time. Consequently, it is now possible to solve the traffic grooming problem to optimality for 16-node rings in a few seconds, under our objective function.

© Copyright 2012 by Zeyu Liu

All Rights Reserved

On Routing and Wavelength Assignment in WDM Networks

by  
Zeyu Liu

A dissertation submitted to the Graduate Faculty of  
North Carolina State University  
in partial fulfillment of the  
requirements for the Degree of  
Doctor of Philosophy

Computer Science

Raleigh, North Carolina

2012

APPROVED BY:

---

Dr. Rudra Dutta

---

Dr. Matthias Stallmann

---

Dr. David Thuent

---

Dr. George Rouskas  
Chair of Advisory Committee

## DEDICATION

To my great parents,  
Liangdian Liu and Jingzhi Li,  
for their endless love.

To my wonderful wife, Lei,  
for her constant support and care.

To my lovely son, Ethan,  
for all the joy he brings me.

## BIOGRAPHY

Zeyu Liu was born and brought up in Jinan, China in 1984. He received his B.S. degree in Telecommunications Engineering in Zhejiang University, Hangzhou, China, in 2008. Since August 2008, he has been a full-time PhD student at Computer Science Department of North Carolina State University, Raleigh, North Carolina, USA.

During his PhD study, he was a Software Engineer intern with Ericsson Inc., San Jose, CA, in the summer of 2010. He has received a Certificate of Accomplishment in Teaching from the NC State Graduate School. As part of this program, Zeyu lectured extensively for Dr. Rouskas' CSC 579 (Fall 2010, 2012), CSC 401 (Spring 2011), and CSC 316 (Fall 2012) courses. Zeyu received Outstanding Teaching Assistant Award by Computer Science Department in 2011. He was also selected to present his research at the 6th Annual NC State Graduate Research Symposium and was honored in Recognition of Outstanding Research.

After graduation, Zeyu will join IBM as the next step of his career.

Zeyu is married to Lei Tian, in Raleigh, NC, and they have a lovely son Ethan.

## ACKNOWLEDGEMENTS

I would like to give my sincere thanks to Dr. George Rouskas for believing in me and providing me expert guidance throughout my research. He certainly changed the course of my life and left his footprint in my professional career. This dissertation would have not been possible without his patient help and constant support. Discussions with him on different topics excited my research ideas and strengthened my interest in pursuing a doctoral degree. My thanks also go to the rest of my committee members, Dr. Rudra Dutta, Dr. Matthias Stallmann and Dr. David Thuente, who gave me the great help and insightful comments on my research. I thank them all for their invaluable inputs. I would also want to give my great thanks to our DGP Dr. Douglas Reeves and former DGP Dr. David Thuente (again) for their gracious support on my internship, department transfer and many other graduate advisory. They saved me from a lot of troubles.

I am also grateful to my senior labmates Anjing Wang and Mohan Iyer, who gave me a lot of personal suggestions and encouragement as well as the research inspirations. To Hui Wang, who worked with me on certain area of our research and for the wide ranging discussions. To my other friends in the Department of Computer Science, without whom I would have not been able to enjoy my graduate life. This work is dedicated to my great parents who have given me constant support throughout my life and encouraged me during my graduate studies. My special thanks also go to my wonderful wife, Lei Tian, who has supported me with love and care during the tough days, and for the lovely son Ethan she has given birth to.

Finally, I would like to acknowledge the National Science Foundation for partly supporting the research in this dissertation under grant CNS-1113191.

# TABLE OF CONTENTS

<b>List of Tables</b> . . . . .	<b>vii</b>
<b>List of Figures</b> . . . . .	<b>viii</b>
<b>Chapter 1 Introduction</b> . . . . .	<b>1</b>
1.1 The Routing and Wavelength Assignment (RWA) Problem . . . . .	1
1.2 Related Work . . . . .	2
1.3 Contributions . . . . .	3
1.4 Structure of the Dissertation . . . . .	5
<b>Chapter 2 Existing ILP Formulations</b> . . . . .	<b>7</b>
2.1 Link Formulation . . . . .	7
2.2 Path Formulation . . . . .	10
2.3 Maximal Independent Set (MIS) Formulation . . . . .	11
2.4 Comparison among the three . . . . .	15
<b>Chapter 3 RWA in Ring Networks: Exact, Fast Formulations Based On MIS Decomposition</b> . . . . .	<b>16</b>
3.1 MIS Decomposition-2 . . . . .	17
3.2 MISD-4 . . . . .	19
3.3 Generalized MIS Decomposition Formulation - MISD-2 <sup>x</sup> . . . . .	24
3.4 Size and Scalability of MISD Formulations . . . . .	28
3.5 Experimental Study . . . . .	29
3.6 MIS Decomposition Formulation in Mesh Networks . . . . .	32
<b>Chapter 4 New, Fast Formulations Based on Path-based ILPs</b> . . . . .	<b>34</b>
4.1 Optimal Symmetric RWA Solutions . . . . .	35
4.1.1 Symmetric Traffic Demands . . . . .	36
4.1.2 Arbitrary Traffic Demands . . . . .	40
4.2 Further Improvements to the ILP Formulation . . . . .	42
4.2.1 Incorporating Information from Heuristics . . . . .	42
4.2.2 Path Selection Algorithm . . . . .	44
4.3 Experimental Study . . . . .	44
4.3.1 Scalability Comparison . . . . .	45
4.3.2 Quality of Optimal Symmetric Solution . . . . .	48
4.4 Concluding Remarks . . . . .	49
<b>Chapter 5 New, Fast Link-based ILP Formulation with Wise Link Selection</b> . . . . .	<b>50</b>
5.1 Speed up Link-based Formulation with Link Selection Algorithms . . . . .	51
5.1.1 Complexity of Link-based Formulation . . . . .	51
5.1.2 Link Selection Algorithms - Remove Redundant Variables . . . . .	53
5.2 Speed and Quality Analysis of New Link-based Formulation . . . . .	55



5.2.1	Number of variables of New Link-based Formulation vs. Parameter $k$ . . .	55
5.2.2	Trade-off between Solution Quality and Running Time . . . . .	56
5.2.3	Solution Quality Advantage over Path Formulation . . . . .	57
5.3	Experimental Study . . . . .	58
5.3.1	$k$ -Thres vs. $k$ -Path . . . . .	59
5.3.2	Running Time Comparison . . . . .	61
5.3.3	Solution Quality Comparison . . . . .	63
5.3.4	Conclusion . . . . .	64
<b>Chapter 6 Scalable Optimal Traffic Grooming in WDM Rings Incorporating Fast RWA Formulation . . . . .</b>		<b>66</b>
6.1	Introduction to Traffic Grooming . . . . .	66
6.2	ILP Formulation of the Traffic Grooming Problem . . . . .	67
6.2.1	Objective Function . . . . .	68
6.2.2	Constraints . . . . .	69
6.3	RWA in Traffic Grooming . . . . .	71
6.4	Experimental Study . . . . .	72
6.5	Concluding Remarks . . . . .	76
<b>Chapter 7 Conclusion and Future Work . . . . .</b>		<b>77</b>
<b>References . . . . .</b>		<b>79</b>
<b>Appendix . . . . .</b>		<b>85</b>
Appendix A	Exact MISD-2 <sup>x</sup> formulation . . . . .	86

## LIST OF TABLES

Table 2.1	Comparison among Link, Path, MIS formulations . . . . .	15
Table 3.1	Algorithm to calculate core sets . . . . .	22

## LIST OF FIGURES

Figure 1.1	Lightpaths in wavelength routed WDM network . . . . .	2
Figure 1.2	Symmetry problem in Link & Path formulations . . . . .	3
Figure 2.1	Illustration on $c_{ij}^{lw}$ variable . . . . .	8
Figure 2.2	Multicommodity flow equation at node $n$ . . . . .	9
Figure 2.3	RWA as graph coloring problem . . . . .	12
Figure 2.4	Maximal independent sets in 3-node ring network . . . . .	13
Figure 3.1	MISD-2 . . . . .	17
Figure 3.2	Network parts in MISD-4 . . . . .	19
Figure 3.3	Path set partitions in MISD-4 . . . . .	20
Figure 3.4	Path graph partitions in MISD-4 . . . . .	20
Figure 3.5	Core Sets & MISs . . . . .	21
Figure 3.6	Link divisions of the network in MISD-8 . . . . .	24
Figure 3.7	Clockwise path set partitions in MISD-8 . . . . .	25
Figure 3.8	Clockwise path graph in MISD-8 . . . . .	27
Figure 3.9	MIS Representation in MISD-8 . . . . .	27
Figure 3.10	Problem size in MIS/core set decision variables . . . . .	28
Figure 3.11	Problem size in nonzero items in formulations . . . . .	30
Figure 3.12	RWA solution times vs. $N$ ( $W=120$ ) . . . . .	31
Figure 3.13	Size of largest network can be solved for a given number of wavelength within 3000 sec . . . . .	32
Figure 4.1	RWA instance for the proof of Lemma 4.1.1: (a) optimal symmetric solution to the original RWA problem, (b) one optimal solution to the RWA-1 problem, (c) another optimal solution to the RWA-1 problem . . .	37
Figure 4.2	CPU time comparison, $K = 2$ , $T_{max} = 2$ . . . . .	46
Figure 4.3	CPU time against $T_{max}$ , $K = 2$ , NSF and EON networks . . . . .	47
Figure 4.4	CPU time against $K$ , $T_{max} = 2$ , NSF and EON networks . . . . .	47
Figure 4.5	Optimality comparison for NSFNet, $T_{max} = 2$ , $K = 2$ . . . . .	48
Figure 5.1	Illustration on $c_{ij}^{lw}$ variable . . . . .	51
Figure 5.2	Multicommodity flow equation at node $n$ . . . . .	53
Figure 5.3	Number of $c_{ij}^{wl}$ variables in German network using two link selection algorithms . . . . .	56
Figure 5.4	Trade-off between speed and solution quality . . . . .	57
Figure 5.5	An illustration on the advantage of $k$ -path link selection algorithm . . . .	58
Figure 5.6	$k$ -thres algorithm: Running time and solution value vs. $k$ in German Network, $t_{max} = 2$ . . . . .	60
Figure 5.7	$k$ -path algorithm: Running time and solution value vs. $k$ in German Network, $t_{max} = 2$ . . . . .	60

Figure 5.8	$k$ -thres algorithm: Running time and solution value vs. $k$ in German Network, $t_{max} = 6$ . . . . .	61
Figure 5.9	$k$ -path algorithm: Running time and solution value vs. $k$ in German Network, $t_{max} = 6$ . . . . .	62
Figure 5.10	$k$ -Path algorithm: Running time and solution value vs. $k$ in NSF Network, $t_{max} = 2$ . . . . .	62
Figure 5.11	$k$ -Path algorithm: Running time and solution value vs. $k$ in NSF Network, $t_{max} = 6$ . . . . .	63
Figure 5.12	Running time of new link formulation with two link selection algorithms, compared with original link-based and path-based formulations . . . . .	64
Figure 5.13	Solution value of new link formulation with two link selection algorithms against $t_{max}$ , compared with original link-based and path-based formulations . . . . .	65
Figure 6.1	CPU time comparison vs. $N$ , $\alpha = 0.2$ . . . . .	73
Figure 6.2	CPU time comparison vs. $N$ , $\alpha = 0.5$ . . . . .	74
Figure 6.3	CPU time comparison vs. $N$ , $\alpha = 0.8$ . . . . .	74
Figure 6.4	CPU time comparison vs. $T_{max}$ at $N = 16$ . . . . .	75
Figure 6.5	CPU time comparison vs. $W$ at $N = 16$ . . . . .	75

# Chapter 1

## Introduction

### 1.1 The Routing and Wavelength Assignment (RWA) Problem

In today's optical networks, wavelength division multiplexing (WDM) technology is widely adopted. The technology uses a number of distinct wavelengths to implement separate channels [53]. With WDM, the enormous low-loss bandwidth of optical medium can be exploited efficiently by simultaneously carrying up to hundreds of wavelengths in one fiber.

In wavelength routed WDM networks, traffic is carried by logical connections implemented using lightpaths from sources to destinations space[52]. These lightpaths, also referred to as  $\lambda$ -channels, are purely in the optical domain, and there is no need for signal processing between electrical and optical domains. In Figure 1.1, two lightpaths in a small network are shown, each lightpath represented by a solid line of a different color.

Each lightpath in a WDM network must be assigned a path and wavelength through the network. This is referred to as the Routing and Wavelength Assignment (RWA) problem. A feasible assignment for the problem must satisfy two constraints [52]:

- *Wavelength continuity constraint.* The same wavelength must be assigned to all the links along the path traversed by a lightpath. In Figure 1.1, this constraint is represented by using a single color for each lightpath.
- *Distinct wavelength constraint.* If two or more lightpaths share a common link, each must be assigned a distinct wavelength. In Figure 1.1, this constraint requires that the two lightpaths sharing a link be represented by two different colors.

RWA is a fundamental problem in the engineering, control, and design of optical networks, and arises in most network design applications, including traffic grooming [7, 63, 77], survivability design [25, 24], and traffic scheduling [19, 30]. Because of the two constraints mentioned above, there is tight coupling between routing and wavelength assignment. As a result, the

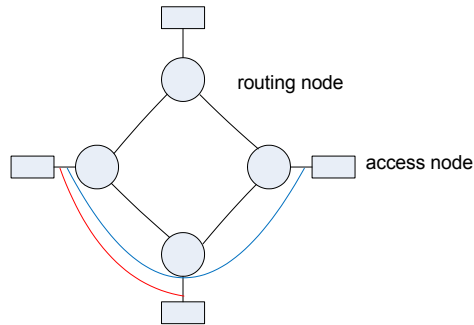


Figure 1.1: Lightpaths in wavelength routed WDM network

RWA problem is significantly more difficult than routing problems in electronic networks [57] where such coupling does not exist.

Formally, the RWA problem can be stated as follows in terms of input, output, constraints, and objective

- *Input*: the network topology and a set of connection requests.
- *Output*: the lightpaths to be established (one per connection request), each lightpath defined by the path along which it is set up and a wavelength.
- *Constraints*: wavelength continuity constraint, distinct wavelength constraint, maximum number of wavelengths on a fiber (only for the maxRWA objective below).
- *Objective*:
  - minRWA*: establish all connection requests using the minimum number of wavelengths.
  - maxRWA*: maximize the number of requests that are established given the maximum number of wavelengths that each fiber can support.

Both the minRWA and maxRWA problems are NP-hard; for a proof, the reader is referred to [39].

## 1.2 Related Work

The optimal solution to RWA problem may be obtained by using Integer Linear Programming (ILP) formulations. Existing ILP formulations may be classified as link-based [46], path-based [51], or maximal independent set (MIS)-based [51]. The former two have a symmetry problem, in that the solution is highly symmetric with respect to wavelength permutations, as shown in

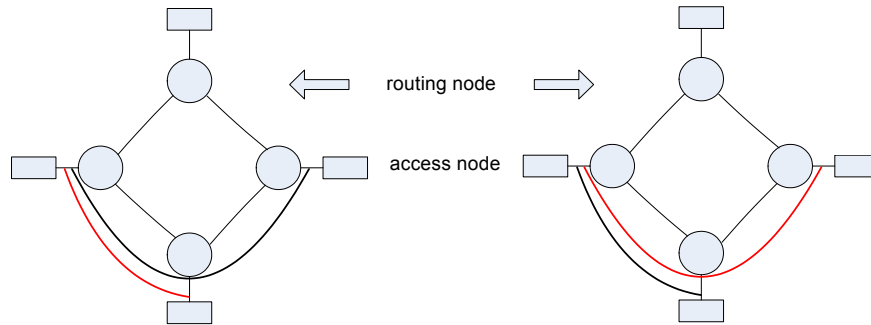


Figure 1.2: Symmetry problem in Link & Path formulations

Figure 1.2. Specifically, any permutation of the solution wavelengths represents an equivalent optimal solution, hence an ILP solver (e.g., ILOG CPLEX) may spend a significant amount of time examining solutions that do not improve the objective function. Consequently, the symmetry property represents a crucial bottleneck in solving real-life WDM networks that are capable of supporting a large number (more than 100, with current technology) of wavelengths. Moreover, all the three formulations suffer from a severe scalability problem. Specifically, the number of variables and constraints in all three formulations grows rapidly as the network size grows. Especially in the MIS-based formulation, the number of MIS's grows exponentially with the total number of paths in the network, making this approach impractical as the network size increases. We will discuss the existing ILP formulations in detail in Chapter 2.

Because of the inherent complexity of the RWA problem, many heuristic algorithms have been proposed to solve it [42]. Most heuristic approaches divide the problem into two sub-problems, one for routing lightpaths and one for assigning wavelengths, and solve each separately [36, 47]. However, it is difficult to characterize the quality of solutions obtained by such heuristics; importantly, considering each sub-problem separately may fail to find feasible solutions even if one exists.

### 1.3 Contributions

RWA is a fundamental problem in optical network design and optimization. However, existing optimal approaches experience severe scalability issue. As we will demonstrate later, existing ILP formulations (whether link-, path-, or MIS-based) cannot tackle the RWA problem on large rings up to the maximum size of SONET/SDH networks (equal to sixteen nodes), not to mention mesh network topologies representative of backbone or regional networks. In this dissertation, we improve all three existing formulations greatly and extend the good result to

traffic grooming problem, which includes RWA as a subproblem.

The first part of our work is regarding the RWA problem in ring networks. It is based on the observation that the current optical transport infrastructure is largely based on SONET/SDH ring networks that may support more than one hundred wavelengths on each fiber link. Therefore, new approaches for solving the RWA problem optimally on large ring networks are of high practical value for network operators. Since the link- and path-based formulations have a symmetry problem, we focus on the MIS-based formulation. The latter is “future-proof” in that as we will show in the next chapter, its size is independent of the number of wavelengths, and thus, it is not affected by advances in WDM technology. The challenge with the MIS formulation is the exponential increase in the number of MIS decision variables with the size of network. To overcome this issue, we propose a new, exact ILP formulation that dramatically reduces the problem size. The key idea is to decompose the path set of the MIS formulation recursively into several partitions, and represent the MIS formulation recursively into several partitions, and represent each original MIS by the smaller MISs calculated in each of the partitions. We refer to this ILP formulation as the MIS decomposition with  $2^x$  partitions, or MISD- $2^x$ , where  $x$  is a parameter representing the number of times the decomposition has been effected. Experimental study to be presented indicates that MISD-8 improves the time required to obtain an optimal solution by three or more orders of magnitude, compared to existing formulations, making it possible to solve 16-node rings in only a few seconds.

Secondly, we extend our study to mesh networks. As backbone and regional networks evolve from ring to mesh, optimal RWA solutions for general topologies are becoming important to network designers and operators. Unfortunately, current optimization methods cannot be used to solve optimally mesh network instances arising in practice. Even the MIS decomposition could not scale well in mesh networks due to the greater number of MIS generated in mesh topologies. We then introduce the concept of a symmetric RWA solution and develop a new, fast path-based formulation for obtaining such solutions. Experimental study indicates that the approach improves the performance of the original path-based formulation by 2 orders of magnitude in terms of running time. With this new proposed formulation, we can solve mesh topologies representative of backbone and regional networks in a reasonable time. The scalability of this approach makes it possible to characterize the performance of heuristics on large network topologies in RWA problem. Specifically, our experimental study shows that solutions given by the proposed approach are 20% – 60% better than those given by LFAP, a very well-performed heuristics. This reveals the large solution quality difference between ILPs and heuristics for the first time, and it gives the network operators choices to select a much-better-quality solution with little sacrifice of running time.

Thirdly, we continue to seek even better solutions with link-based formulation. As link-based formulation takes links as entities of interest, it provides the overall optimal solution



among the three types of ILPs, but it lacks scalability due to the large number of variables in the formulation. We successfully reduce the problem size by proposing a new, fast formulation with wise link selection. This new approach reduces the problem size by pruning the redundant link decision variables. The formulation scales well to mesh topologies representative of backbone and regional networks. Simulation results show that it decreases the running time by 2 orders of magnitude while providing even-better-quality solutions than path-based and MIS-based formulation. More importantly, this approach applies not only to the link-based formulation of the RWA problem, but also to ILP formulations for any problems that use multicommodity flow equations as their core constraints. As a result, a large variety of network design problem could benefit from this technique.

Additionally, we extend our study to traffic grooming, a network design problem that includes RWA as a subproblem. We present a scalable formulation for the traffic grooming problem in WDM ring networks, incorporating the fast MIS decomposition formulation to RWA problem. Our experimental study indicates that the new formulation results in an improvement of up to 2 orders of magnitude in running time. Consequently, it is now possible to solve the traffic grooming problem to optimality for 16-node rings in a few seconds, under our objective function.

The works in this dissertation have several practical benefits:

- They make it possible to solve existing WDM network extremely fast, allowing network operators to carry out “what-if” analysis practically and efficiently;
- They have the potential to speed up solutions to several optical network design problems that include RWA as a subproblem, such as traffic grooming [40, 41, 58], survivability design [50, 49], and traffic scheduling [48, 54]; and
- They make it possible to characterize the performance of heuristics on large networks, and develop new efficient heuristics.

## 1.4 Structure of the Dissertation

The rest of the dissertation is organized as follows. In Chapter 2 we discuss the existing ILP formulations and quantify the size of each in terms of the number of decision variables and constraints. In Chapter 3, we introduce a new, exact formulation for ring networks based on decomposition of the MIS set. In Chapter 4, we introduce the concept of a symmetric RWA solution and develop a new, fast path-based formulation for obtaining such solutions. In Chapter 5, a fast link-based formulation with link selection algorithm to solve mesh topologies representative to backbone networks is proposed. Chapter 6 extends our RWA result to the

traffic grooming problem and presents a scalable formulation for traffic grooming in WDM ring networks. Chapter 7 concludes the dissertation and briefly discusses future research directions.

## Chapter 2

# Existing ILP Formulations

In this chapter, we present and analyze the path-, link-, and MIS-based ILP formulations for the minRWA problem. Formulations for the maxRWA problem are similar, and are omitted.

In the formulations, we will use  $G(V, E)$  to represent the network topology<sup>1</sup>, where  $V$  is the set of nodes and  $E$  is the set of links in the network. We consider bidirectional networks, hence a link  $l \in E$  between two nodes  $s$  and  $d$  represents two fibers in opposite directions connecting the two nodes. Let  $N = |V|$  be the number network nodes. We also let  $W$  denote the number of wavelengths available at any fiber link. The given traffic demand is represented by an  $N \times N$  matrix  $T = [t_{sd}]$ , where  $t_{sd}$  is a non-negative integer denoting the number of lightpaths to be set up from node  $s$  to node  $d$ ; matrix  $T$  need not be symmetric, i.e., in general we assume that  $t_{sd} \neq t_{ds}$ .

In the formulations, we will use  $l$  as the link index,  $w$  as the wavelength index,  $k$  as the path index, and  $m$  as the MIS index. Additional notation will be introduced as needed.

### 2.1 Link Formulation

The link formulation is based on expressing the RWA problem as a multicommodity flow problem space[46]. Let us define the following sets of decision variables:

- $c_{ij}^{lw} \in \{0, 1\}$ : binary variable that indicates whether there exists a lightpath from node  $i$  to node  $j$  that uses wavelength  $w$  on link  $l$  (see Figure 2.1)
- $u^w \in \{0, 1\}$ : binary variable that indicates whether wavelength  $w$  is used anywhere in the network
- $\omega_{total}$ : number of wavelengths used in the whole network

With these notations, the link ILP formulation can be expressed as:

---

<sup>1</sup>The formulations we present are valid for general topology networks, not just rings.

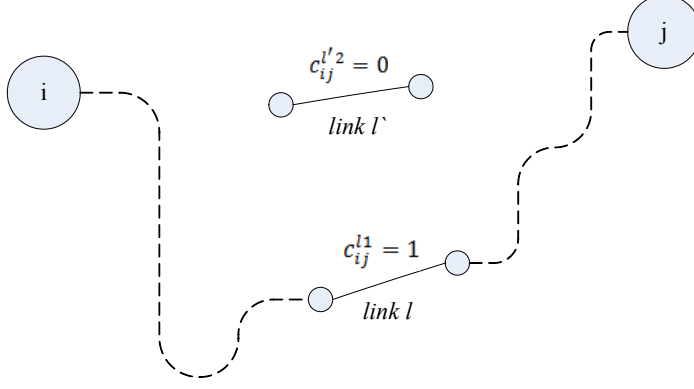


Figure 2.1: Illustration on  $c_{ij}^{lw}$  variable

*Minimize* :  $\omega_{total}$

*Subject to:*

$$\sum_{\substack{\text{links } l \\ \text{outgoing from } n}} c_{ij}^{lw} - \sum_{\substack{\text{links } l \\ \text{incoming to } n}} c_{ij}^{lw} = \begin{cases} 0, & n \neq i, j; \\ t_{ij}, & n = i; \\ -t_{ij}, & n = j. \end{cases} \quad \forall n, i, j \in V, \forall w \quad (2.1)$$

$$\sum_{i,j} c_{ij}^{lw} \leq 1, \quad \forall l \in E, \forall w \quad (2.2)$$

$$\sum_{i,j} \sum_l c_{ij}^{lw} \leq u^w N(N-1)|E|, \quad \forall w \quad (2.3)$$

$$W_{total} \geq wu^w, \quad \forall w \quad (2.4)$$

$$u^w = 0, 1, \quad \forall w; \quad c_{ij}^{lw} = 0, 1, \quad \forall i, j, l, w \quad (2.5)$$

Expression (2.1) are the multicommodity flow equations at node  $n$ . Specifically, if  $n$  is an intermediate node in the path from some source  $i$  to some destination  $j$ , the traffic coming in should be equal to the traffic going out, as such traffic is not dropped at, or originates from, this node, hence the left hand side of (2.1) is equal to zero. If  $n$  is the source node  $i$ , the first sum of the left hand side is equal to the traffic  $t_{ij}$  to node  $j$  and the second sum is zero. Similarly, if  $n$  is the destination node  $j$ , the second sum of the left hand side is equal to  $t_{ij}$  and the first sum is zero. This set of constraints ensure that all traffic demands are satisfied. Moreover,

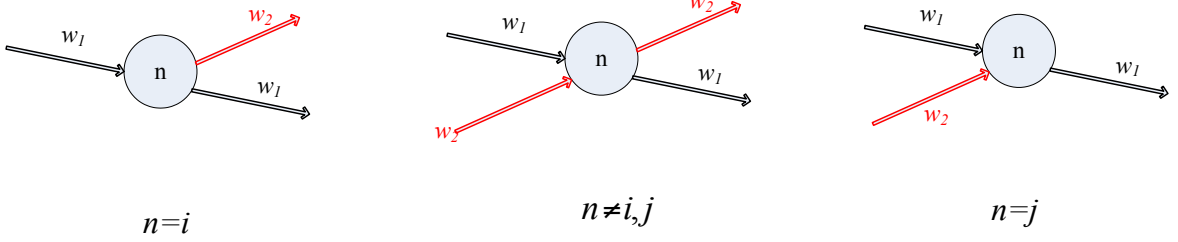


Figure 2.2: Multicommodity flow equation at node  $n$

they also take care of the wavelength continuity constraints, because for any intermediate node  $n$  (neither source nor destination), the right hand side of the equation will be 0, ensures that if one wavelength comes in, the same wavelength will go out. Expression (2.2) represent the distinct wavelength constraints of the RWA problem, such that no two connections share the same wavelength on one link. Expression (2.3) make sure that  $u^w$  is set to 1 if wavelength  $w$  is used on any link by any connection. Expression (2.4) count the number of used wavelengths by making  $W_{total}$  equal to the index of the highest wavelength used. Expression (2.5) are the integrality constraints for the decision variables.

Let us now turn our attention to the scalability of the link ILP formulation, which is a function of the formulation size. This size, in turn, is determined by the number of decision variables and constraints. The number of the  $c_{ij}^{lw}$  variables is equal to  $N(N-1)|E|W$  for general topology networks; for ring networks, this reduces to  $N(N-1)(2N)W$ . There are also  $W$  variables  $u^w$ , and the decision variable  $\omega_{total}$ . Hence, the total number of variables in the link formulation for ring networks is  $O(N^3W)$ .

In terms of the number of constraints (ignoring the integrality constraints (2.5)), expression (2.1) corresponds to  $N^3W$  constraints, expression (2.2) yields  $|E|W$  constraints, expression (2.3) consists of  $W$  constraints, as does expression (2.4). Overall, the formulation consists of  $O(N^3W)$  constraints.

Note also that all the main variables in the formulation are tied to a specific wavelength. As a result, the optimal solution explicitly specifies the assignment of wavelengths to lightpaths, and as such it is highly symmetric with respect to wavelength permutations. In other words, if  $\omega_{total}$  is the number of wavelengths in the optimal solution, there exist  $\omega_{total}!$  alternative optimal solutions each corresponding to one permutation of the  $\omega_{total}$  wavelengths. Hence, the ILP solver may explore a large number of solutions that do not improve the objective function, limiting the scalability of the link ILP formulation to realistic networks with a large number of wavelengths.

## 2.2 Path Formulation

There is another straightforward ILP formulation often discussed in the literature (e.g., [44, 51]), referred to as path-based formulation. In this formulation, the available paths between node pairs are generated in advance, using an all-pair k-shortest path algorithm [37, 55, 43]. Therefore, the path topology of the network is added to the formulation as a set of additional inputs. We denote  $P$  as the total number of path candidates in the network. Specifically, we denote the  $k$ -th path from node  $i$  to node  $j$  as  $p_{ij,k}$ , and use binary variables  $X_{ij,k}^l$  to indicate whether path  $p_{ij,k}$  uses link  $l$ . Note that in ring networks, there are only two available paths between each node pairs, i.e., clockwise and counterclockwise.

Let us define the following set of decision variables:

- $c_{ij,k}^w \in \{0, 1\}$ : binary variable that indicates whether there exists a lightpath assigned wavelength  $w$  on path  $p_{ij,k}$
- $u^w \in \{0, 1\}$ : binary variable that indicates whether wavelength  $w$  is used anywhere in the network
- $\omega_{total}$ : number of wavelengths used in the whole network

With these notations, the path ILP formulation can be expressed as:

$$\text{Minimize : } W_{total}$$

*Subject to:*

$$\sum_k \sum_w c_{ij,k}^w = t_{ij}, \quad \forall i, j \in V \quad (2.6)$$

$$\sum_{i,j} \sum_k c_{ij,k}^w X_{ij,k}^l \leq 1, \quad \forall l \in E, \forall w \quad (2.7)$$

$$\sum_{i,j} \sum_k c_{ij,k}^w \leq u^w P, \quad \forall w \quad (2.8)$$

$$W_{total} \geq \sum_w u^w, \quad \forall w \quad (2.9)$$

$$u^w = 0, 1, \quad \forall w; \quad c_{ij,k}^w = 0, 1, \quad \forall i, j, k, w \quad (2.10)$$

Expression (2.6) ensures that all the traffic demands are satisfied. Specifically, the sum of all the wavelengths used by all  $K$  paths between node  $i$  and  $j$ , should be equal to the traffic demand between these two nodes. Expression (2.7) represents the distinct wavelength

constraints of the RWA problem, such that no two lightpaths share the same wavelength on one link. Since a path is the smallest unit to assign wavelength, the wavelength continuity constraints are implicitly satisfied in the path formulation. Expression (2.8) makes sure that  $u^w$  is set to 1 if wavelength  $w$  is used on any path. Expression (2.9) counts the number of used wavelengths by making  $W_{total}$  equal to the index of highest wavelength used. Expression (2.10) represents the integrality constraints for the decision variables.

Let's now turn our attention to the scalability of the path formulation. In terms of the number of decision variables, the set of variables  $c_{ij,k}^w$  have the largest number, which is equal to  $N(N-1)KW$  for the general topology; in a ring network, this number is  $N(N-1)(2W)$  as there are two paths between each node pair. There are also  $W$   $u_w$  variables and the decision variable  $W_{total}$ . Hence, the total number of variables in the formulation for ring networks is  $O(N^2W)$ .

In terms of the number of constraints (ignoring the integrality constraints (10)), expression (2.6) corresponds to  $N(N-1)$  constraints, which is  $2NW$  in a ring network; expression (2.7) yields  $|E|W$  constraints, which is  $2NW$  in ring networks; each of expressions (2.8) & (2.9) consist of  $W$  constraints respectively. Overall, the total number of constraints in the path formulation is  $O(NW)$ .

As in the link formulation, all the main variables in the path-based formulation are also tied to a specific wavelength. Hence, the path formulation suffers from the symmetry problem as well. As discussed already in the link formulation, this problem will severely decrease the performance of path formulation when used in modern networks deploying a large number of wavelengths.

### 2.3 Maximal Independent Set (MIS) Formulation

An alternative ILP formulation that overcomes the symmetry problem was introduced by Ramaswami and Sivarajan [51, 36]. This approach formulates the RWA problem as a graph coloring problem. Since the concept of maximal independent set (MIS) is used in the approach, this ILP formulation is referred to as MIS formulation.

To apply this approach, the first step is to transfer the original network graph into a path graph such that

- the paths in the original network graph are transformed to vertices in the new graph and
- two vertices in the path graph are connected if and only if the corresponding paths in the network share a common link.

To illustrate this, Figure 2.3 gives an example of a 3-node ring network, in which the network graph  $G$  is converted into path graph  $G_p$ . Paths in the network graph, as vertices in the path

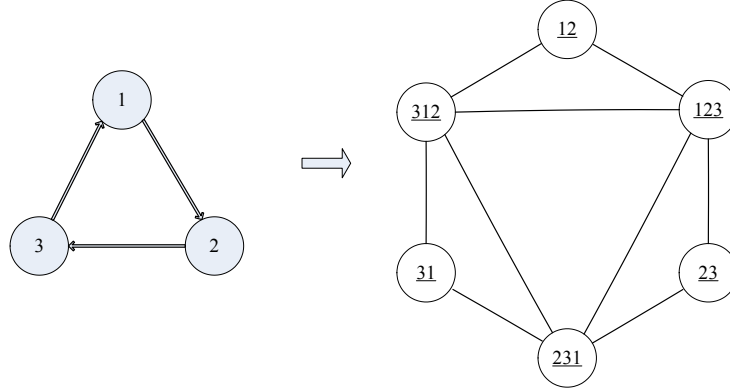


Figure 2.3: RWA as graph coloring problem

graph, are denoted by the sequence of nodes they traverse. As shown in the figure, 6 paths in total are found in the 3-node ring network, i.e., 12, 23, 31,123, 231, 312. If any two paths share a common link (e.g. 12 and 123), the fact will be represented as an edge between the two corresponding vertices in the path graph (for instance, nodes 12 and 123 are connected in  $G_p$ ).

Now, the RWA problem may be formulated as a graph coloring problem for the path graph such that multiple colors (each corresponding to a wavelength) are available to assign to the vertices with the constraint that no two adjacent vertices are assigned the same color. Moreover, in the minRWA problem, the number of colors used needs to be minimized to satisfy the traffic demands requested to the corresponding paths. As a well-studied problem, this multiple coloring problem can be optimally solved with the help of maximal independent sets: all vertices in the same maximal independent set (MIS) will be assigned the same color, since there are no connections between any 2 vertices within the same independent set; vertices that fall in different maximal independent sets will be assigned different colors, according to the definition of *maximal* independent set. Figure 2.4 provides an example of all MIS's in a 3-node ring network to illustrate this method. As we can see, four MIS's are enumerated in the path

graph, i.e., MIS (a) - (d) as shown in the figure. If there is a traffic matrix  $\begin{pmatrix} 0 & 1 & 0 \\ 1 & 0 & 1 \\ 1 & 0 & 0 \end{pmatrix} =$

$\begin{pmatrix} 0 & 1 & 0 \\ 0 & 0 & 1 \\ 1 & 0 & 0 \end{pmatrix} + \begin{pmatrix} 0 & 0 & 0 \\ 1 & 0 & 0 \\ 0 & 0 & 0 \end{pmatrix}$ , then MIS a & b should be selected to assign two different wavelengths respectively.

In MIS formulation, the MIS's of path graph are calculated in advance, and are additional set of inputs besides the network topology and traffic demands. Specifically, we use binary variable  $Y_{ij,k}^m$  to indicate whether path  $p_{ij,k}$  belongs to MIS  $m$ . Let us also define the set



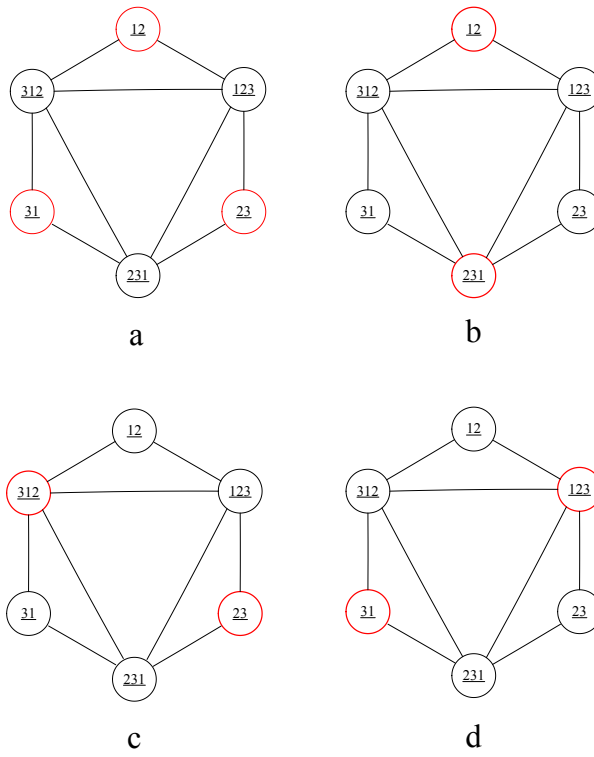


Figure 2.4: Maximal independent sets in 3-node ring network

of decision variables  $v^m$  as the number of wavelengths assigned to MIS  $m$ . We denote the number of lightpaths on path  $p_{ij,k}$  as  $b_{ij,k}$ . With the notations introduced above, the MIS-based formulation may be written as:

$$\text{Minimize : } W_{total}$$

*Subject to:*

$$\sum_k b_{ij,k} = t_{ij}, \quad \forall i, j \in V \quad (2.11)$$

$$\sum v^m Y_{ij,k}^m \geq b_{ij,k}, \quad \forall i, j \in V, \forall k \quad (2.12)$$

$$W_{total} \geq \sum_m v^m \quad (2.13)$$

$$v^m : \text{ integer}, \quad \forall m; \quad b_{ij,k} : \text{ integer}, \quad \forall i, j, k \quad (2.14)$$

Expression (2.11) ensures that all the traffic demands are satisfied. Specifically, the number of all the wavelengths used by all  $K$  paths between node  $i$  and  $j$  should be equal to the traffic demand between these two nodes. Expression (2.12) is used to assign sufficient number of wavelengths to each path, by ensuring that the sum of numbers of wavelengths assigned to all MIS including that path is no less than the traffic demands over it. Expression (2.13) counts the number of used wavelengths by adding up the number of wavelengths assigned to each MIS. Finally, expression (2.14) represents the integrality constraints for the variables.

Note that there are no constraints in the MIS formulation corresponding to either the wavelength continuity constraint or the distinct wavelength constraint. The former is implicitly satisfied by the same reason discussed in path formulation; the latter is taken care of by the property of an independent set, as any two paths in the same MIS will not share a common link.

Let us turn our attention to the scalability of the MIS formulation. The three sets of decision variables are  $b_{ij,k}$ ,  $v^m$  and  $W_{total}$ , among which the set of  $v^m$  variables has the largest number. The number of  $v^m$  variables is the same as the number of MIS, which is upper bounded by  $3^{N_p/3}$ . Since in ring networks,  $N_p = 2N(N-1)$ , the number of variables in the MIS formulation is  $O(3^{N^2/3})$ . This will be an extremely large number as the network size grows. In terms of the number of constraints, among the three sets (excluding the integrality constraints), expression (2.12) has the largest number, which is  $N(N-1)K$ . In ring network, this is equal to  $2N(N-1)$ . Hence, the number of constraints in the MIS-based formulation is in  $O(N^2)$ .

Finally, after reviewing all the decision variables in MIS formulation, we observe that none

Table 2.1: Comparison among Link, Path, MIS formulations

	# of variables	# of constraints	symmetric
Link	$O(N^3W)$	$O(N^3W)$	YES
Path	$O(N^2W)$	$O(NW)$	YES
MIS	$O(3^{N^2/3})$	$O(N^2)$	NO

is tied to a specific wavelength; instead, the focus is on the *number* of wavelengths assigned to each MIS. As a result, the MIS formulation overcomes the wavelength symmetry problem. This feature entitles MIS formulation the ability to solve RWA problems with any number of wavelengths available in the network, which is very useful in solving modern WDM networks that have a large number of wavelengths supported on a single fiber.

## 2.4 Comparison among the three

Having discussed the path-, link-, and MIS-based formulations, we list the important properties of the three in Table 2.1 as a comparison. First, let us look at the number of constraints. Considering the number of available wavelengths  $W$  is usually much larger than the number of nodes  $N$  in modern optical networks, the MIS formulation has the least number of constraints among the three. The reason could be revealed by looking at how much network information is included in the three ILP formulations. The link formulation starts purely from the original network topology without any additional inputs; The path formulation calculates the paths between each nodes pairs and includes them as an additional set of inputs to the formulation. Finally, the MIS formulation not only has all paths calculated but also includes the independent sets of paths in the formulation. As a result, the MIS-based formulation reduces the complexity of ILP solving.

Moreover, unlike the link- or path-based formulations, the MIS formulation overcomes wavelength symmetry problem. As a result, MIS formulation is more capable in solving the RWA problem in realistic WDM networks with easily up to hundreds of wavelength available.

On the other hand, the performance of the MIS formulation is limited by the bottleneck of the enormous number of variables. In fact, since the number of MIS decision variables grows exponentially with the network size, MIS formulation becomes impractical for large networks.

## Chapter 3

# RWA in Ring Networks: Exact, Fast Formulations Based On MIS Decomposition

As we discussed in the previous chapter, although the MIS formulation overcomes the symmetry problem, its scalability is limited by the enormous problem size. To decrease the problem size, we propose a new method of decomposing path sets into three partitions and represent the MISs by smaller MISs calculated in each partition [56]. In this chapter, we will introduce the decomposition method and generalize it to dividing the network to  $2^x$  partitions. By implementing this generalized form, we divide the network into partitions recursively, and form MISs of the path graph using the MISs calculated in different partitions separately. This maximal independent set decomposition (MISD) method effectively reduces the formulation size, and does not sacrifice the benefit of MIS formulation. We use MISD- $2^x$  to refer to the algorithm that divides the path set into  $2^x$  partitions.

Since vast parts of the current infrastructure are based on SONET/SDH rings, we focus on the discussion of the MIS decomposition approach in ring networks in this chapter. Experimental study shows that our approach gains a nearly 4 orders of magnitude decrease in running time compared to the existing formulations. The approach applies to the RWA problem in mesh networks but the scalability is limited due to the enormous number of MIS decision variables in mesh networks. The RWA problem in mesh networks is addressed in the next two chapters.

In the rest of this chapter, the key idea of MISD is introduced in detail. Section 3.1 and 3.2 discuss the MISD-2 and MISD-4 formulations respectively. Section 3.3 provides a general formulation for MISD formulations with any number of decompositions. Section 3.4 makes a comparison among the suite of MISD formulations and discusses the trade off between variables and constraints in the formulations. At the end of this chapter, experimental study in Section

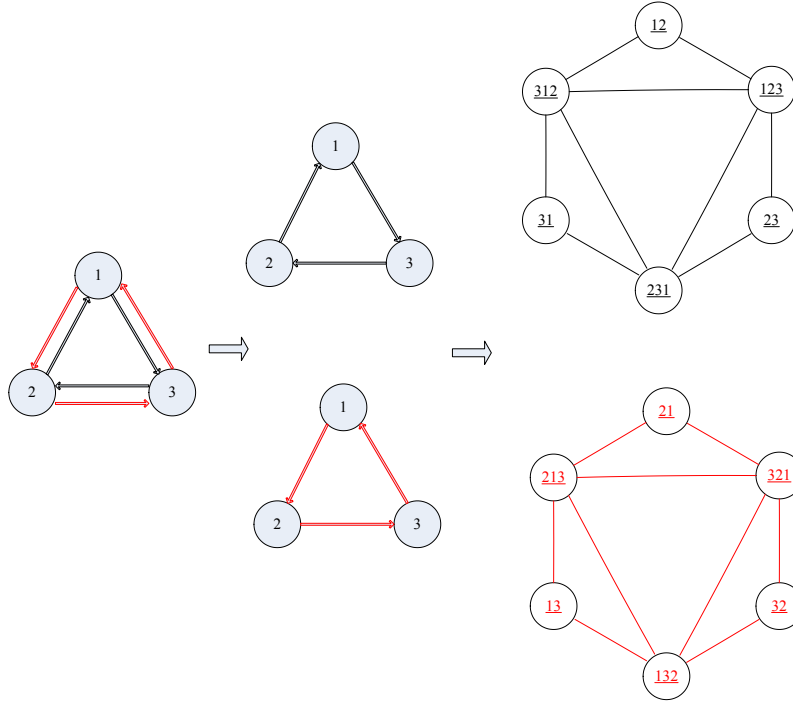


Figure 3.1: MISD-2

3.5 compares the efficiency of existing ILP formulations and the MISD formulations.

### 3.1 MIS Decomposition-2

The first decomposition formulation is based on the observation that any clockwise path does not intersect with any counter-clockwise path. To take advantage of this feature of a ring network, this method divides the network topology into two parts (i.e., two separate rings with opposite directions), which partitions the path graph  $G_p$  into two completely separate subgraphs  $G_p^{cw}$  and  $G_p^{ccw}$ . Therefore, a maximal independent set  $m$  of  $G_p$  can be represented by the union of some MIS  $m_{cw}$  in the first subgraph  $G_p^{cw}$  and some MIS  $m_{ccw}$  in the second subgraph  $G_p^{ccw}$ . To better illustrate this idea, an example is given in Figure 3.1. A three-node ring network is divided into two components, i.e., the clockwise ring with black color in the figure and the counter-clockwise ring with red color. As a result, the path graph is partitioned into two subgraphs, with 6 paths each (in the right side of figure). So we have  $m = m_{cw} \cup m_{ccw}$ . Also, if we denote the set of all  $m_{cw}$  as  $M_{cw}$ , the set of all  $m_{ccw}$  as  $M_{ccw}$ , then the number of MISs in the original path graph,  $|M|$ , could be represented by the product of  $|M_{cw}|$  and  $|M_{ccw}|$ , i.e.,  $|M| = |M_{cw}| \times |M_{ccw}|$ , and  $|M_{cw}| = |M_{ccw}| = \sqrt{|M|}$ . Again as in the example in Figure 3.1,  $|M_{cw}| = |M_{ccw}| = 4$ , while  $|M| = 16$ . In other words, the MISD-2 formulation provides a

great decrease in the number of decision variables compared to the original MIS formulation.

To further express the formulation, we denote  $X_{ij,k}^m$  as binary variables which indicate whether  $p_{ij,k}$  belongs to MIS  $m$  in ring  $k$  ( $k = cw, ccw$ ). (As shown in Figure 2.3, path 12 belongs to MIS 0, hence  $X_{12,0}^0 = 1$ ; but it does not belong to MIS 2, therefore  $X_{12,0}^2 = 0$ .)

We have the following set of outputs:

- $b_{ij,k} \in \{0, 1\}$ : number of wavelengths assigned to  $p_{ij,k}$
- $v_k^m \in \{0, 1\}$ : number of wavelengths assigned to MIS  $m$  in ring  $k$  ( $k = cw, ccw$ )
- $\omega_{total}$ : number of wavelengths used in the whole network

Then, the MISD-2 formulation may be expressed as follows:

$$\text{Minimize : } W_{total}$$

Subject to:

$$\sum_k b_{ij,k} = t_{ij}, \quad \forall i, j \in V \quad (3.1)$$

$$\sum_{m \in M_k} v_k^m X_{ij,k}^m \geq b_{ij,k}, \quad \forall i, j \in V, k = cw, ccw \quad (3.2)$$

$$W_{total} \geq \sum_{m \in M_k} v_k^m, \quad k = cw, ccw \quad (3.3)$$

$$v^m : \text{ integer}, \quad \forall m; \quad b_{ij,k} : \text{ integer}, \quad \forall i, j, k \quad (3.4)$$

Compared with the original MIS formulation in Chapter 2, only two sets of expressions (3.2) & (3.3) are different in the MIS decomposition-2 formulation. Expressions (3.2) correspond to expressions (2.12) of the MIS formulation, which represent the relationships between the numbers of wavelengths assigned on MISs and the numbers of wavelengths needed on each single path. This set of constraints ensures that each path is assigned a sufficient number of wavelength. Expressions (3.3) correspond to expressions (2.13) of the MIS formulation, and ensure that  $W_{total}$  represents the least number of wavelengths needed to satisfy all the traffic. Because both rings have a separate set of MISs, the same wavelengths may be assigned to MISs in different rings.  $W_{total}$  will be equal to the larger number of wavelengths used in either of the two rings.

By reviewing the scalability of MIS decomposition-2 formulation, it may be observed that the number of constraints remains the same as in the MIS formulation, i.e.,  $O(N^2)$ , but the number of variables becomes the square root of that in the MIS formulation, as discussed in the beginning of this chapter. This results in a dramatic decrease of the problem size, therefore

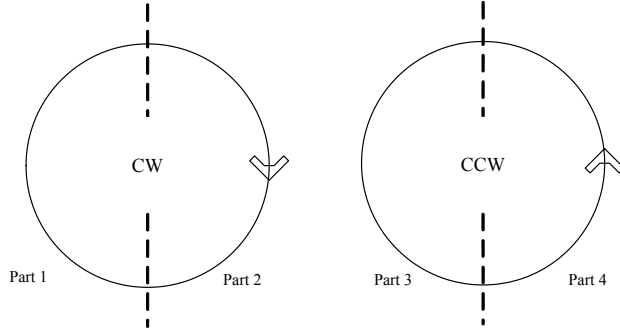


Figure 3.2: Network parts in MISD-4

a much better performance is gained by MISD-2 over MIS formulation. Further discussion will be provided in the experimental study in Section 3.5.

### 3.2 MISD-4

In the former section, we showed how to divide the path graph into two disjoint compositions so as to make the problem size much smaller. To further reduce the problem size, we now extend this approach by decomposing the network into more partitions. As shown in Figure 3.2, we divide the network topology into 4 parts, 2 for each directional ring. As a result, each of the path graphs  $G_p^{cw}$  and  $G_p^{ccw}$  is divided into three subgraphs, respectively. Figure 3.3 takes  $G_p^{cw}$  as an example, using path partitions of the clockwise ring to illustrate this decomposition. Graph  $G_p^{ccw}$  is handled in an identical manner. As shown in the figure, path partition 0 consists of all the paths containing only links from the left half-ring, corresponding to nodes in path subgraph  $G_p^{cw,0}$  in Figure 3.4; path partition 1 consists of all the paths containing only links from the right half-ring, corresponding to nodes in path subgraph  $G_p^{cw,1}$ . These two partitions are selected in the sense that no path in partition 0 shares a common link with any path in partition 1, and vice versa, and therefore there are no links between any node in  $G_p^{cw,0}$  and any node in  $G_p^{cw,1}$ . Afterward, all remaining paths will be included in the third partition, which we call a core partition. It consists of all the paths containing links from both the left half-ring and the right half-ring, which are the paths that cross the two halves, corresponding to nodes in path subgraph  $G_p^{cw,core}$ . (Since there are totally 46 connections between the 12 nodes in  $G_p^{cw}$ , for clarity of presentation, we omit these connections in Figure 3.4.)

Unlike the MISD-2 formulation, the three subgraphs in  $G_p^{cw}$  are not completely disjoint, so a MIS in  $G_p^{cw}$  may not be simply represented by the union of MIS in smaller subgraphs. Instead, we have to introduce a new set definition, referred to as core set. A core set consists of the nodes in  $G_p^{cw,core}$  which are the maximal subset of a MIS in  $G_p^{cw}$ , in other words, it includes the

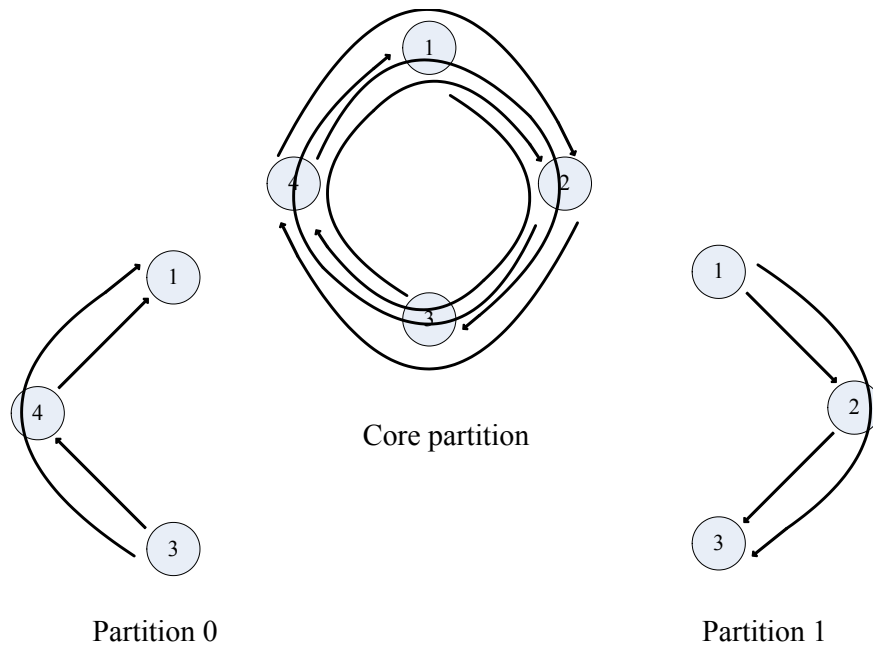


Figure 3.3: Path set partitions in MISD-4

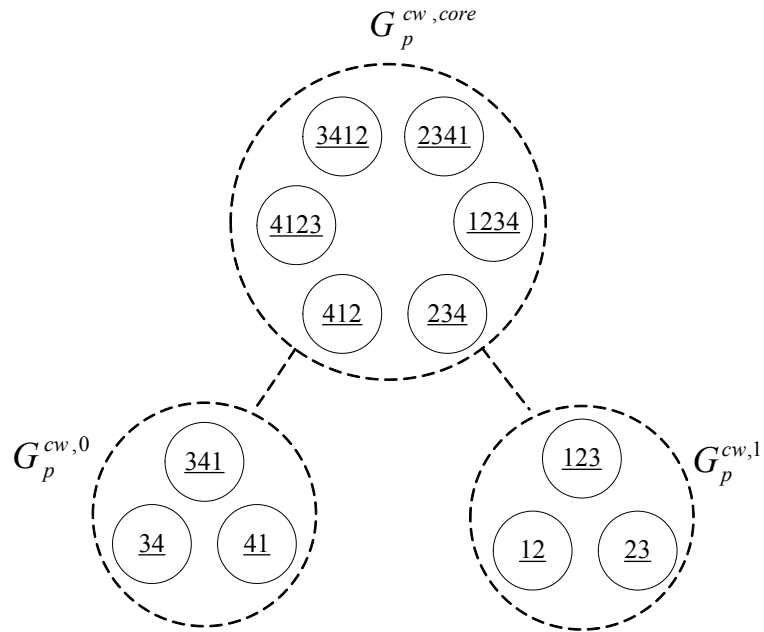


Figure 3.4: Path graph partitions in MISD-4



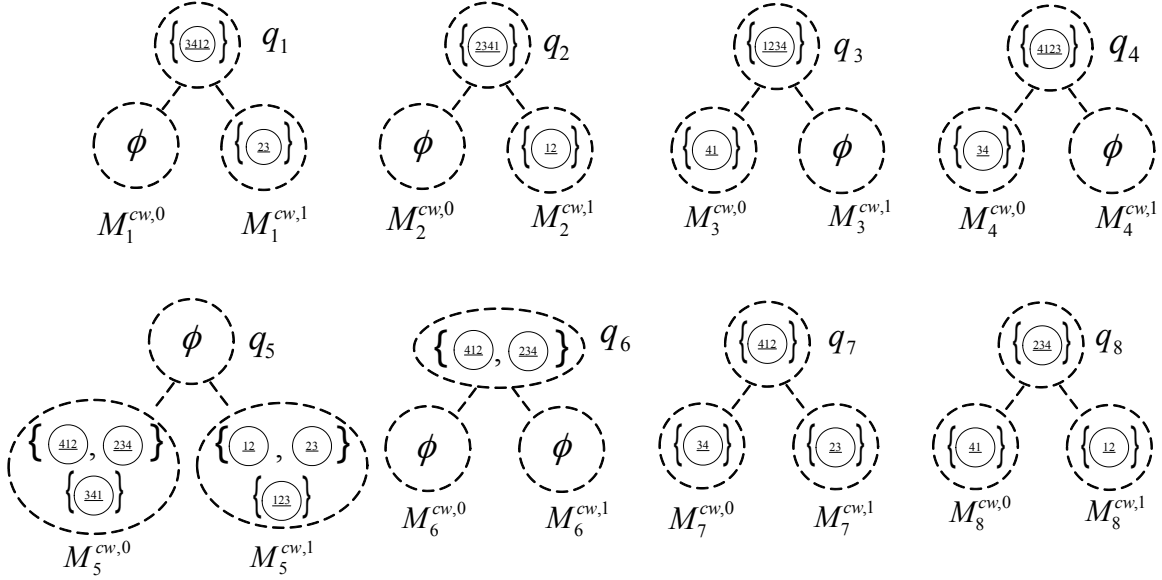


Figure 3.5: Core Sets & MISs

intersection of a MIS in  $G_p^{cw}$  and  $G_p^{cw,core}$ . Consequently, a MIS  $m_{cw}$  in  $G_p^{cw}$  is now represented by the union of some MIS  $m_{cw,0}$  in  $G_p^{cw,0}$ , some MIS  $m_{cw,1}$  in  $G_p^{cw,1}$ , and some core set  $q$ , i.e.,  $m_{cw} = m_{cw,0} \cup q \cup m_{cw,1}$ .

Similar to MIS's of the subgraphs in the MISD-2 formulation, core sets are calculated and included as variables in the MISD-4 formulation. We denote the set of all core sets as  $Q$ . The algorithm to calculate  $Q$  is stated in Table 3.1. Afterwards, for each core set  $q \in Q$ , the two sets of corresponding MISs in  $G_p^{cw,0}$  and  $G_p^{cw,1}$  are selected to compose MISs in  $G_p^{cw}$ , and we name them as  $M_q^{cw,0}$  and  $M_q^{cw,1}$  respectively. Then any MIS  $m_{cw,0} \in M_q^{cw,0}$  and any MIS  $m_{cw,1} \in M_q^{cw,1}$  will form a MIS in  $G_p^{cw}$  with core set  $q$ .

Figure 3.5 gives an example of all MIS's of  $G_p^{cw}$  represented by smaller MIS's and core sets in a 4-node ring network. Eight core sets are calculated from  $G_p^{cw,core}$  (including the empty set  $\emptyset$ ). For each of them,  $M_q^{cw,0}$  and  $M_q^{cw,1}$  are calculated. As a result, 11 MISs of  $G_p^{cw}$  in total are represented by the smaller MISs and core sets.

To introduce core sets into the MISD-4 formulation, we define  $X_{ij,k}^q$  as the binary variable indicating whether path  $p_{ij,k}$  belongs to core set  $q \in Q_k$ . Also, let us define the following sets of decision variables:

- $v_q^{k,core}$ : number of wavelengths assigned to core set  $q$  in  $k$ -th ring,  $k = cw, ccw$
- $v_{q,m}^{k,r}$ : number of wavelengths assigned to MIS  $m \in M_q^{k,r}$ ,  $k = cw, ccw$ ,  $r = 0, 1$

Table 3.1: Algorithm to calculate core sets

---

Initialize  $Q_k =$  maximal independent sets in  $G_p^{cw,k}$ ,  $k = 0, 1$ ,  
**for** each core set  $q \in Q_k$  do  
  **for** each node  $p \in q$  do  
    **if**  $p$  has a link to a node  $r \in G_p^{cw,0} \cup G_p^{cw,1}$ , and  
      none of the nodes in  $q \setminus \{p\}$  have a link to that node  
    **then** append the set  $q \setminus \{p\}$  to  $Q_k$   
  **end if**  
  **end for**  
**end for**  
append  $\emptyset$  to  $Q_k$

---

With all the notations introduced above, the MIS decomposition-4 formulation may be written as:

*Minimize :  $W_{total}$*

*Subject to:*

$$\sum_k b_{ij,k} = t_{ij}, \quad \forall i, j \in V \quad (3.5)$$

$$\sum_{q \in Q_k} v_q^{k,core} X_{ij,k}^q \geq b_{ij,k}, \quad \forall p_{ij,k} \in G_p^{k,core}, k = cw, ccw \quad (3.6)$$

$$\sum_{q \in Q_k} \sum_{m \in M_q^{k,r}} v_{q,m}^{k,r} X_{ij,k}^m \geq b_{ij,k}, \quad \forall p_{ij,k} \in G_p^{k,r}, \quad k = cw, ccw, \quad r = 0, 1 \quad (3.7)$$

$$v_q^{k,core} = \sum_{m \in M_q^{k,r}} v_{q,m}^{k,r}, \quad \forall q \in Q_k, \quad k = cw, ccw, \quad r = 0, 1 \quad (3.8)$$

$$W_{total} \geq \sum_{q \in Q_k} v_q^{k,core}, \quad k = cw, ccw \quad (3.9)$$

$$b_{ij,k}, \quad v_q^{k,core}, \quad v_{q,m}^{k,r} : \quad integer \quad (3.10)$$

Expression (3.5) is comparable to expression (3.1) in MISD-2 formulation, and ensures that all the traffic demands are satisfied. Expressions (3.6) and (3.7) are comparable to expression (3.2), and are used to assign sufficient number of wavelength to each path in such a way that the sum of numbers of wavelengths assigned on MIS/core sets that includes a certain path is no less than the number of traffic demands over it. Specifically, (3.6) ensures that traffic demands on each path included in  $G_p^{k,core}$  satisfied; similarly, (3.7) takes care of every path included in  $G_p^{k,0}$  &  $G_p^{k,1}$ . Expression (3.8) is used to ensure consistency between wavelength assignment in different partitions. Since  $m_{cw} = m_{cw,1} \cup q \cup m_{cw,2}$ , the specific  $m_{cw,0}, q, m_{cw,1}$  used to form the same MIS  $m_{cw}$  should have the same number of wavelength assigned. Expressions (3.9) count the number of used wavelengths by adding up the number of wavelengths assigned to each core set. Because the two rings have distinct core sets, the same wavelengths may be assigned to core sets in different rings. Finally,  $W_{total}$  will be equal to the larger number of wavelengths used in the two rings.

Let us now analyze the scalability of the MISD-4 formulation. Since the MISD-4 formulation is built on the basis of MISD-2 by representing the MIS variables of the MISD-2 formulation as the union of three smaller sets (one core set and two MIS's), the number of variables in MISD-4 depends on the number of core sets and corresponding MIS's in the smaller subgraph. Since we are calculating MIS in a smaller subgraph containing fewer nodes, the number of MIS variables will have an exponential decrease compared to that in MISD-2 formulation. On the other

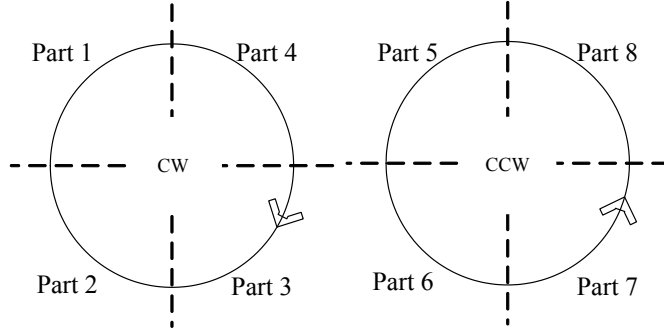


Figure 3.6: Link divisions of the network in MISD-8

hand, this decrease in variables is possible only at the expense of an increase in the number of constraints. This is due to the extra set of constraints to ensure consistency on assigned wavelengths between core sets and corresponding independent sets. The number of these extra constraints is the same as the number of core sets, which is a small number compared to the large number of variables that are eliminated. Therefore, the trade-off between decrease of variables and increase of constraints is very beneficial to the performance of MISD-4 formulation. Section 3.4 provides a detailed discussion along with numerical results further demonstrating this fact.

### 3.3 Generalized MIS Decomposition Formulation - MISD- $2^x$

We may further extend the MISD-4 formulation, by dividing the path sets into more partitions recursively, generalizing the MIS decomposition formulation with arbitrary number of partitions.

In a MISD- $2^x$  formulation, the ring network is divided into two directional rings, with  $2^{x-1}$  parts on each ring. According to these  $2^{x-1}$  parts on each ring, the path sets of each ring are partitioned into  $2^x - 1$  partitions with  $x$  levels as a tree topology. The lowest level of path partitions consists of paths containing only links within each network part; the second lowest level of path partitions includes paths containing only links from the adjacent two network parts, and so on. The highest level of path partitions consists of paths that are across the left half-ring and right half-ring. An example of MISD-8 is shown in Figure 3.6. There are seven partitions for the clockwise paths. The lowest level of partitions are labeled 4, 5, 6, 7, and each consists of paths that only use links within network part 1, 2, 3, 4, respectively. The second lowest level contains two partitions, where partition 2 consists of paths that use links in (and only in) both parts 1 & 2, while partition 3 consists of paths that use links in (and only in) both parts 3 & 4. The top level partition consists of all remaining paths, i.e. paths that use links in both half-rings.

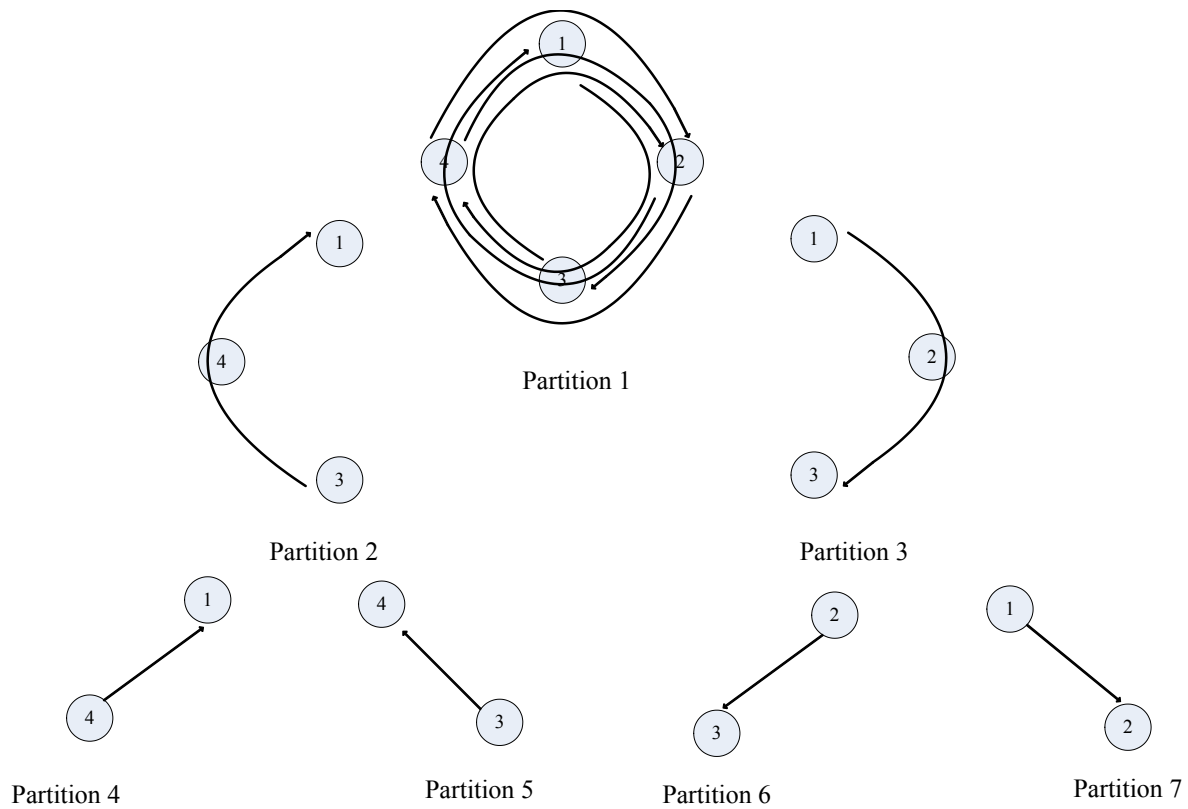


Figure 3.7: Clockwise path set partitions in MISD-8

When presented as a path graph, shown in Figure 3.8, it is easily seen that all the leaf subgraphs,  $G_p^{cw,4}$ ,  $G_p^{cw,5}$ ,  $G_p^{cw,6}$  and  $G_p^{cw,7}$  in MISD-8 are mutually disjoint. The only connections among the subgraphs are between the child subgraphs and parent subgraphs. Therefore, a MIS in  $G_p^{cw}$  can be represented by the union of core sets in the parent subgraph and MISs in the child subgraph respectively. Starting from the root of the subgraph tree, a MIS  $m_{cw}$  in  $G_p^{cw}$  may be represented by the union of a MIS  $m_{cw,2}$  in  $G_p^{cw,2}$ , a core set  $q_{cw,1}$  in  $G_p^{cw,1}$  and a MIS  $m_{cw,3}$  in  $G_p^{cw,3}$ , i.e.,  $m_{cw} = m_{cw,2} \cup q_{cw,1} \cup m_{cw,3}$ . Recursively, MIS  $m_{cw,2}$  may be further substituted by the union of  $m_{cw,4}$  in  $G_p^{cw,4}$ , core set  $q_{cw,2}$  in  $G_p^{cw,2}$  and  $m_{cw,5}$  in  $G_p^{cw,5}$ , i.e.,  $m_{cw,2} = m_{cw,4} \cup q_{cw,2} \cup m_{cw,5}$ . Performing a similar representation for  $m_{cw,3}$ , we have  $m_{cw,3} = m_{cw,6} \cup q_{cw,3} \cup m_{cw,7}$ . In the generalized MISD- $2^x$ , this representation continues to be performed recursively, until it reaches the leaf subgraph in the subgraph tree. Therefore, a MIS in  $G_p^{cw}$  may be represented by the union of MIS in leaf subgraphs and core sets in non-leaf subgraphs, e.g.,  $m_{cw} = (m_{cw,4} \cup q_{cw,2} \cup m_{cw,5}) \cup q_{cw,1} \cup (m_{cw,6} \cup q_{cw,3} \cup m_{cw,7})$  in MISD-8 case as shown in Figure 3.9.

Having discussed the key idea underlying the generalized MISD- $2^x$ , now let us turn our attention to the ILP formulation. Since all core sets and MIS of subgraphs in different levels need to be calculated out and included as decision variables, the exact MISD- $2^x$  formulation has very complicated expressions. For the sake of simplicity and continuity for readers, only basic formulation structures are given in this section. The exact mathematical expressions of this formulation may be found in Appendix A.

$$\text{Minimize : } W_{total}$$

Subject to:

$$\sum_k b_{ij,k} = t_{ij}, \quad \forall i, j \in V \quad (3.11)$$

$$\sum_{\text{all } m \text{ containing } p_{ij,k}} \text{wavelength assignment on MIS } m \geq b_{ij,k}, \quad \forall \text{ leaf subgraph} \quad (3.12)$$

$$\sum_{\text{all } q \text{ containing } p_{ij,k}} \text{wavelength assignment on core set } q \geq b_{ij,k}, \quad \forall \text{ non-leaf subgraph} \quad (3.13)$$

$$\text{wavelength assignment on core set } q = \sum_{\text{all } m \text{ corresponding to } q} \text{wavelength assignment on MIS } m, \quad (3.14)$$

\(\forall\) non-leaf subgraph

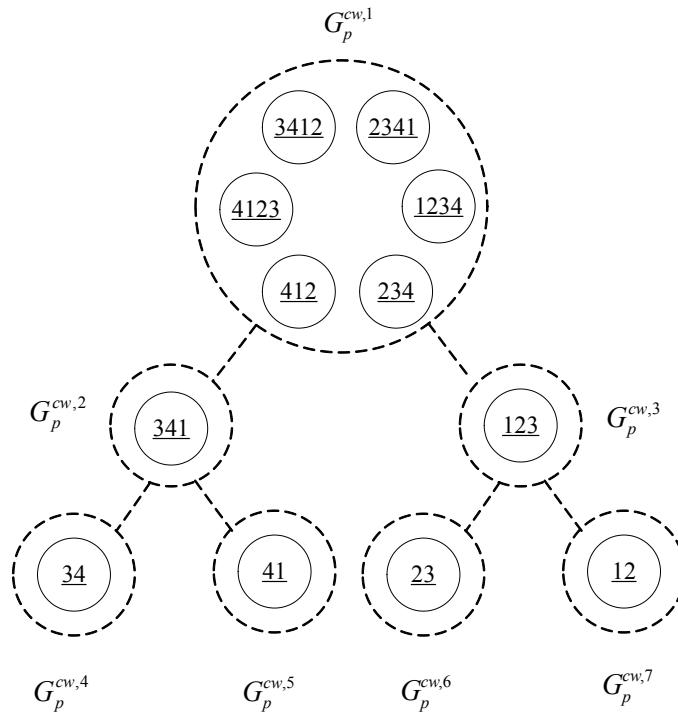


Figure 3.8: Clockwise path graph in MISD-8

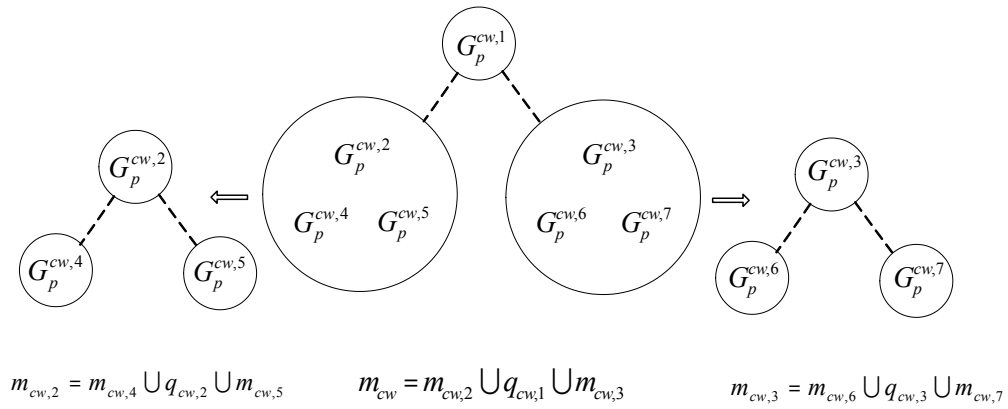


Figure 3.9: MIS Representation in MISD-8

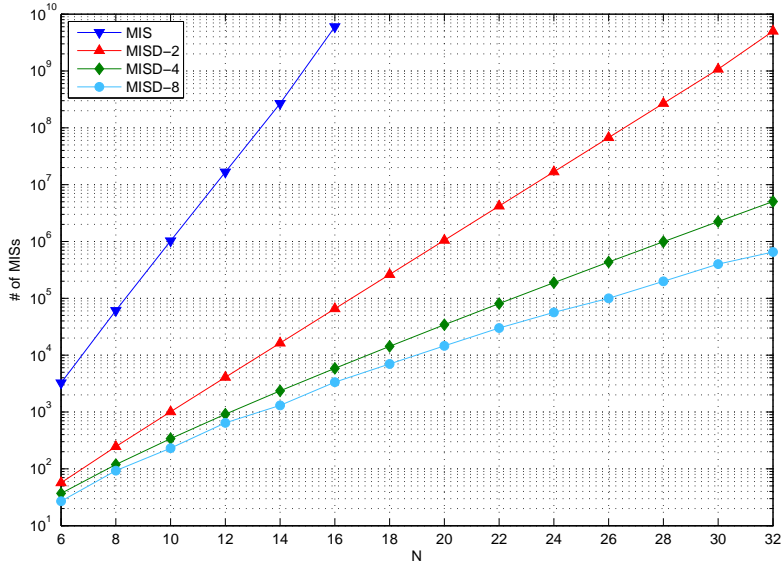


Figure 3.10: Problem size in MIS/core set decision variables

$$W_{total} \geq \sum_{\text{all } q \text{ in root subgraph}} \text{wavelength assignment on core set } q \quad (3.15)$$

$$\text{integrality constraints} \quad (3.16)$$

Expressions (3.12) (3.13) make sure that a sufficient number of wavelengths is assigned to each path. Expressions (3.3) are used to keep consistency between wavelength assignment in different partitions. Expression (3.15) counts the number of used wavelengths by adding up the number of wavelengths assigned to each core set in root subgraph.

### 3.4 Size and Scalability of MISD Formulations

As discussed in earlier sections, the more partitions the network is divided into, the fewer decision variables the MISD formulation will include, but the more constraints the formulation will add. In this section, we present numerical results to compare the number of MIS/core set decision variables in different MISD formulations, so as to understand how the trade-off between decreasing variables and increasing constraints influences performances of these ILP formulations.

Figure 3.10 presents the number of MIS decision variables in the MIS and MISD-2 formu-



lations, and the total number of MIS/core set decision variables in the MISD-4 and MISD-8 formulations. As we can see, the number of MIS's in the MISD-2 formulation is the square root of those in MIS formulations. This is consistent with the discussion in Section 3.1, as the ring network consists of two disjoint subnetworks of the same size. In the network instance with 10 nodes, the MISD-2 formulation represents a 3 order of magnitude decrease in the number of MISs. Still, with further decomposition, the number of MIS/core set decision variables in MISD-4 continues to cut down, with a 2 order of magnitudes decrease compared to that in MISD-2 at 24 nodes. Finally, the number of MIS/core set decision variables is further reduced with a MISD-8 decomposition. Although the rate of decrease slows compared to the drop between MISD-2 and MISD-4 formulations, we observe nearly one order of magnitude decrease at 32 nodes. To sum up, as the number of decompositions grows, the number of decision variables in MISD formulations keeps decreasing, but this decrease is getting slower and its impact is evident only as the network size increases.

As we discussed in Section 3.2, the MISD approach trades off the number of variables with the number of constraints so as to achieve a better scalability in terms of network size. The decrease in the number of variables does come with the expense of an increase in the number of constraints, the number of which is equal to the number of core sets. However, this increase in constraints is comparatively low compared to the great decrease in number of variables. For example, for a 16-node ring network instance, the number of variables has a large drop from around 70000 in MISD-2 formulation to 2000 in MISD-4 formulation, while the number of constraints only increases by 953. As a result, we are eliminating a large amount of variables with the little expense of adding a small number of constraints.

To further prove the benefits that we obtain in the trade-off between variable and constraints, consider the problem size in terms of the number of nonzero items in the four MIS-based formulations, which takes both variables and constraints into account. As shown in Figure 3.11, compared to the MISD-2 formulation, the MISD-4 formulation has a much smaller problem size for all network instances. Also, the problem size of the MISD-8 formulation is very close to that in MISD-4 formulation when the network is smaller than 12 nodes, but becomes clearly smaller when network grows larger. Therefore, MISD formulations with up to 8 decompositions are all getting benefits in the trade-off between variables and constraints. This conclusion will also be proved by the experimental study in next section.

### 3.5 Experimental Study

In this section, we present experimental results to compare the efficiencies of MISD formulations and the three kinds of existing formulations (Link, Path, MIS). In all comparisons, results are obtained through the IBM Ilog CPLEX 11 optimization tool on a cluster of compute nodes

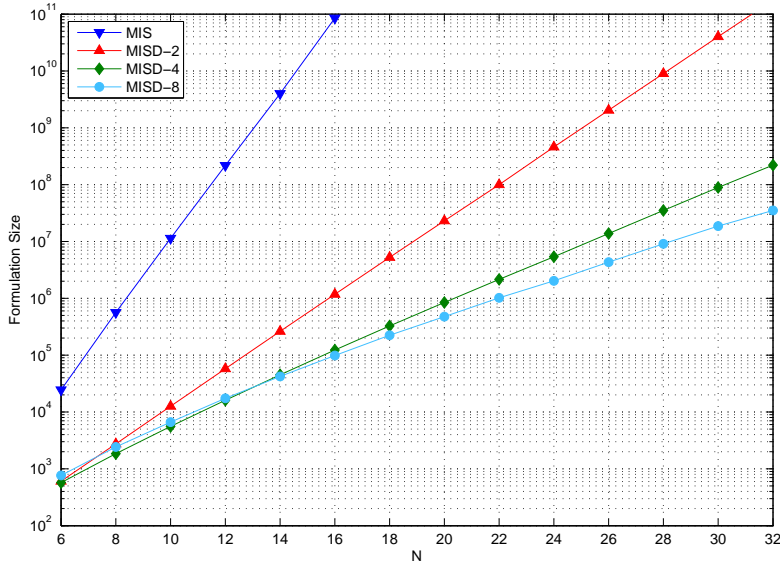


Figure 3.11: Problem size in nonzero items in formulations

with dual Woodcrest Xeon CPU at 2.33GHz with 1333MHz memory bus and 4MB L2 cache.

For the first comparison, we used 6 formulations (Link, Path, MIS, MISD-2, MISD-4, MISD-8), to solve the RWA problem in ring networks on identical sets of network instances. In this set of instances, network size varies from 6 to 24 nodes. Traffic demands  $t_{ij}$  from node  $i$  to node  $j$  are generated randomly in the interval of  $[0, 3]$  and the number of wavelengths  $W$  is selected as 120, which is representative of today’s WDM technology. The experimental results are shown in Figure 3.12, which are all obtained as the average of 30 runs with different random traffic demands. The solution times of minRWA problem using 6 different formulations are plotted (in logarithmic scale) as a function of network size. Note that the “tLim” sign in time axle indicates that the solution time has exceeded 2 CPU hours of time limit, and the “mem” sign indicates that the problem size is too large to fit in the machine memory.

As the experimental result shows, the RWA problem for a network with more than 10 nodes can not be solved by the link formulation within 2 hours. Also, in the range of its capability, the link formulation requires the longest time to solve the problem among the 6 formulations. The path formulation has a comparatively better performance than the link formulation: it can find the optimal solution for network of up to 16 nodes. This is consistent with the comparison analysis in Section 2.4 that the path formulation has a good extent of decrease in the number of both variables and constraints compared to the link formulation. The MIS formulation runs faster than the former two formulations in small networks with up to 8 nodes. However, as the

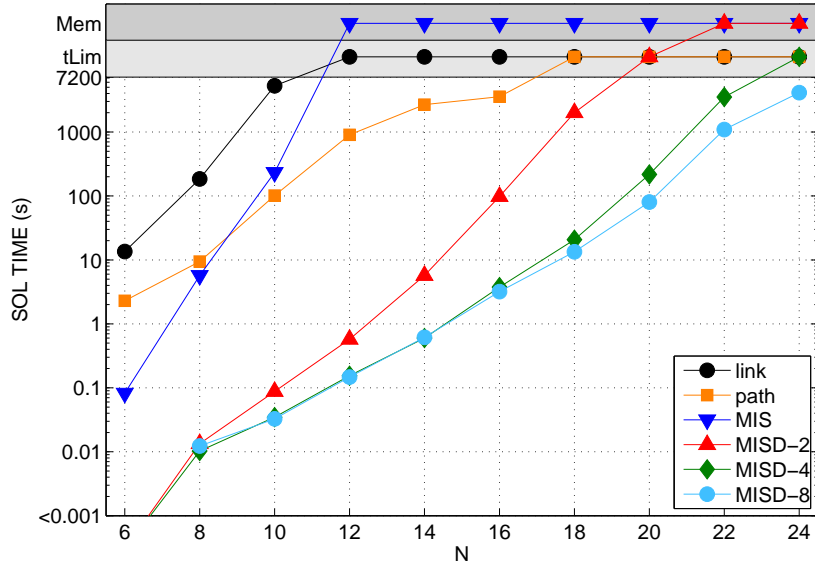


Figure 3.12: RWA solution times vs.  $N$  ( $W=120$ )

network size gets larger, the exponential increase in the number of variables makes it run out of memory. The proposed MISD formulations performs much better than the other three. The MISD-8 formulation, particularly, may optimally solve a network with up to 24 nodes with the 2-hour limit, and obtains the solution for 16 node network within just 3 seconds. As a result, it gains 8 more nodes than any other existing formulations in solving capability, and three orders of magnitude decrease in solving times for any network size. Noting the fact that the largest size of existing SONET ring is 16 nodes, and that the MISD formulations do not suffer from the wavelength symmetry problem, we conclude that MISD-8 can solve the RWA problem for any existing ring network with any number of wavelength in a very practical time.

The second comparison results are presented in Figure 3.13, which are the largest problem sizes in network instances that can be solved within 3000 sec according to different number of wavelengths. The gray area indicates the problem is infeasible, which means the needed number of wavelengths is larger than the one provided. Note that the MIS and MISD formulations are independent of  $W$ , so the curves are straight lines as their solving capability does not depend on  $W$ . Even when the provided number of wavelengths is less than sufficient, they still could present the optimal solutions with needed number of wavelengths. To the contrast, the link and path formulations suffer from the wavelength symmetry problem, as a result, their solving capability becomes obviously worse as the provided number of wavelengths grows. Numerically, MISD-8 formulations has the best performance among all six, which could solve network instances with

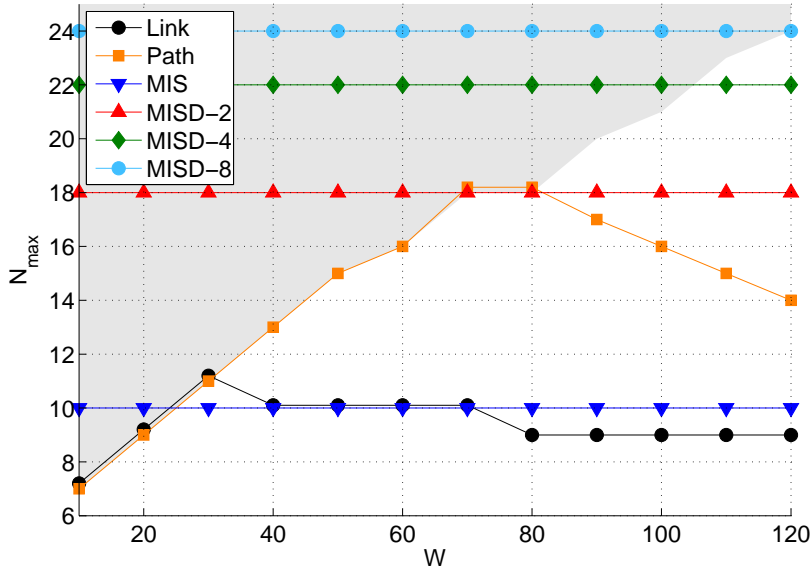


Figure 3.13: Size of largest network can be solved for a given number of wavelength within 3000 sec

up to 24 nodes. MISD-4 and MISD-2 formulations also have good scalability close to MISD-8. On the other hand, all three of the conventional formulations fall behind MISD formulations. Within the 3000 sec time limit, the link and MIS formulations provide the ability to solve only less-than-10-nodes ring networks, and the path formulation’s performance is severely restricted when the provided number of wavelengths grows larger than 80.

To sum up, the experimental study indicates that the suite of MISD formulations significantly overperforms conventional ILP formulations in solving the RWA problem in WDM ring networks, and dramatically extends the network size that can be solved optimally.

### 3.6 MIS Decomposition Formulation in Mesh Networks

Now that we have demonstrated that the MIS Decomposition Formulation performs well in WDM ring networks, it is natural to explore its potential and performance in WDM mesh networks. In fact, the same idea applies to mesh network and works well. However, the scalability of MISD formulation is highly limited due to the enormous number of MIS decision variables in mesh networks.

First of all, the idea of MIS decomposition works in mesh networks well. Links in mesh networks may be partitioned into two sets easily. Paths that contain links in only one of the

two sets, will compose the smaller partitions of the MIS decomposition, while the paths that contain links in both of the two sets will be included in the core partition. By directly utilizing the same idea used in ring networks, the MIS decomposition can be applied to mesh network instances.

However, unlike ring networks, general mesh networks are not able to be divided into two partitions such that no intersections are possible between paths from different partitions. As a result, the number of MIS decision variables can not achieve the dramatic decrease as in the ring network instances. Therefore, with the same network size, the number of MIS decision variables are dramatically larger than that in ring network. As a consequence, although MIS decomposition works well in large ring networks, it can not tackle even normal-sized mesh networks, as it requires extraordinarily large memory to run the ILP formulation in CPLEX. This makes the MIS decomposition limited in its scalability in mesh network application.

On the other hand, the number of decision variables in path-based ILP formulations remains the same, therefore it remains the same solution time as in ring network. As a result, path-based formulation shows its advantages over MIS decomposition formulation in mesh network applications.

From the above observations, rather than MIS decomposition approach, we will further explore the path-based formulation in mesh networks. In fact, the discussion in the following chapter will show that it actually succeeds in reducing the problem size.

## Chapter 4

# New, Fast Formulations Based on Path-based ILPs

As backbone and regional networks evolve from ring to mesh, optimal RWA solutions for general topologies are becoming important to network designers and operators. However, as discussed in the previous chapter, the MIS decomposition formulation faces scalability issues in mesh networks, which makes it impractical for mesh topologies representative of backbone networks. On the other hand, the path-based formulation has the advantage of keeping the problem size similar to that in ring networks. In this chapter, we present a new path-based ILP formulation for tackling the RWA efficiently on mesh network topologies encountered in practice. To this end, we propose a series of techniques to bring down the problem size in path-based formulations, including:

- introducing the concept of a symmetric RWA solution and developing a new, fast formulation for obtaining such solutions, and
- introducing the output from fast heuristics as part of the input to ILP formulation (i.e., limiting the number of wavelengths and introducing cuts in the solution search).

Experimental study in the end of the chapter indicates that the techniques work well and improve the performance of the original path-based formulation by orders of magnitude in terms of running time. We also demonstrate that optimal symmetric solutions, in addition to their practical advantages, often achieve the overall optimal or a value very close to it. With this new proposed formulation, we can solve mesh topologies representative of backbone and regional networks efficiently.

The chapter is organized as follows. In Section 4.1 we introduce the concept of a symmetric RWA solution and develop a new, fast formulation for obtaining such solutions, while in Section 4.2 we show how to further improve this formulation. In Section 4.3, we present

an experimental study that demonstrate the effectiveness of our formulation in solving problem instances representative of existing backbone networks, and we conclude the chapter in Section 4.4.

## 4.1 Optimal Symmetric RWA Solutions

In this section and the next, we present a set of techniques to scale the path ILP formulation to problem instances encountered in practice. In this work, we assume that routing is symmetric, i.e., for all source-destination pairs  $(s, d)$ , path  $p_{sd,k}$ ,  $k = 1, \dots, K$ , from node  $s$  to node  $d$  consists of the same physical links as path  $p_{ds,k}$  from node  $d$  to node  $s$ , but in the opposite direction. We now introduce the concept of a symmetric RWA solution.

**Definition 4.1.1 (Symmetric RWA solution)** *Without loss of generality, assume that for a node pair  $(s, d)$  we have that  $t_{sd} \leq t_{ds}$ . For RWA problem instances with symmetric routing, we define a symmetric solution to be such that:*

$$c_{sd,k}^w = c_{ds,k}^w, \quad \forall w, k, \quad \forall s, d : t_{sd} \leq t_{ds}. \quad (4.1)$$

*In other words, for each demand between source  $s$  and destination  $d$  for which there is a symmetric demand from  $d$  to  $s$ , the two demands are assigned the same path (in opposite directions) **and** the same wavelength<sup>1</sup>.*

It has long been recognized [3] that symmetric routing offers many advantages, including better network capacity planning and utilization, faster problem resolution, and more consistent traffic flow characteristics in terms of delay, cost, and other metrics. Several Internet protocols, including RSVP, NTP, and multicast (e.g., reverse path forwarding) rely upon routing symmetry, despite the fact that symmetric routing of fine granularity flows is not guaranteed in today’s multi-provider Internet [17]. On the other hand, optical transport networks are designed, deployed and engineered by a single provider, hence symmetric routing of lightpaths may be easily achieved within such a backbone or regional network. Our definition of a symmetric RWA solution goes one step further, requiring that symmetrically routed lightpaths also use the same wavelength. This additional requirement simplifies significantly the ILP formulation (and hence, the search for a solution) *with little, if any, sacrifice* in terms of optimality compared to general asymmetric solutions, as we explain and quantify in Section 4.3.

It is possible to obtain an optimal symmetric solution by introducing constraints (4.1) into the ILP formulation (2.6)-(2.10). However, the resulting formulation would be larger, and hence, less scalable than the original one. In the following, we present a decomposition technique that

---

<sup>1</sup>Note that a symmetric solution does not constrain demands that do not have a symmetric counterpart.

makes it possible to obtain an optimal symmetric RWA solution in times that are orders of magnitude faster than solving the formulation (2.6)-(2.10).

The key idea of our approach is to decompose the original problem into two smaller subproblems such that *only one* of these needs to be solved using an ILP. The optimal solution to the second subproblem is determined by symmetry, without the need to solve another ILP. Combined, the two solutions form an optimal symmetric solution for the original problem. Each subproblem consists of a different subset of all source-destination pairs, and hence includes only the corresponding part of the traffic demand matrix and path subset of the original problem. Consequently, the first subproblem can be solved using a slightly modified path ILP formulation whose size is significantly smaller than that of the original formulation shown in (2.6)-(2.10).

Next, we describe an intuitive decomposition that is applicable to instances with symmetric traffic demands; in the following subsection, we present a generalized version of the decomposition for arbitrary traffic matrices.

#### 4.1.1 Symmetric Traffic Demands

In this subsection we make the additional assumption that traffic demands are symmetric, i.e.,  $t_{sd} = t_{ds}$ ,  $\forall s, d \in V$ ; we will remove this assumption in the next subsection. Let us define two new traffic matrices  $T^1 = [t_{sd}^1]$  and  $T^2 = [t_{sd}^2]$  as:

$$t_{sd}^1 = \begin{cases} t_{sd}, & s < d \\ 0, & \text{otherwise} \end{cases} ; t_{sd}^2 = \begin{cases} t_{sd}, & s > d \\ 0, & \text{otherwise} \end{cases} \quad (4.2)$$

and the corresponding path sets:

$$\mathcal{P}^1 = \{p_{sd,k} \in \mathcal{P} | s < d\}, \mathcal{P}^2 = \{p_{sd,k} \in \mathcal{P} | s > d\} \quad (4.3)$$

Note that  $T^1$  and  $T^2$  are lower and upper diagonal matrices, respectively, such that  $T^1 + T^2 = T$  and  $(T^1)^T = T^2$ , and that  $\mathcal{P}^1 \cup \mathcal{P}^2 = \mathcal{P}$ .

Consider the decomposition of the original RWA problem into two subproblems, RWA-1 and RWA-2, such that the input to RWA-1 is traffic matrix  $T^1$  and path set  $\mathcal{P}^1$ , and the input to RWA-2 is  $T^2$  and  $\mathcal{P}^2$ . With this pair of symmetric subproblems, one is naturally led to the following two-step decomposition algorithm (SYM-RWA).

---

#### Algorithm SYM-RWA

1. Solve optimally subproblem RWA-1.
2. Construct a *symmetric solution* for subproblem RWA-2, as defined in expression (4.1), where  $c_{sd,k}^w$  is the solution from Step 1.



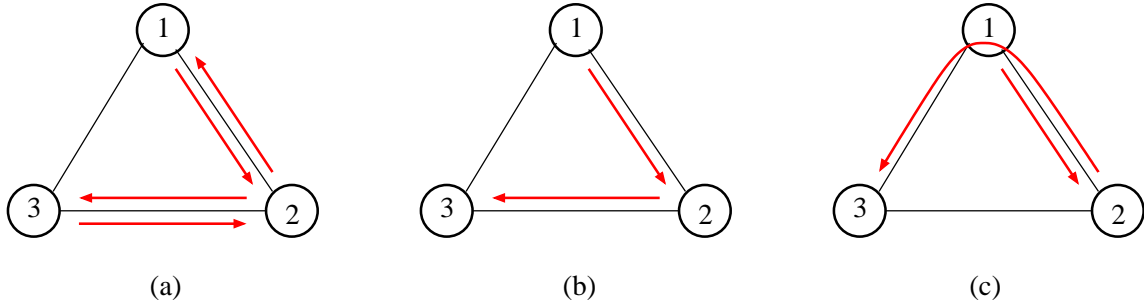


Figure 4.1: RWA instance for the proof of Lemma 4.1.1: (a) optimal symmetric solution to the original RWA problem, (b) one optimal solution to the RWA-1 problem, (c) another optimal solution to the RWA-1 problem

---

Subproblem RWA-1 may be solved optimally in Step 1 using a *reduced* version of the ILP formulation (2.6)-(2.10) after making the following changes:

- the new binary variables are  $\{c_{sd,k}^w : s < d\}$ ;
- the new traffic constraints are those in (2.7) with  $s < d$ ; and
- the new distinct wavelength constraints are those in (2.7) for links  $l$  used by paths in  $\mathcal{P}^1$ .

This ILP formulation for RWA-1 has only one-half the decision variables  $\{c_{sd,k}^w\}$  and one-half the traffic constraints (2.7) of the original formulation, i.e., those corresponding to the paths and traffic demands, respectively, included in the RWA-1 subproblem. The reduced formulation may also have fewer distinct wavelength constraints (2.8), if some of the links in the network are not used by paths of this subproblem. Hence, the decomposition algorithm can be applied to larger problem instances than is possible by tackling directly the original RWA problem through the ILP; we quantify the scalability of SYM-RWA in Section 4.3.

The question then arises whether solving only one subproblem optimally and constructing a symmetric solution for the other subproblem yields an optimal symmetric solution for the original RWA problem. In Lemma 4.1.1, we show that if the ILP formulation in (2.6)-(2.10) is used in Step 1 of the SYM-RWA algorithm (after removing the unnecessary variables and constraints, as we discussed above), then the resulting symmetric solution may not be optimal (or even feasible) for the original problem. We then show how to modify the ILP formulation in (2.6)-(2.10) so that the SYM-RWA algorithm will always yield an optimal symmetric solution for the original problem.

**Lemma 4.1.1** *Consider an RWA problem instance with symmetric routing and symmetric traffic demands, and the subproblems RWA-1 and RWA-2 as defined above. If, in Step 1 of the*

*SYM-RWA algorithm, the ILP formulation in (2.6)-(2.10) is used to solve one of the subproblems, then the symmetric solution obtained by the algorithm may not be an optimal (or feasible) symmetric solution for the original RWA problem.*

**Proof.** We will construct a simple instance to show that the SYM-RWA algorithm may not always find an optimal symmetric solution. Consider an RWA instance with  $N = 3$  nodes arranged in a ring topology, as shown in Figure 4.1, and traffic matrix  $T = \begin{pmatrix} 0 & 1 & 0 \\ 1 & 0 & 1 \\ 0 & 1 & 0 \end{pmatrix}$ . The

path set consists of the clockwise and counter-clockwise paths between the node pairs with non-zero demands. The optimal symmetric solution to this problem is shown in Figure 4.1(a) and requires only one wavelength.

There exist two optimal solutions, shown in Figures 4.1(b) and 4.1(c), respectively, that require a single wavelength for subproblem RWA-1 with traffic matrix  $T^1 = \begin{pmatrix} 0 & 1 & 0 \\ 0 & 0 & 1 \\ 0 & 0 & 0 \end{pmatrix}$ . If Step 1

of the SYM-RWA algorithm returns the first solution, then in Step 2 the symmetric solution to the RWA-2 subproblem will yield the overall optimal symmetric solution in Figure 4.1(a). However, if the solution in Figure 4.1(c) is returned by Step 1 of the algorithm, then Step 2 of the algorithm cannot construct a feasible symmetric solution (e.g., since the lightpath from node 2 to node 1 in the RWA-2 subproblem will share the link  $2 \rightarrow 1$  with the lightpath from node 2 to node 3 in Figure 4.1(c), and hence it cannot be assigned the same wavelength). In fact, given the solution to RWA-1 in Figure 4.1(c), a solution to RWA-2 that uses symmetric paths (but not wavelengths) necessarily requires one additional wavelength, such that the combined symmetric solution to the original problem is suboptimal.

To understand the reason underlying the negative result expressed by Lemma 4.1.1, observe that in the ILP formulation, subproblems RWA-1 and RWA-2 are coupled only through the distinct wavelength constraints (2.8). Once the decision variables  $\{c_{sd,k}^w\}$  corresponding to RWA-2 are removed from the formulation used to solve RWA-1, the coupling between the two subproblems is also removed. Let us return to the solution of RWA-1 shown in Figure 4.1(c) for the problem instance in the proof of Lemma 4.1.1. While this solution is optimal for the RWA-1 subproblem in isolation, it does not take into account the coupling between path  $2 \rightarrow 1 \rightarrow 3$  that only appears in this subproblem and path  $2 \rightarrow 1$  that only appears in subproblem RWA-2.

Fortunately, there is an easy way to account for this coupling by modifying slightly the distinct wavelength constraints (2.8) in the ILP formulation used to solve subproblem RWA-1. The key observation is that, although half of the paths (i.e., those that appear only in RWA-2) and the corresponding decision variables are no longer in the formulation used to solve RWA-1, due to symmetric routing, these removed paths are symmetric to the paths of RWA-1.

In Figure 4.1(c), for instance, path  $2 \rightarrow 1$  is not part of the formulation for RWA-1, but its symmetric path  $1 \rightarrow 2$  is.

Based on the above observation, we introduce a new set of binary parameters:

- $Z_{sd,k}^l \in \{0, 1\}$ : indicates whether link  $l$  is used by either path  $p_{sd,k}$  or its symmetric path  $p_{ds,k}$ .

Similar to the binary parameters  $X_{sd,k}^l$  used in (2.8), parameters  $Z_{sd,k}^l$  are fixed (constant) given the path set  $\mathcal{P}^1$  of RWA-1. We also introduce a new set of distinct wavelength constraints to replace the ones in (2.8) that are expressed in terms of the  $X_{sd,k}^l$  parameters. The new constraints, as they apply to subproblem RWA-1, are:

- bidirectional distinct wavelength constraints:

$$\sum_{s,d \in V: s < d} \sum_{k=1}^K c_{sd,k}^w Z_{sd,k}^l \leq 1, \quad \forall l \in A, \forall w \quad (4.4)$$

These bidirectional constraints restore the coupling between the two subproblems in the ILP formulation used to solve subproblem RWA-1. Returning to the problem instance of Lemma 4.1.1, note that these constraints would prevent the lightpaths  $1 \rightarrow 2$  and  $2 \rightarrow 1 \rightarrow 3$ , shown in Figure 4.1(c), from being assigned the same wavelength, as the latter lightpath uses link  $2 \rightarrow 1$  which is the symmetric of the link used by the former lightpath. Consequently, the solution shown in Figure 4.1(c) would require two wavelengths, making it suboptimal. Therefore, Step 1 of the SYM-RWA algorithm would return the optimal solution to RWA-1 shown in Figure 4.1(b), ensuring that the symmetric solution constructed in Step 2 is the optimal symmetric solution of Figure 4.1(a).

We now have the following result.

**Lemma 4.1.2** *Consider an RWA problem instance with symmetric routing and symmetric demands, and the subproblems RWA-1 and RWA-2 as defined above. If, in Step 1 of the SYM-RWA algorithm, subproblem RWA-1 is solved using the ILP formulation in (2.6)-(2.10) after replacing the distinct wavelength constraints (2.8) with the bidirectional constraints (4.4), then the solution obtained by the algorithm is an optimal symmetric solution for the original RWA problem.*

**Proof.** By definition, we have that  $Z_{sd,k}^l = X_{sd,k}^l + X_{ds,k}^l$ , for all  $s, d, k, l$ . Therefore, we can rewrite (4.4), for all  $l$  and  $w$ , as:

$$\sum_{s,d \in V: s < d} \sum_{k=1}^K c_{sd,k}^w X_{sd,k}^l + \sum_{s,d \in V: s < d} \sum_{k=1}^K c_{sd,k}^w X_{ds,k}^l \leq 1. \quad (4.5)$$

Since at most one of  $X_{sd,k}^l$  and  $X_{ds,k}^l$  may be equal to one, the above set of constraints is equivalent to the two sets:

$$\sum_{s,d \in V: s < d} \sum_{k=1}^K c_{sd,k}^w X_{sd,k}^l \leq 1, \quad \forall l \in A, \forall w \quad (4.6)$$

$$\sum_{s,d \in V: s < d} \sum_{k=1}^K c_{sd,k}^w X_{ds,k}^l \leq 1, \quad \forall l \in A, \forall w \quad (4.7)$$

The two sets of constraints (4.6) and (4.7) is equivalent to the set of constraints (2.8) after setting  $c_{sd,k}^w = c_{ds,k}^w$  for all  $s, d, k, w$ . Therefore, solving subproblem RWA-1 and then constructing a symmetric solution for RWA-2, as indicated in the statement of the lemma, results in an optimal symmetric solution for the original RWA problem.

Note that the proof does not depend on the form of the objective function, hence this decomposition technique is applicable to RWA variants with different objective functions.

#### 4.1.2 Arbitrary Traffic Demands

Now let us assume that traffic demands are arbitrary and not symmetric, i.e.,  $\exists s, d \in V : t_{sd} \neq t_{ds}$ . To accommodate such asymmetric demands, we generalize the decomposition approach such that each of the two subproblems, RWA-1 and RWA-2, includes only one-half of the source-destination pairs and paths of the original problem, as before, but one subproblem (say, RWA-1) contains more traffic demands than the other. The new decomposition is such that algorithm SYM-RWA can be applied directly, except that it is now necessary that the subproblem solved optimally in Step 1 of the algorithm be the one (RWA-1) with the larger traffic demands.

Let  $O^1$  and  $O^2$  be sets of ordered pairs of nodes such that:

$$(s, d) \in \begin{cases} O^1, & t_{sd} > t_{ds} \vee (t_{sd} = t_{ds} \wedge s < d) \\ O^2, & \text{otherwise.} \end{cases} \quad (4.8)$$

In other words, the traffic demand between an ordered pair  $(s, d) \in O^1$  is at least as large as the traffic demand between the corresponding pair  $(d, s) \in O^2$ . In the decomposition, the traffic matrices  $T^1 = [t_{sd}^1]$  and  $T^2 = [t_{sd}^2]$  of the two subproblems RWA-1 and RWA-2, respectively, are constructed as:

$$t_{sd}^1 = \begin{cases} t_{sd}, & (s, d) \in O^1 \\ 0, & \text{otherwise} \end{cases}; t_{sd}^2 = \begin{cases} t_{sd}, & (s, d) \in O^2 \\ 0, & \text{otherwise} \end{cases} \quad (4.9)$$

The corresponding path sets are:

$$\mathcal{P}^1 = \{p_{sd,k} \in \mathcal{P} | (s, d) \in O^1\}; \mathcal{P}^2 = \{p_{sd,k} \in \mathcal{P} | (s, d) \in O^2\} \quad (4.10)$$

Let  $t_{sd}^{min} = \min\{t_{sd}, t_{ds}\}$ , and  $t_{sd}^+ = t_{sd} - t_{sd}^{min}$ . We can rewrite the traffic demands of matrix  $T^1$  as:

$$t_{sd}^1 = \begin{cases} t_{sd}^{min} + t_{sd}^+, & (s, d) \in O^1 \\ 0, & \text{otherwise} \end{cases} \quad (4.11)$$

With this notation, traffic matrix  $T^1$  can be written as  $T^1 = T^{1,1} + T^{1,2}$ , where  $T^{1,1}$  is the transpose of  $T^2$  and  $T^{1,2}$  contains the additional traffic demands  $t_{sd}^+$  that are present in  $T^1$ .

We solve the original RWA problem using the same decomposition algorithm SYM-RWA we described in the previous subsection. The main difference is that the ILP formulation is further modified to account for the fact that subproblem RWA-1 has a “heavier” traffic matrix than subproblem RWA-2. Specifically, there are two types of demands in RWA-1, those that have a symmetric demand in RWA-2 and those that do not; the two types are accounted for differently in the modified formulation:

- for traffic demands in  $T^{1,1}$  for which a symmetric demand exists in  $T^2$ , use the parameter  $Z_{sd,k}^l$ , and
- for traffic demands in  $T^{1,2}$  for which a symmetric demand does not exist in  $T^2$ , use the parameter  $X_{sd,k}^l$ .

To express the new ILP formulation, we define the following two sets of variables that replace variables  $\{c_{sd,k}^w\}$ :

- $d_{sd,k}^w \in \{0, 1\}$ : binary variable that indicates whether there exists a lightpath assigned wavelength  $w$  on path  $p_{sd,k}$  to carry traffic in  $T^{1,1}$ .
- $e_{sd,k}^w \in \{0, 1\}$ : binary variable that indicates whether there exists a lightpath assigned wavelength  $w$  on path  $p_{sd,k}$  to carry traffic in  $T^{1,2}$ .

The following modified formulation is used to solve RWA-1 in Step 1 of the SYM-RWA algorithm:

$$\text{minimize: } W_{high} \quad (4.12)$$

subject to:

- traffic constraints:

$$\sum_{k=1}^K \sum_{w=1}^W d_{sd,k}^w = t_{sd}^{min}, \quad (s, d) \in O^1 \quad (4.13)$$

$$\sum_{k=1}^K \sum_{w=1}^W e_{sd,k}^w = t_{sd}^+, \quad (s, d) \in O^1 \quad (4.14)$$

- distinct wavelength constraints:

$$\sum_{(s,d) \in O^1} \sum_{k=1}^K (d_{sd,k}^w Z_{sd,k}^l + e_{sd,k}^w X_{sd,k}^l) \leq 1, \quad \forall l \in A, \forall w \quad (4.15)$$

- wavelength usage constraints:

$$\sum_{(s,d) \in O^1} \sum_{k=1}^K (d_{sd,k}^w + e_{sd,k}^w) \leq U^w P, \quad \forall w \quad (4.16)$$

- highest wavelength index constraints:

$$W_{high} \geq w U^w, \quad \forall w \quad (4.17)$$

- integrality constraints:

$$U^w = 0, 1, \quad \forall w; \quad d_{sd,k}^w = 0, 1, \quad e_{sd,k}^w = 0, 1, \quad \forall s, d, k, w \quad (4.18)$$

Finally, we have the following result.

**Lemma 4.1.3** *Consider an RWA problem instance with symmetric routing and arbitrary demands, and the subproblems RWA-1 and RWA-2 as defined above. If, in Step 1 of the SYM-RWA algorithm, subproblem RWA-1 is solved using the ILP formulation in (4.12)-(4.18), then the solution obtained by the algorithm is an optimal symmetric solution for the original RWA problem.*

**Proof.** The proof is similar to the proof of Lemma 4.1.2, and is omitted.

## 4.2 Further Improvements to the ILP Formulation

### 4.2.1 Incorporating Information from Heuristics

We may further improve the scalability of the new ILP formulation by incorporating information from fast, high-quality heuristic algorithms for the RWA problem. We adopt the LFAP algorithm [29], a fast and conceptually simple heuristic that we have found to perform consistently well across a range of topologies [59].

For each problem instance to solve, we first run the LFAP algorithm to obtain a feasible solution that uses  $W_{LFAP}$  distinct wavelengths. The algorithm takes less than one half of a second even for large networks of forty or more nodes, yet it provides an upper bound (=  $W_{LFAP}$ ) on the optimal solution, that can be used to (1) effect a further reduction in the size of the ILP formulation, and (2) speed up the optimization procedure. We discuss each of these aspects next.

## Reducing the Number of Variables in the Formulation

Referring to the general formulation for symmetric RWA solutions in (4.12)-(4.18), we observe that the number of variables  $d_{sd,k}^w$  and  $e_{sd,k}^w$  and the number of wavelength usage and highest index constraints is a function of the number of wavelengths  $W$ . In the absence of any upper bound on the number of wavelengths required for a particular problem instance, one might initialize  $W$  to a value (e.g., the number supported by DWDM technology) that may be much larger than necessary. Doing so would have a negative impact on the ILP solver due to: (1) an increase in the size of the formulation; for instance, for each additional input wavelength, the number of  $d_{sd,k}^w$  and  $e_{sd,k}^w$  variables increases as  $O(KN^2)$ , and (2) the symmetry problem, since the number of equivalent solutions obtained by wavelength permutations is proportional to  $W!$ .

As we explain in the next section, we have found that LFAP in many cases constructs solutions that use 25% more wavelengths than the optimal one. Therefore, given the output  $W_{LFAP}$  of the LFAP algorithm, we set the number of wavelengths in the formulation (4.12)-(4.18) to  $W = \lceil 0.8 \times W_{LFAP} \rceil$ . (If this value turns out to be too low, CPLEX, the optimization tool we use, typically determines quickly that the problem is infeasible, and can then be invoked again with a higher value.)

## Include Goal Cut in the Optimization Procedure

In the process of searching for an optimal solution, CPLEX manages a branch-and-cut search tree in which the root node represents the entire problem and every other node represents a subproblem to be solved [35]. It initializes the search procedure by processing the root node and continues until either it finishes processing all the nodes or it breaks some constraints.

In order to process a node, CPLEX first solves the continuous relaxation of the corresponding subproblem by removing the integrality constraints. If any predefined cuts is violated in the solution to the relaxed subproblem, CPLEX adds the cuts to the subproblem and re-solves it, iterating until no cuts are violated. The node will be removed from the search tree, if the relaxed subproblem is infeasible. After solving the relaxed subproblem, the solution is checked with the integrality constraints. If they are satisfied, CPLEX updates the current best solution if necessary. Otherwise, CPLEX splits the node problem into smaller subproblems and add them to the search tree to be processed.

CPLEX allows users to control the integer feasibility test and the creation of subproblems by specifying goal cuts in the branch-and-cut tree. A goal cut may force subproblems to become infeasible, such that the corresponding nodes are removed without examining the solutions in those subtrees. Therefore, we introduce a goal cut with the output of the heuristic, such that any nodes that would lead to solutions with objective value higher than  $W = \lceil 0.8 \times W_{LFAP} \rceil$  are removed, speeding up the optimization procedure.

## 4.2.2 Path Selection Algorithm

Observe that an optimal solution obtained by a path-based ILP formulation is optimal only among the set of solutions that are feasible with the path set  $\mathcal{P} = \{p_{sd,k}\}$  provided as input to the problem. Therefore, the  $K$  candidate paths for each source-destination pair must be selected carefully to ensure that the optimal solution is close to the overall optimal that would be obtained through a link-based formulation (note, however, that the latter is a type of multicommodity flow formulation that does not scale to networks with more than a small number of nodes and wavelengths).

The  $K$  paths for each source-destination pair may be obtained as the  $K$  shortest paths [11], the  $K$  disjoint shortest paths [10], or using some other criteria [13]. In this work, we adopt the increasing-cost  $K$ -shortest path algorithm that was proposed in [6], and that we have found to work well in practice. Specifically, the algorithm initializes the cost of all links in the network to the same value. For each node pair, every time a shortest path is found, the cost of each link along this path is increased by a fixed factor  $f \geq 1$ , such that the new cost is equal to the old cost times  $f$ . As a result, new paths are likely to select different links, which in turn leads to fewer collisions with respect to wavelength assignment. Therefore the path candidates constructed by the algorithm are closer to the overall path solution space. However, the algorithm cannot altogether avoid sharing some good links among the  $K$  paths between one node pair, due to the fact that it is based on finding shortest paths. Note also that, by varying the cost increase factor  $f$ , this algorithm may produce paths that lie anywhere in the spectrum between the  $K$  shortest paths and the  $K$  disjoint shortest paths. For the experiments that we present in the following section, we have used  $f = 2$ , a value that was found in [6] to produce the best results.

## 4.3 Experimental Study

In this section, we present the results of an experimental study we conducted to investigate the performance of the optimal symmetric RWA formulation in terms of scalability (running time) and quality of solution. All results were obtained by running the IBM Ilog CPLEX 11 optimization tool on a cluster of identical compute nodes with dual Woodcrest Xeon CPU at 2.33GHz with 1333MHz memory bus, 4GB of memory and 4MB L2 cache.

Our study involves a large set of problem instances defined on several network topologies with random traffic matrices. In particular, we consider the following topologies: (1) the 14-node, 42-(directed) link NSFNet [31]; (2) the 17-node, 52-link German network [12]; (3) the 20-node, 78-link EON network [22]; and (4) a 32-node, 106-link USA topology [59]. These networks have irregular topologies of increasing size that are representative of existing backbone networks, and have been used extensively in optical networking research. For each topology, we



generate  $K = 2, 3$ , or 4 symmetric paths between each source-destination pair in the manner we discussed in Section 4.2.2.

For each network topology, we consider several problem instances. For each problem instance, the traffic demand matrix  $T = [t_{sd}]$  is generated by drawing the (integer) traffic demands (in units of lightpaths) uniformly at random in the interval  $[0, T_{max}]$ . We generate both symmetric (i.e.,  $t_{sd} = t_{ds}$  for all  $s, d$ ) and asymmetric traffic matrices. Each data point in the figures we present in this section represents the average of 10 random problem instances for the given topology and value of parameters  $K$  and  $T_{max}$ .

### 4.3.1 Scalability Comparison

Let us first investigate the scalability of the the new formulation. Figure 4.2 compares the original formulation (2.6)-(2.10) for the RWA problem to the new formulation (4.12)-(4.18) in terms of running time, for the four networks. Recall that the original formulation obtains the overall optimal solution given the input path set, whereas the new formulation obtains the optimal symmetric solution for the same path set. The figure plots, in logarithmic scale, the CPU time it takes for CPLEX to find an optimal solution under symmetric and asymmetric traffic. We imposed a limit of 20 CPU hours for CPLEX to find a solution; if it failed to do so within the 20-hour limit, we terminated the execution run and plotted the data point in the light gray area of the figure labeled “tLim.” For the results shown in Figure 4.2, there are  $K = 2$  paths between each source-destination pair and the traffic matrix (symmetric or asymmetric) was generated by setting  $T_{max} = 2$ .

As we can see, the original path ILP formulation can find the optimal solution within the 20-hour limit for the NSF, German, and EON topologies, but not for the 32-node USA topology. Also, the running time for a given topology is the same regardless of whether traffic is symmetric or asymmetric, as the number of variables in the formulation depends on the size of the network and the traffic load (which depends on  $T_{max}$ ), not on the form of the traffic matrix. The new formulation, on the other hand, performs much better than the original one. For symmetric traffic, we observe a reduction of more than two orders of magnitude in running time compared to the original formulation, and the 32-node topology can be solved in only about 3 hours. For asymmetric traffic, the new formulation achieves a reduction in running time of more than one order of magnitude (up to a factor of 25), solving the 32-node network in about 16 hours. The main reason for the higher running time in the case of asymmetric traffic is due to the additional variables that need to be included in the formulation, as we explained in Section 4.1.2. Importantly, symmetric instances on the NSF, Germany, and EON topologies may be solved in about one minute, while asymmetric instances on the same topologies take about ten minutes to solve; the large increase in running time for the USA topology is due

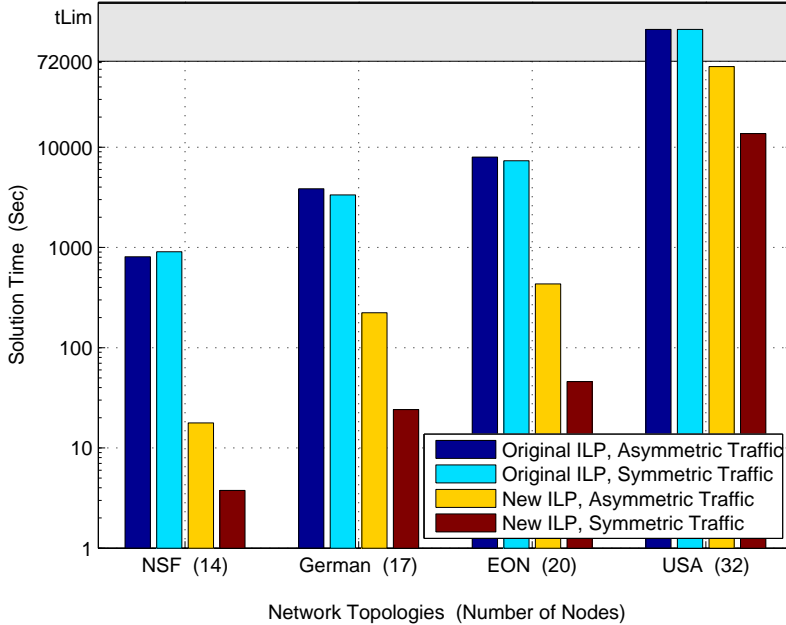


Figure 4.2: CPU time comparison,  $K = 2$ ,  $T_{max} = 2$

not only to the size of the network, but also to the much larger number of wavelengths needed to accommodate the demands. As a result, the new formulation makes it possible to solve network sizes of practical size fast enough to allow network designers and operators to perform extensive “what-if” analysis so as to investigate large numbers of scenarios regarding forecast demands. We have obtained similar results for several other topologies, including regular (torus) topologies; these are omitted due to space constraints.

Figure 4.3 plots the running time of the new formulation for the NSF and EON networks as a function of the value of parameter  $T_{max}$ . We observe that the running time increases with the traffic load, as expected, due to the larger number of wavelengths needed to accommodate the traffic. Note that a value of  $T_{max} = 8$ , the highest one considered in this experiment, corresponds to an average of four lightpaths between a source-destination pair (in each direction); for the NSF and EON networks, the optimal solution for this value would require more than 50 and 70 wavelengths, respectively (refer also to Figure 4.5 for NSFNet). Although such instances are well beyond what can be realized in deployed networks, the new formulation is capable of solving them efficiently.

Finally, Figure 4.4 plots the running time of the new formulation as a function of the number  $K$  of candidate paths, for the NSF and EON networks and  $T_{max} = 2$ . Again, the running time increases with  $K$  due to the larger number of variables in the formulation. Nevertheless, the

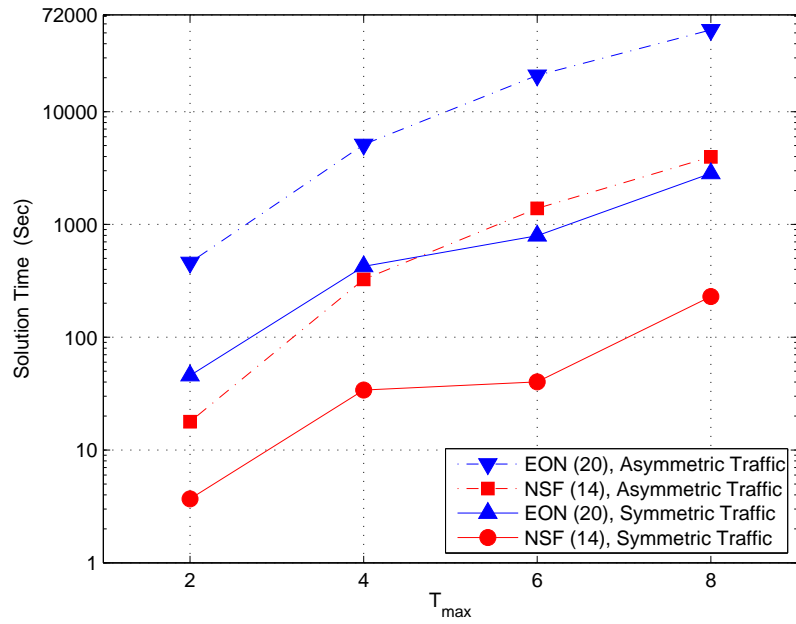


Figure 4.3: CPU time against  $T_{max}$ ,  $K = 2$ , NSF and EON networks

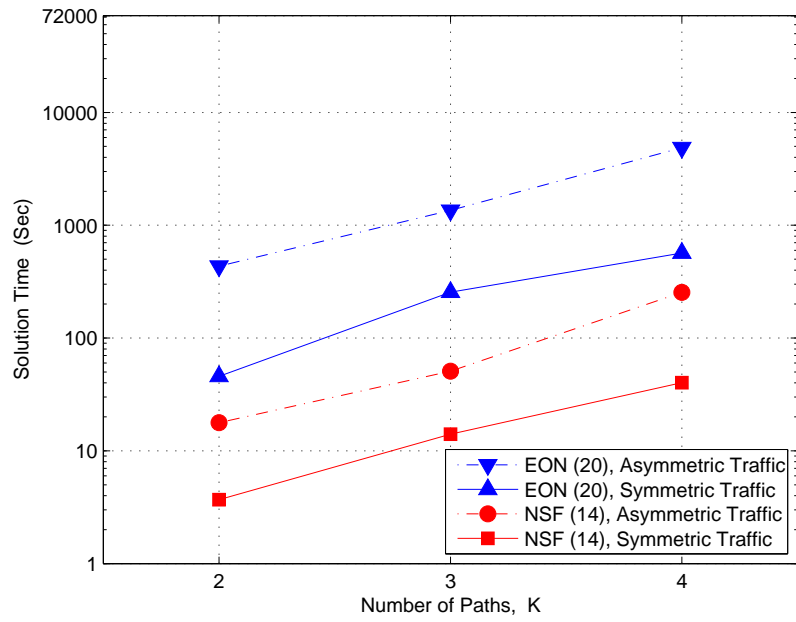


Figure 4.4: CPU time against  $K$ ,  $T_{max} = 2$ , NSF and EON networks

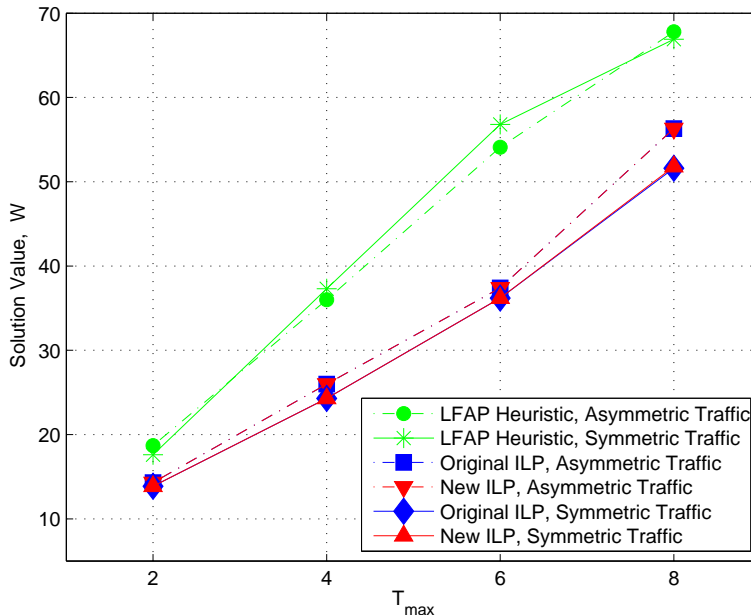


Figure 4.5: Optimality comparison for NSFNet,  $T_{max} = 2$ ,  $K = 2$

new formulation makes it possible to solve realistic instances in a short amount of time. We also note that, of the 80 instances (i.e., ten instances per data point) we run with  $K > 2$ , only one instance resulted in an optimal value better (by a single wavelength) than the one obtained with  $K = 2$ .

### 4.3.2 Quality of Optimal Symmetric Solution

Let us now turn our attention to the quality of the optimal symmetric solution. Figure 4.5 plots the value of the solution returned by the original formulation, the new formulation, and the LFAP heuristic [29] for NSFNet, as a function of  $T_{max}$ . Recall that LFAP and the original formulation consider the whole solution space, while the new formulation only considers symmetric solutions to the RWA problem as defined in (4.1). The new formulation obtained the *same* optimal solution as the original formulation for 79 of 80 instances from which the results in the figure are generated. There was only one instance ( $T_{max} = 8$ , symmetric traffic) for which the optimal symmetric solution required two additional wavelengths (52 versus 50 for the overall optimal). We obtained similar results for the EON network (not shown), in which the new formulation resulted in the same optimal solution as the original one over all 80 instances. These findings confirm the intuitive view that, except in rare cases when the demand matrix creates severe bottlenecks, optimal symmetric solutions are also optimal overall.

We also observe that LFAP, one of the best heuristic algorithms for the RWA problem, constructs solutions that are between 25-60% higher than the optimal one in the NSF network. Hence, while LFAP is quite fast, relying on such a heuristic algorithm may result in significantly higher costs in deploying and operating the optical network. Our new formulation, on the other hand, achieves an excellent tradeoff between running time and optimality.

## 4.4 Concluding Remarks

We have presented a new ILP formulation to construct optimal symmetric solutions to the RWA problem, that scales well to network topologies encountered in practice and enables network designers and operators to carry out extensive what- if analysis. We also demonstrated that optimal symmetric solutions, in addition to their practical advantages, often achieve the overall optimal or a value very close to it.

## Chapter 5

# New, Fast Link-based ILP Formulation with Wise Link Selection

In previous chapters, we improved MIS-based formulation and path-based formulation respectively, which perform reasonably well in practical instances in the RWA problem. However, both of the two approaches need to pre-calculate a set of path candidates manually as the input of ILP formulation, which limits the optimality of the solutions. Additionally, for MIS-based formulation, due to the enormous number of MISs generated in mesh network topologies, its scalability is limited to a very small size, which makes it hardly applicable to practical networks.

As discussed in Chapter 2, link-based formulation provides the overall optimality due to the fact that it considers links as entities of interests. However, the scalability of link-based formulation is also limited due to the great number of links considered in the routes of all source-destination node pairs. In this chapter, we improve the formulation with a wisely-selected set of links to consider for each particular node pairs. This new approach reduces the problem size by pruning the redundant link decision variables, while still practically maintaining solution optimality. The formulation scales to mesh topologies representative of backbone and regional networks. Simulation results show that this approach could speed up the running time by orders of magnitude while providing better-quality solutions than path-based formulation and MIS-based formulation. What is more important is, this approach is applicable not only to the link-based formulation for RWA problem, but also to ILP formulations for any problems that use multicommodity flow equations.

In Section 5.1 we review the complexity of link-based formulation and introduce two link selection algorithms to reduce the problem size. In Section 5.2 we analyze how the new approach decreases running time and maintains solution quality. In Section 5.3 we conduct an

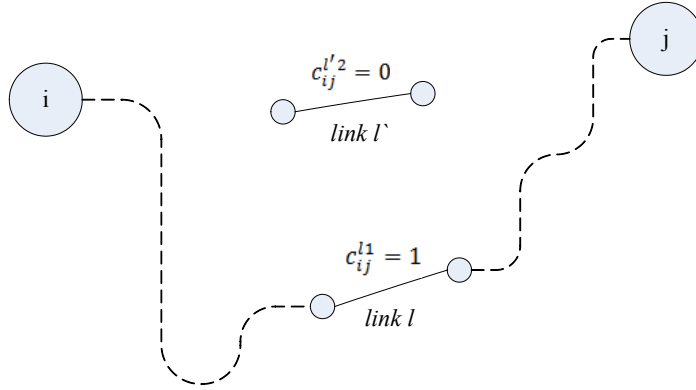


Figure 5.1: Illustration on  $c_{ij}^{lw}$  variable

experimental study on the new formulation to show the effectiveness of the approach.

## 5.1 Speed up Link-based Formulation with Link Selection Algorithms

In this section, we review the complexity of link-based ILP formulation to RWA problem, and look into how to reduce the number of variables in the formulation.

### 5.1.1 Complexity of Link-based Formulation

Let us first recall the detail of link-based formulation.

The link formulation is based on expressing the RWA problem as a multicommodity flow problem[46]. Let us define the following sets of decision variables:

- $c_{ij}^{lw} \in \{0, 1\}$ : binary variable that indicates whether there exists a lightpath from node  $i$  to node  $j$  that uses wavelength  $w$  on link  $l$  (see Figure 5.1)
- $u^w \in \{0, 1\}$ : binary variable that indicates whether wavelength  $w$  is used anywhere in the network
- $\omega_{total}$ : number of wavelengths used in the whole network

With these notations, the link ILP formulation can be expressed as:

*Minimize* :  $\omega_{total}$

*Subject to:*

$$\sum_{\substack{\text{links } l \\ \text{outgoing from } n}} c_{ij}^{lw} - \sum_{\substack{\text{links } l \\ \text{incoming to } n}} c_{ij}^{lw} = \begin{cases} 0, & n \neq i, j; \\ t_{ij}, & n = i; \\ -t_{ij}, & n = j. \end{cases} \quad \forall n, i, j \in V, \forall w \quad (5.1)$$

$$\sum_{i,j} c_{ij}^{lw} \leq 1, \quad \forall l \in E, \forall w \quad (5.2)$$

$$\sum_{i,j} \sum_l c_{ij}^{lw} \leq u^w N(N-1)|E|, \quad \forall w \quad (5.3)$$

$$W_{total} \geq wu^w, \quad \forall w \quad (5.4)$$

$$u^w = 0, 1, \quad \forall w; \quad c_{ij}^{lw} = 0, 1, \quad \forall i, j, l, w \quad (5.5)$$

Expressions (5.1) are the multicommodity flow equations at node  $n$ . Specifically, if  $n$  is an intermediate node in the path from some source  $i$  to some destination  $j$ , the traffic coming in should be equal to the traffic going out, as such traffic is not dropped out, or originates from, this node, hence the left hand side of (5.1) is equal to zero. If  $n$  is the source node  $i$ , the first sum of the left hand side is equal to the traffic  $t_{ij}$  to node  $j$  and the second sum is zero. Similarly, if  $n$  is the destination node  $j$ , the second sum of the left hand side is equal to  $t_{ij}$  and the first sum is zero. This set of constraints ensures that all traffic demands are satisfied. Moreover, they also take care of the wavelength continuity constraints, because for any intermediate node  $n$  (neither source nor destination), the right hand side of the equation will be 0, ensures that if one wavelength comes in, the same wavelength will go out. Expressions (5.2) represent the distinct wavelength constraint of the RWA problem, such that no two connections share the same wavelength on one link. Expressions (5.3) make sure that  $u^w$  is set to 1 if wavelength  $w$  is used on any link by any connection. Expressions (5.4) count the number of used wavelengths by making  $W_{total}$  equal to the index of the highest wavelength used. Expressions (5.5) are the integrality constraints for the decision variables.

Let us now turn our attention to the scalability of the link ILP formulation, which is a function of the formulation size. This size, in turn, is determined by the number of decision variables and constraints. The number of the  $c_{ij}^{lw}$  variables is equal to  $N(N-1)|E|W$  for general topology networks. There are also  $W$  variables  $u^w$ , and the decision variable  $\omega_{total}$ . Hence, the



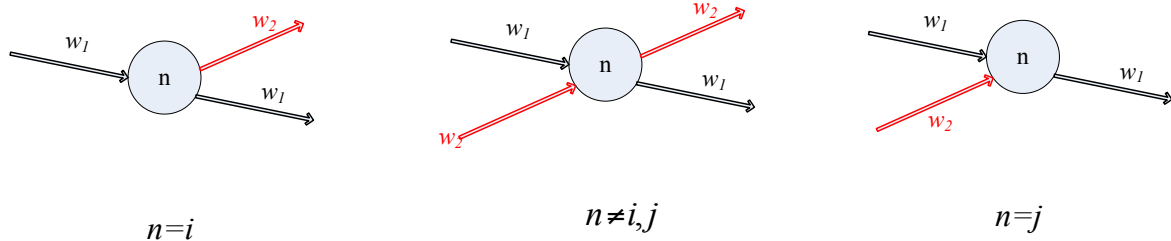


Figure 5.2: Multicommodity flow equation at node  $n$

total number of variables in the link formulation for general network topologies is  $O(N^2|E|W)$ .

In terms of the number of constraints (ignoring the integrality constraints (5.5)), expressions (5.1) correspond to  $N^3W$  constraints, expressions (5.2) yield  $|E|W$  constraints, expressions (5.3) consists of  $W$  constraints, as does expression (5.4). Overall, the formulation consists  $O(N^3W)$  constraints.

### 5.1.2 Link Selection Algorithms - Remove Redundant Variables

After reviewing the complexity of link-based formulation, it is obvious that the problem size of link-based formulation seriously limits the scalability of the approach. Now we discuss how to reduce the problem size while maintaining the good solution quality.

Looking into the constraint (5.1), we found that each single link in the network is considered as a candidate to carry traffic demands between each node pair, which ends up a great amount of  $c_{ij}^{lw}$  variables. However, this does not make practical sense in real situations. Particularly, to carry traffic demands between a certain node pair in the middle of the network while saving network resources, the network operator will not choose a route that goes over the edge of the network. Instead, we want to select only necessary links as candidates to compose routes between each specific source-destination node pair, and if we do so, we will gain great benefits in running time while still practically maintaining optimality.

We then propose the following two approaches to select links wisely.

#### Select links close to the source and destination nodes

The idea for this selection algorithm is to select those links close to the source *and* destination, which could most possibly contribute as parts of the routes between the two nodes.

After calculating the shortest path between each node pairs, we define the distance between any two nodes as the number of hops over the shortest path between these two nodes. We denote the distance between node  $i$  and  $j$  as  $dist(i, j)$ . Then the candidate links for each source-destination pair are selected according to the distance of the two end-points of the link.

Specifically, a link  $l$  with two end-points  $i$  and  $j$  is considered for traffic demand between node  $s$  and  $d$ , if and only if the following requirement fulfills:

$$dist(s, i) + dist(j, d) + 1 \leq dist(s, d) + thres \quad (5.6)$$

where  $thres$  is a parameter at our choice. A good  $thres$  value can limit the number of links to be considered, so that we could get a good balance between the running time and optimality. The choice of  $thres$  will be discussed in the following section. We call this link selection algorithm as  $k$ - $thres$  algorithm.

### Select links on the route of $k$ -shortest paths

One concern to the above link selection algorithm is that simply selecting links close to the source and destination nodes may not always yield to the best solution in practical. The importance of the links may depend on the relative positions as well. Hence we introduce the following selection algorithm with the help of  $k$ -shortest path algorithm.

The main idea of this algorithm is to calculate the  $k$ -shortest path between each source-destination node pairs, and select those links on the routes of the  $k$ -shortest paths of a node pair to consider as the link set of that node pair. We call this link selection algorithm as  $k$ - $path$  algorithm. There are basically two advantages on this algorithm.

- The links selected are closer to the best set for practical results. The position of the link, as well as the distance of the link from the source and destination, is important to take into account when considering a good link candidate. Using only the distance threshold as a selection factor, the link set may contain some redundant candidates while losing some necessary ones. On the other hand, for those links on the routes of  $k$ -shortest path of a node pair, they are the links that are most likely to carry traffic between the specific node pair.
- The number of total links needed to be considered is smaller than  $k$ - $thres$  algorithm. To get a better solution,  $k$ - $thres$  algorithm needs to pick a larger threshold number, and  $k$ - $path$  algorithm needs to adopt a larger  $k$ . With the increasing of threshold, the threshold algorithm will end up with a proportionally increasing number of total links needed to be considered in a general topology. However, the  $k$ -shortest paths may reuse a lot of links among themselves, therefore the larger  $k$  won't dramatically increase the number of total links considered.

The performance of these two approaches will be analyzed with experimental study later on.

Using either of the two link selection algorithms defined above, we could successfully decrease the problem size in the following aspects:

- **Decrease the number of variables.** The dominant set of variables are  $c_{ij}^{lw}$ , and there are  $O(N^2|E|W)$  of them. In other words, the complexity of the formulation depends on the number of  $c_{ij}^{lw}$  variables. When every link is considered for each node pairs, there are *# of links*  $\times$  *# of node pairs* possibilities. By taking only the necessary links into consideration, we cut down the number of links greatly and therefore the number of  $c_{ij}^{lw}$  variables.
- **Decrease the number of constraints.** The link selection will decrease the number of constraint (5.1) - (5.3). For constraint (5.1), the original formulation has to consider every single node  $n$  in the network, with a flow equation. While in the new approach, we just need to take into consideration the nodes that exist as end points in the selected link set only.

In the following section, we will have a further discussion on how this new approach will decrease the time and maintain optimality practically.

## 5.2 Speed and Quality Analysis of New Link-based Formulation

In this section, we will analyze how the running time and solution quality change in link-based formulation with link selection algorithm, and study the trade-off between these two.

### 5.2.1 Number of variables of New Link-based Formulation vs. Parameter $k$

As we discussed before, the problem size depends on the number of variables and number of constraints in multicommodity flow equation, especially on the number of  $c_{ij}^{lw}$  variables. We will analyze and illustrate how the number of  $c_{ij}^{lw}$  variables changes with the parameter  $k$  in the two link selection algorithms.

First of all, the number of  $c_{ij}^{wl}$  variables is determined by the total number of link candidates for all source-destination node pairs. In  $k$ -thres algorithm, when  $k = 0$  the total number of link candidates are the sum of number of links on the shortest path between every node pair. When  $k$  grows, the number of links increases as the algorithm select more links that are close to the shortest paths. The increasing speed varies on different topologies, but proportional to the degree of the networks. Gradually, the increasing will slow down when  $k$  is set to a certain value as almost all links are within  $k$ -distance away from the shortest path. Consequently, as a general rule, the number of variables will increase rapidly as  $k$  grows, but begins to slow down the increasing speed as  $k$  grows too large.

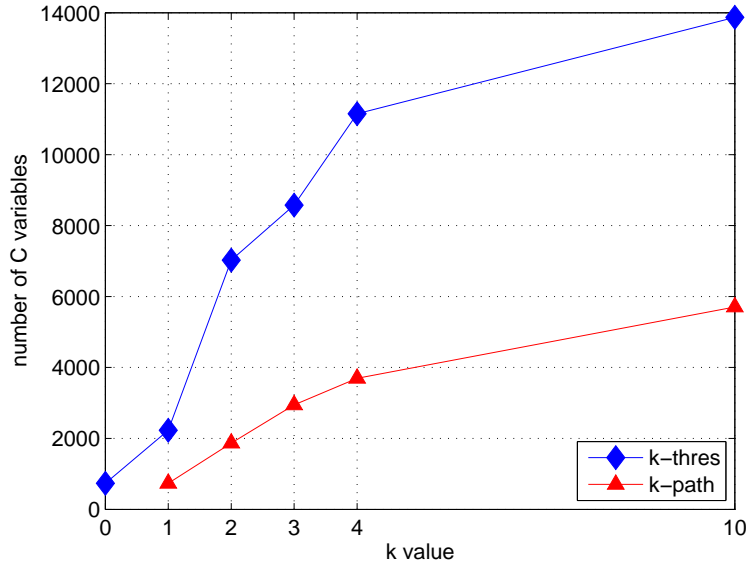


Figure 5.3: Number of  $c_{ij}^{wl}$  variables in German network using two link selection algorithms

On the other hand, the change in the number of variables in the  $k$ -path algorithm will follow the similar pattern but with a few differences. First, the  $k$  value starts from 1, instead of 0, and the link candidate set generated by  $k$ -path algorithm when  $k = 1$  is equivalent to that in  $k$ -thres algorithm when  $k = 0$ , which includes only links on the routes of the shortest path between each source-destination node pair. Second, although the number of variables will also increase as  $k$  grows, the increasing speed is slower than that in  $k$ -thres algorithm. The reason is due to the fact that the  $k$  shortest paths will reuse a good amount of links and therefore the number of links in the candidate set is generally smaller than those in  $k$ -thres algorithm.

Now let us use the 17-node, 52-link German network as an illustration, to show how the number of variables changes in both link selection algorithms. Figure 5.3 plots the curves of number of  $c_{ij}^{wl}$  variables vs.  $k$  in  $k$ -thres and  $k$ -path algorithms, respectively. As we analyzed, in the figure we could see that the number of variables are the same in  $k$ -path algorithm when  $k = 1$  and  $k$ -thres algorithm when  $k = 0$ . Moreover, number of variables in both link selection algorithms increases as  $k$  grows, but that in  $k$ -thres algorithm have a faster increasing speed.

### 5.2.2 Trade-off between Solution Quality and Running Time

As we just discussed, the number of  $c_{ij}^{wl}$  variables will decrease as  $k$  increases, therefore running time of the formulation will increase accordingly as the problem size grows and the solution value will decrease as we include more choices in the routing assignment. As a result, there is a

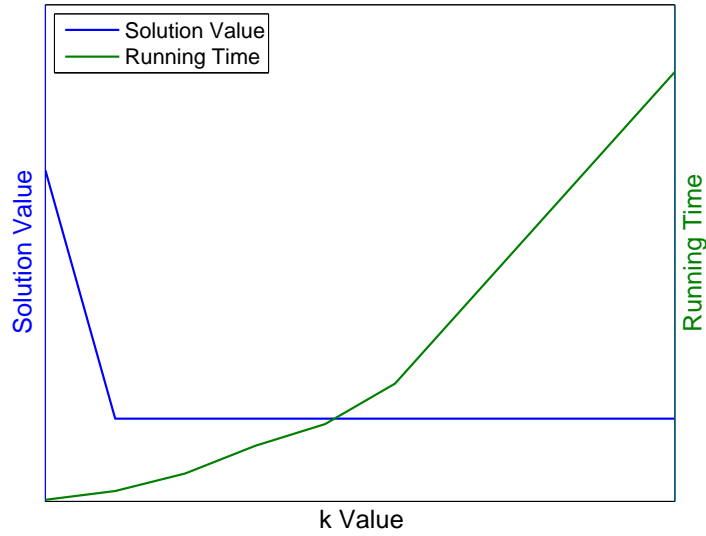


Figure 5.4: Trade-off between speed and solution quality

trade-off between solution quality and running time when selecting parameter  $k$ . Fortunately, the solution value will stop decreasing after a certain  $k$  value, as including more links to consider will not help with the solution any more, in other words, all the necessary links for each node pairs are selected already with this  $k$  value.

To illustrate this, Figure 5.4 plots the trend of changes of the running time and solution value against  $k$ . As shown in the figure, when  $k$  grows the running time curve will go up. On the other hand, when  $k$  grows, the solution value curve will go down and then stay flat. Because the solution decreases when more information included, until one point it reaches the optimal value and then will no longer be able to decrease.

Consequently, in order to get a practically optimal result as well as a reasonably fast running time, we need to look carefully into the  $k$  value and find out the point that solution curve starts to flatten. We will address this issue in the experimental study in the following section.

### 5.2.3 Solution Quality Advantage over Path Formulation

Having discussed the solution quality of the new link formulation with link selection algorithm, one may have a direct question that whether link formulation with  $k$ -path algorithm performs better than path-based formulation with  $k$ -shortest path pre-calculated, in terms of solution quality. In fact, the answer is YES.

Admittedly, both formulations adopt  $k$ -shortest path algorithm in some way. Especially,

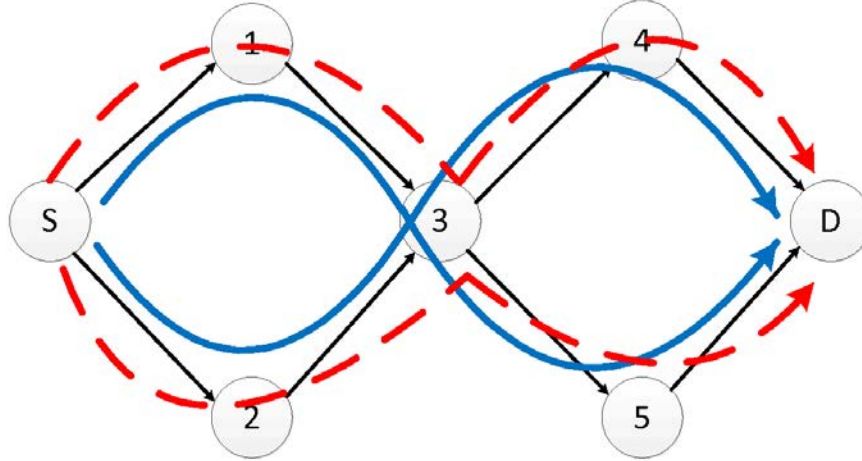


Figure 5.5: An illustration on the advantage of  $k$ -path link selection algorithm

the link formulation with  $k$ -path algorithm only selects links on the routes of the  $k$ -shortest paths between each source-destination node pairs. However, the fact that it considers links as entities of interest makes the link formulation contain much more information when selecting routes in RWA problem. Let us use a very simple example to illustrate this statement.

Figure 5.5 draws part of the network that includes a source node  $s$ , a destination node  $d$  and the related links. When using path-based formulation with  $k$ -shortest path pre-calculated ( $k = 2$ ), two shortest paths are generated, as the two blue routes marked in the figure. When the formulation looks for solution, it takes the two routes and only the two routes for possible candidate routes between node pair  $s$ - $d$  to carry traffic demands. However, the link formulation with  $k$ -path algorithm does not limit the route candidates artificially, but selects all the links on the two routes, and makes any possible combination of the links according to constraints in the formulation, to carry traffic. Specifically, in this example, not only the two blue routes, but also the two red dotted routes could be possible combination of the selected links. In other words, the link formulation with  $k$ -path algorithm has much more information when doing the routing assignment and therefore provide better solution quality over path-based formulation with  $k$ -shortest paths. Experimental study in the following section will also support this conclusion.

### 5.3 Experimental Study

In this section, we present the results of an experimental study we conducted to investigate the performance of the new link-based formulation with wise link selection approach in terms of scalability and quality of solution. All results (obtained using both link-based and path-based formulations) were obtained by running the IBM Ilog CPLEX 12 optimization tool on a cluster

of identical compute nodes with dual Woodcrest Xeon CPU at 2.33GHz with 1333MHz memory bus, 4GB of memory and 4MB L2 cache.

To best illustrate the practical network environment, our study involves a large set of problem instances defined on several network topologies with random traffic matrices. In particular, we consider the following topologies: (1) the 11-node, 52-(directed) link Cost-239 network; (2) the 14-node, 42-(directed) link NSFNet [31]; (3) the 17-node, 52-link German network [12]; and (4) the 20-node, 78-link EON network [22].

These networks have irregular topologies of increasing size that are representative of existing backbone networks, and have been used extensively in optical networking research. For each topology, we generate the traffic demand matrix  $T = [t_{sd}]$  by drawing the (integer) traffic demands (in units of lightpaths) uniformly at random in the interval  $[0, T_{max}]$ .

### 5.3.1 $k$ -Thres vs. $k$ -Path

Let us first compare the two path selection algorithms. Figure 5.6 and 5.7 present the solution value and running time against threshold  $k$ , using  $k$ -thres and  $k$ -path algorithm respectively. The figures plot the curves in German network, with  $t_{max}$  set to 2. The left y axis labels the solution value,  $W$ , while the right y axis labels the running time in CPU seconds. The x axis labels parameter  $k$ , either the threshold in  $k$ -thres algorithm, or the number of shortest path in  $k$ -path algorithm. Note that  $k$  starts from 0 in  $k$ -thres algorithm, while  $k$  starts from 1 in  $k$ -path algorithm. Also note that  $k = 0$  in  $k$ -thres is equivalent to  $k = 1$  in  $k$ -path algorithm, which both mean that we only consider links on *the* shortest path.

From the figures, using both link selection algorithms, we could see the solution value (minimum number of wavelengths needed) dropped rapidly as  $k$  grows to 2 and then remains the same afterwards. Another observation is that with  $k$ -thres algorithm, the running time grows rapidly with the increasing of  $k$ , but with  $k$ -path algorithm, the running time grows much slower with the increasing of  $k$ . Specifically, at  $k = 2$ , the running time of new link formulation with  $k$ -thres algorithm is around 300s, while that of link formulation with  $k$ -path algorithm is around 8000s. When  $k$  grows up to 10, the running time with  $k$ -thres raises high up to 64000s, while that with  $k$ -path still below 2400s. This difference matches our analysis of the two link selection algorithm in Section 5.2.

Now let us look at Figure 5.8 and 5.9, which plots the results of similar simulations but with  $t_{max}$  set to 6. From the figures, the running time of link formulation with  $k$ -thres algorithm quickly reaches out the simulation limit we set (36 hours) after  $k = 2$ , and could not provide any solution when  $k > 2$ . To the contrary, link formulation with  $k$ -path algorithm only takes around 3600 seconds to give solution when  $k = 2$ , and even when  $k = 10$  the running time is still below the time limit. These two figures further demonstrate the advantage of  $k$ -path link

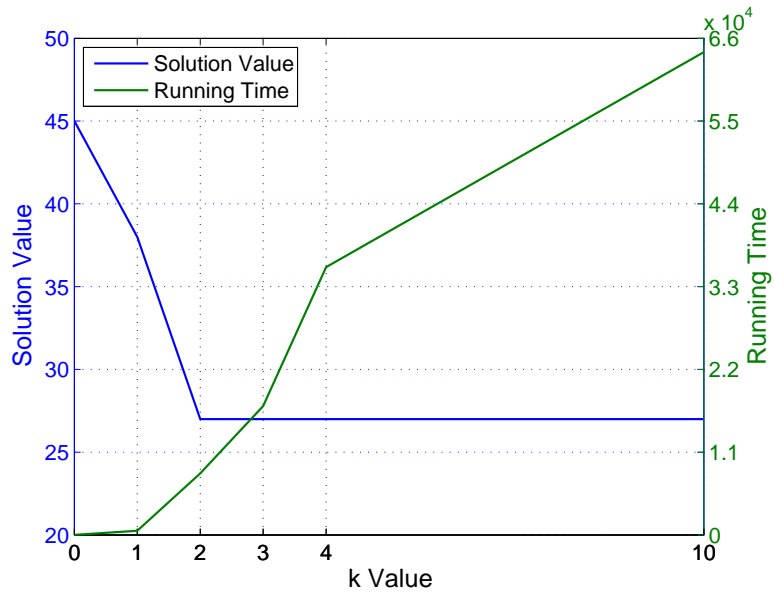


Figure 5.6:  $k$ -thres algorithm: Running time and solution value vs.  $k$  in German Network,  $t_{max} = 2$

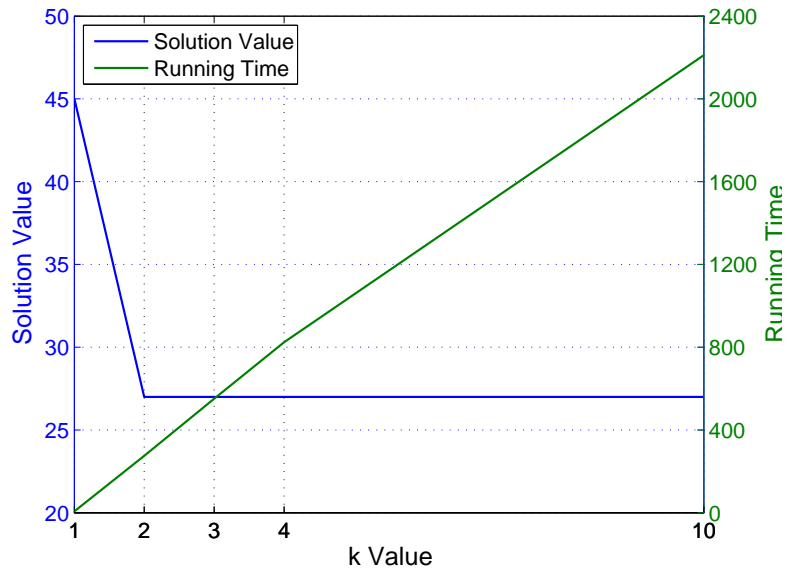


Figure 5.7:  $k$ -path algorithm: Running time and solution value vs.  $k$  in German Network,  $t_{max} = 2$



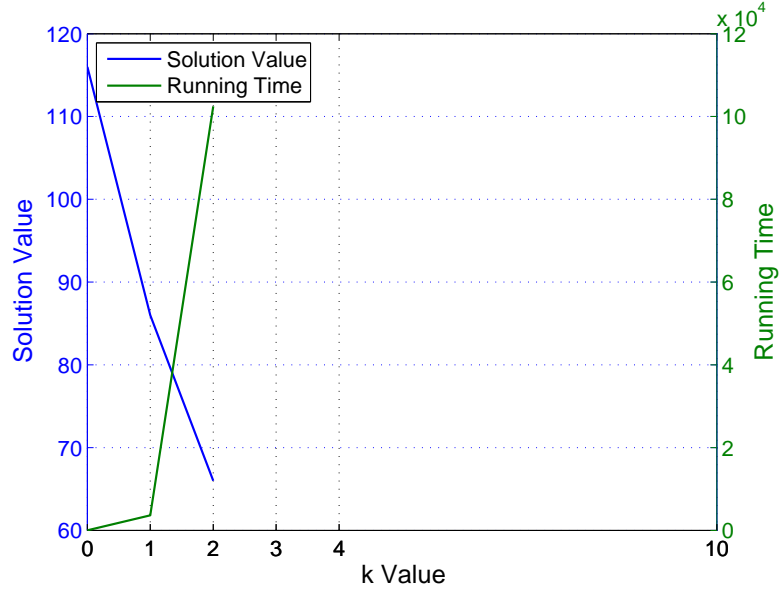


Figure 5.8:  $k$ -thres algorithm: Running time and solution value vs.  $k$  in German Network,  $t_{max} = 6$

selection algorithm over  $k$ -thres algorithm. The running time difference of these two algorithms matches with the analysis of number of  $c_{ij}^{wl}$  variables in Section 5.2.

Note the fact that in all figures above, setting  $k = 2$  in both link selection algorithms is able to provide same solution as original link-based formulation. This is generally true for all network topologies we have investigated in this chapter. For example, Figure 5.10 and 5.3.1 plot the simulation results in 14-node NSF network using  $k$ -path algorithm, with  $t_{max}$  set to 2 and 6 respectively. In both figures,  $k = 2$  is the point where the link selection algorithm begins to provide the solution same to the optimal solution given by original link-based formulation. Additionally, the running time at  $k = 2$  is very low, which are 11s for  $t_{max} = 2$  and 500s for  $t_{max} = 6$ . In other words,  $k = 2$  is the good choice in the trade off between solution quality and running speed. Hence, for the following simulation, we will use new link-based formulation with link selection algorithms where  $k = 2$ , to study the effectiveness of the new formulation.

### 5.3.2 Running Time Comparison

Now let us investigate the speed performance of new link-based formulation with link selection algorithms. Figure 5.12 presents the running time of the two versions of new link formulation, compared with the original link and path formulation (MIS-based formulation could not solve mesh networks due to the huge number of MISs they have, so we do not even take it into

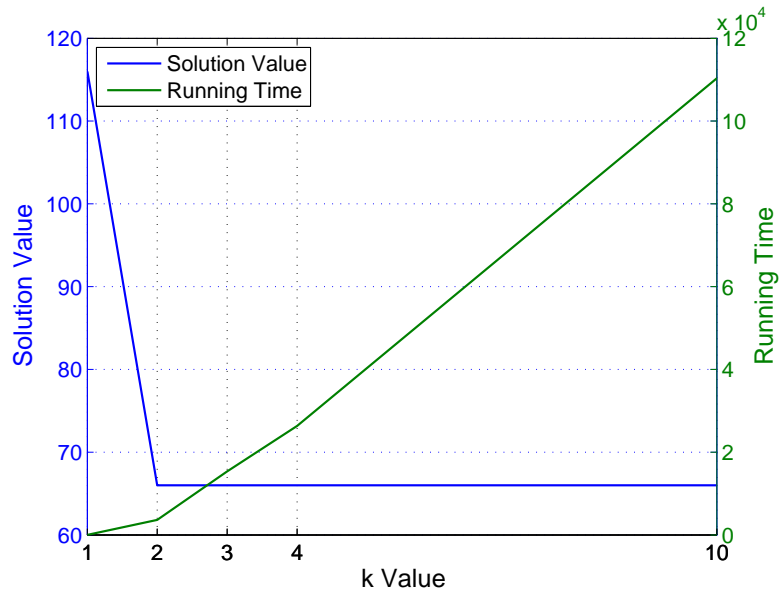


Figure 5.9:  $k$ -path algorithm: Running time and solution value vs.  $k$  in German Network,  $t_{max} = 6$

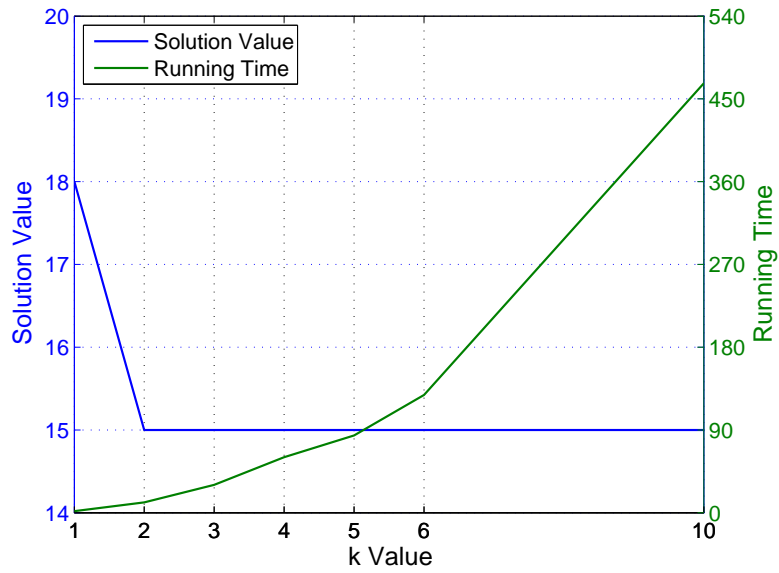


Figure 5.10:  $k$ -Path algorithm: Running time and solution value vs.  $k$  in NSF Network,  $t_{max} = 2$

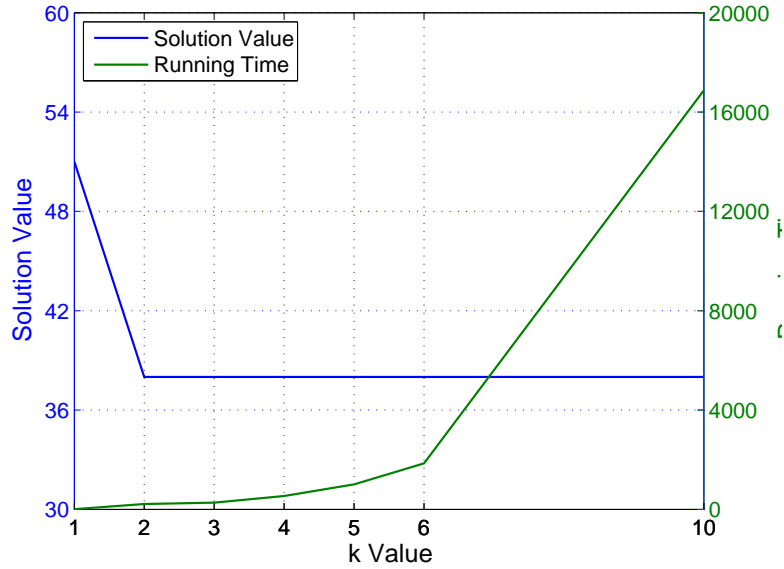


Figure 5.11:  $k$ -Path algorithm: Running time and solution value vs.  $k$  in NSF Network,  $t_{max} = 6$

account in comparison).  $k$  is set to 2 in both link selection algorithms and  $t_{max} = 2$ .

From the figure, original link-based formulation could solve up to 17-node German network, but not the 20-node EON network, within the 20-hour time limit we set. Using the  $k$ -thres link selection algorithm, new link formulation could gain more than an order of magnitude decrease in running time and could solve EON network as well. The new link formulation with  $k$ -path link selection algorithm performs even better, which decrease the running time of original link formulation by more than 2-and-a-half orders of magnitudes, and could solve all 4 network topologies within just a few hundred seconds. Particularly, it even outperforms path-based formulation, which is a totally different technique that takes a much larger unit, path, as entity of interest.

### 5.3.3 Solution Quality Comparison

Finally, let us investigate the quality of solutions provided by our newly-proposed link formulation. Figure 5.13 takes NSF network as an example, and plots the solution value given by original link-based, path-based formulation and new link formulation with  $k$ -path algorithm, given different  $t_{max}$ . In the figure we could see, the new link formulation with link selection algorithm provides all solution values same to the optimal ones given by original link formulation. Moreover, in one of the cases, new link formulation is able to provide better solution

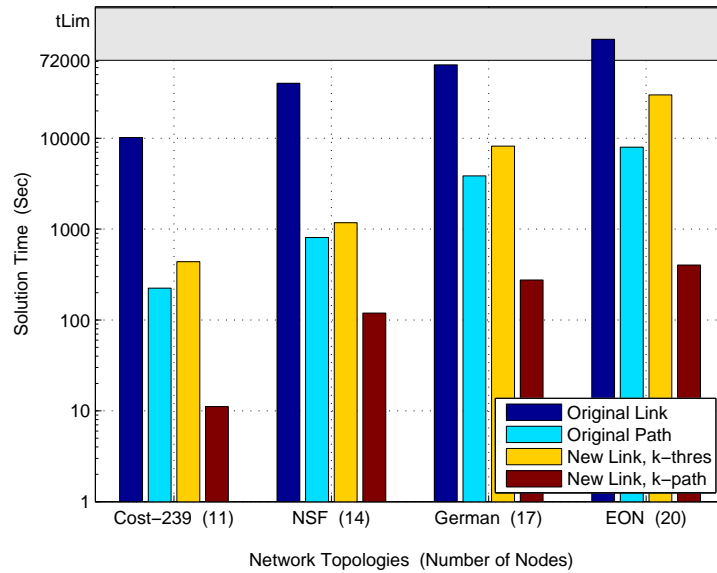


Figure 5.12: Running time of new link formulation with two link selection algorithms, compared with original link-based and path-based formulations

than path formulation (56 vs. 59). In other words, new link formulation with link selection algorithm could provide practically optimal solution and outperforms path formulation in both speed and solution quality.

### 5.3.4 Conclusion

To sum up, the new link formulation with wise link selection algorithm could decrease the running time of original link formulation for more than two-and-a-half orders of magnitudes, and provide the same optimal solution in practical scenarios. It also outperforms path and MIS-based formulations in both running time and solution quality. More importantly, this approach is applicable to ILP formulations for any problems that use multicommodity flow equation as their core constraints.

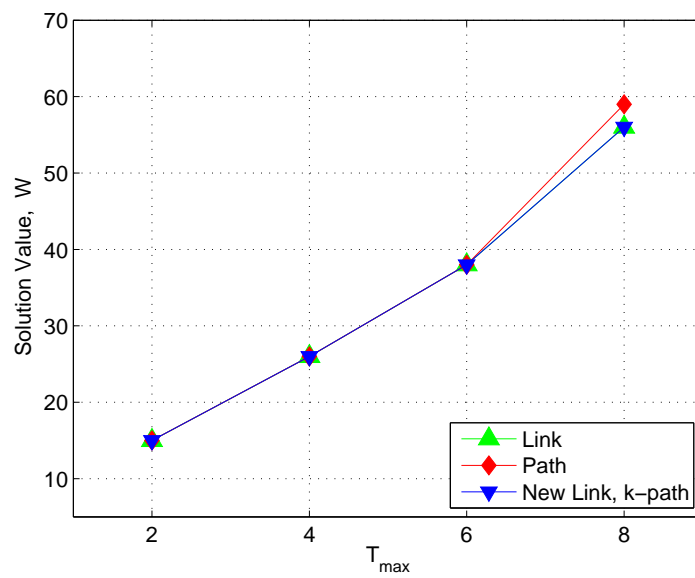


Figure 5.13: Solution value of new link formulation with two link selection algorithms against  $t_{max}$ , compared with original link-based and path-based formulations

## Chapter 6

# Scalable Optimal Traffic Grooming in WDM Rings Incorporating Fast RWA Formulation

Traffic grooming problem is a fundamental and important network design problem that includes routing and wavelength assignment. We present a scalable formulation for the traffic grooming problem in WDM ring networks. Specifically, we modify the ILP formulation to replace the constraints related to routing and wavelength assignment (RWA), typically based on a link approach, with a new set of constraints based on the maximal independent set decomposition (MISD) that we recently developed to solve optimally the RWA problem in ring networks. Our experimental study indicates that the new formulation results in an improvement of up to two orders of magnitude in running time. Consequently, it is now possible to solve the traffic grooming problem to optimality for 16-node rings in a few seconds, under our objective function.

The chapter is structure as follows. In Section 6.1 we give the introduction to traffic grooming problem. In Section 6.2, we present the basic but general ILP formulation for the traffic grooming problem that is the starting point of our work, and we discuss its complexity and limitations. In Section 6.3, we integrate the MISD RWA algorithm to the formulation to traffic grooming problem. In Section 6.4, we present an experimental study that demonstrates the effectiveness of the approach, and we conclude the chapter in Section 6.5.

### 6.1 Introduction to Traffic Grooming

With the help of wavelength division multiplexing (WDM) technology, it is possible to transmit traffic on different wavelengths within the same optical fiber simultaneously. The capacity of

each wavelength can be significantly higher than the magnitude of individual traffic demands. The concept of traffic grooming was introduced in the mid-1990s to address the gap between the channel capacity and individual traffic demands in optical networks. The key idea is to aggregate individual traffic requests onto wavelengths so as to improve bandwidth utilization across the network and minimize the use of network resources. As a result, traffic grooming problem includes grooming assignment, as well as routing and wavelength assignment.

Many variants of traffic grooming have been studied in the literature. Online versions of the problem target network environments in which traffic demands arrive in real time. Since future demands are not known in advance, the main objective of online problems is to minimize blocking probability or maximize throughput. Several heuristics for solving online traffic grooming problems have been developed [66, 65, 68, 75], and simulation was used to demonstrate the effectiveness of the proposed methods.

Offline traffic grooming is a fundamental network design problem that has been shown to be NP-hard [64]. Such network design problems have been formulated as integer linear programs (ILPs) and assume the existence of a traffic matrix representing the demands between node pairs. Basic ILP formulations of the problem are available in [63] and [77]. Typically, the objective is to minimize the total network cost while satisfying all demands (e.g., as in [60, 69]), or to maximize the total revenue by satisfying as many traffic demands as possible given certain capacity (wavelength) constraints (e.g., as in [77]). Since electronic equipment, i.e., switch transceivers or SONET add-drop multiplexers (ADMs), that terminate lightpaths represent a large fraction of the overall network cost, the number of lightpaths established to carry the traffic demands is usually taken as the metric to minimize [69]. Other cost functions have also been considered; for instance, the objective of the study in [62] was to minimize the electronic switching cost of grooming traffic between lightpaths at intermediate switches, while a formulation for energy-efficient traffic grooming, i.e., one that minimizes power consumption in the grooming networks, was presented in [74].

One essential concern about the ILP formulations is that they are solvable only for small network topologies [74]. For larger topologies representative of realistic networks, the ILP formulation cannot be solved to optimality within reasonable amounts of time (e.g., several hours). Therefore, the offline problem has generally been addressed using heuristic algorithms [59, 76]. In the following of this chapter, we develop a scalable optimal traffic grooming formulation incorporating fast RWA formulation.

## 6.2 ILP Formulation of the Traffic Grooming Problem

Consider a connected graph  $G = (N, L)$ , where  $N$  denotes the set of nodes and  $L$  denotes the set of directed links (arcs) in the network. We define  $|N|$  and  $|L|$  as the number of nodes and

links, respectively. Each directed link  $l$  consists of an optical fiber that may support  $W$  distinct wavelengths. Let  $T = [t_{sd}]$  denote the traffic demand matrix, where  $t_{sd}$  is a non-negative integer representing the traffic demand in terms of a unit capacity to be established from source node  $s$  to destination node  $d$ . In general, traffic demands may be asymmetric, i.e.,  $t_{sd} \neq t_{ds}$ . We also make the assumption that  $t_{ss} = 0, \forall s$ . Finally, we denote  $C$  as the capacity of a single wavelength channel in terms of a unit capacity.

In this basic formulation, the entities of interest (i.e., decision variables) are link related. Hence, let us further denote the links outgoing from (incoming to, respectively) node  $n$  as  $L_n^+$  ( $L_n^-$ , respectively).

Let us define the following set of decision variables:

- $t_{ij}^{sd}$ : integer variable that indicates amount of traffic, in terms of unit capacity, from node  $s$  to node  $d$  carried on lightpaths from node  $i$  to node  $j$ ;
- $b_{ij}$ : integer variable that indicates number of lightpaths from node  $i$  to node  $j$ ;
- $b_{ij}^l$ : integer variable that indicates number of lightpaths from node  $i$  to node  $j$  which traverse link  $l$ ; and
- $c_{ij}^{l,w}$ : binary variable that indicates whether a lightpath from node  $i$  to node  $j$  uses wavelength  $w$  on link  $l$ .

In the following subsections, we will discuss the objective function and constraints.

### 6.2.1 Objective Function

In this chapter, we are interested in minimizing the total network cost while satisfying all traffic demands. There are various minimizing objective functions, two of which receive extensive discussion, as shown below.

a). minimizing the total number of lightpaths to be established. This is a most commonly discussed objective in the literature [63], [69]. The corresponding objective function is expressed as

$$\text{minimize: } \sum_{i,j} b_{ij} \quad (6.1)$$

b). minimizing the amount of electronically switched traffic. This objective function is used in [62]. The corresponding objective function is expressed as

$$\text{minimize: } \sum_{i,j} \sum_{s,d} t_{ij}^{sd} - \sum_{s,d} t^{sd} \quad (6.2)$$



Here in this chapter, we propose a combined objective functions, using a weight parameter,  $\alpha$ , to join the two objectives together.

$$\text{minimize: } \alpha \sum_{i,j} b_{ij} + (1 - \alpha) \left( \sum_{i,j} \sum_{s,d} t_{ij}^{sd} - \sum_{s,d} t^{sd} \right) \quad (6.3)$$

Using this objective function, one can consider minimizing the number of lightpaths and the amount of electronically switched traffic at the same time, and control the weight of each objective in the combined function by adjust the parameter  $\alpha$ .

## 6.2.2 Constraints

With the notations defined before, the basic ILP formulation generally used in literatures [74] can then be expressed as:

**Grooming constraints:**

$$\sum_{s,d} t_{ij}^{sd} \leq b_{ij}C, \quad i, j \in N \quad (6.4)$$

$$\sum_{s,d} t_{ij}^{sd} \geq (b_{ij} - 1)C, \quad i, j \in N \quad (6.5)$$

$$\sum_j t_{ij}^{sd} - \sum_j t_{ji}^{sd} = 0, \quad i \in N \setminus \{s, d\}, s, d \in N \quad (6.6)$$

$$\sum_j t_{ij}^{sd} = t^{sd}, \quad s, d \in N \quad (6.7)$$

$$\sum_j t_{js}^{sd} = 0, \quad s, d \in N \quad (6.8)$$

$$\sum_j t_{dj}^{sd} = 0, \quad s, d \in N \quad (6.9)$$

$$\sum_j t_{jd}^{sd} = t^{sd}, \quad s, d \in N \quad (6.10)$$

**Routing constraints:**

$$\sum_{l \in L_n^+} b_{ij}^l - \sum_{l \in L_n^-} b_{ij}^l = 0, \quad n \in N \setminus \{i, j\}, i, j \in N \quad (6.11)$$

$$\sum_{l \in L_i^+} b_{ij}^l = b_{ij}, \quad i, j \in N \quad (6.12)$$

$$\sum_{l \in L_i^-} b_{ij}^l = 0, \quad i, j \in N \quad (6.13)$$

$$\sum_{l \in L_j^+} b_{ij}^l = 0, \quad i, j \in N \quad (6.14)$$

$$\sum_{l \in L_i^-} b_{ij}^l = b_{ij}, \quad i, j \in N \quad (6.15)$$

**Wavelength constraints:**

$$\sum_w c_{ij}^{w,l} = b_{ij}^l, \quad i, j \in N, l \in L \quad (6.16)$$

$$\sum_{i,j} c_{ij}^{w,l} \leq 1, \quad \forall w, l \in L \quad (6.17)$$

$$\sum_{l \in L_n^+} c_{ij}^{w,l} = \sum_{l \in L_n^-} c_{ij}^{w,l}, \quad n \in N \setminus \{i, j\}, i, j \in N, \forall w \quad (6.18)$$

$$\sum_{l \in L_i^+} c_{ij}^{w,l} \leq b_{ij}, \quad i, j \in N, \forall w \quad (6.19)$$

$$\sum_{l \in L_i^-} c_{ij}^{w,l} = 0, \quad i, j \in N, \forall w \quad (6.20)$$

$$\sum_{l \in L_j^+} c_{ij}^{w,l} = 0, \quad i, j \in N, \forall w \quad (6.21)$$

$$\sum_{l \in L_j^-} c_{ij}^{w,l} \leq b_{ij}, \quad i, j \in N, \forall w \quad (6.22)$$

The grooming assignment constraints (6.4) to (6.10) are for grooming traffic into lightpaths over the virtual topology. Constraint (6.4) is the channel capacity constraint that counts the number of lightpaths need to be established between each node pair, while (6.5) ensures that only enough number of lightpaths are to be established. Constraints (6.6) to (6.10) are multi-commodity flow equations that find the traffic route(s) for each connection request.

The routing constraints (6.11) to (6.15) find the routes for each lightpath, utilizing a multi-commodity flow equation, where each lightpath between a node pair corresponds to a single commodity. Constraint (6.11) ensures the number of incoming lightpaths is equal to the number of outgoing lightpaths at any intermediate node. Constraint (6.12) and (6.13) are the lightpath constraints at origin nodes of each lightpath, while constraints and (6.14) and (6.15) are the corresponding constraints for the termination nodes of each lightpath.

The wavelength assignment constraints (6.16) to (6.22) ensures the two wavelength con-

straints in the problem: a). distinct wavelength constraint: (6.17) guarantees that each wavelength can only be used once on any link, i.e., no two lightpaths that share a common link will use the same wavelength; b). wavelength continuity constraint: multi-commodity flow equation (6.18) to (6.22) guarantee that each link on the same lightpath will be assigned the same wavelength. Finally, constraint (6.16) ensures that each lightpath will only use one wavelength.

The scalability of an ILP formulation depends directly on its size, which, in turn, is determined by the number of variables and constraints. The above formulation consists of  $N^2(N-1)^2$  integer variables  $\{t_{ij}^{sd}\}$ ,  $N(N-1)$  variables  $\{b_{ij}\}$ ,  $N(N-1)|L|$  variables  $\{b_{ij}^l\}$ , and  $N(N-1)|L|W$  binary variables  $\{c_{ij}^{l,w}\}$ , for a total of  $O(N^2|L|W)$  variables. For the number of constraints, there are  $N(N-1)(N+2)$  routing constraints,  $O(N(N-1)(N+2)W)$  wavelength constraints, and  $N(N-1)(N+4)$  grooming constraints. Hence there are in total  $O(N^3W)$  constraints in the formulation.

This existing ILP formulation has two main limitations: (1) its size increases rapidly with the size of the network; and (2) they have a symmetry problem in that multiple solutions with the same objective value can be obtained by simply changing the order of wavelengths. Since the ILP solver has to evaluate all  $W!$  distinct optimal solutions, the running time can be unnecessarily long. Hence, these formulations do not scale to networks with 100 or more wavelengths per link that can be realized with current technology.

In the following section, we will present a scalable optimal approach that incorporates our recently developed fast MISD RWA formulation, which response well to the two big challenges above.

### 6.3 RWA in Traffic Grooming

The routing and wavelength assignment problem is a substantial subproblem of traffic grooming, and it takes a large portion of efforts in the optimization procedure of traffic grooming. In fact, RWA problem is a NP-hard problem by itself. Especially when it is combined with the grooming assignment, it adds up the complexity to the whole problem dramatically. In previous chapters of this thesis, we discussed in depth the performance of existing approaches to RWA algorithm and developed an exact decomposition approach for an ILP formulation based on maximal independent sets that makes it possible to obtain optimal solutions to the RWA problem for maximum size (i.e., 16-node) SONET rings in only a few seconds using commodity CPUs. Looking back at the existing ILP formulation to traffic grooming problem above, we find that it utilizes the most complicated RWA ILP formulation, i.e., the link-based formulation, to solve the routing and wavelength assignment subproblem. Although it ensures overall optimality to arbitrary network topologies, the link-based formulation results in an enormous complexity to the approach. Since the recently-developed MISD approach is totally equivalent to link-based

RWA formulation in ring networks, we present the new scalable traffic grooming approach incorporating MISD RWA formulation, so as to greatly increase the efficiency of traffic grooming solution in rings.

Before we introduce the equation substitution, a quick overview of MISD approach could be as follows. MISD is a decomposition approach based on MIS-based formulation. Taking MISD-2 as an example, this approach decomposes the network into two non-intersection partitions. It can perfectly fit in the ILP for traffic grooming problem by substituting Equation (6.11)-(6.22) with (6.23)-(6.25). For more details for the MISD approach and understanding the equations below, reader may refer to Chapter 3.

$$Cl \sum_{k=cw,ccw} b_{ij,k} = b_{ij} \quad i, j \in N \quad (6.23)$$

$$b_{ij,k} \leq \sum_{m \in \mathcal{M}^k} v_m^k X_{ij,k}^m \quad i, j \in N, k = cw, ccw \quad (6.24)$$

$$\sum_{m \in \mathcal{M}^k} v_m^k \leq W \quad k = cw, ccw \quad (6.25)$$

We could see that the whole set of constraints (6.11)-(6.22) regarding routing and wavelength assignment in traffic grooming problem can be substituted by only three constraints shown above. Consequently, the formulation is greatly simplified. Further, using MIS-based approach in RWA, the variables in the formulation is not coupled with a specific wavelength, as a result, one can successfully avoid wavelength symmetry problem.

Moreover, MISD-4 and the general MISD approach MISD-2<sup>x</sup> formulation can be substituted in the traffic grooming ILPs in a similar manner. In this chapter, we will use both MISD-2 and MISD-4 in the new formulation and have a performance evaluation in the following section.

## 6.4 Experimental Study

In this section, we present the results of an experimental study we conducted to investigate the performance of the traffic grooming with MISD, compared to the original approach. All results were obtained by running the IBM Ilog CPLEX 12 optimization tool on a cluster of identical compute nodes with dual Woodcrest Xeon CPU at 2.33GHz with 1333MHz memory bus, 4GB of memory and 4MB L2 cache.

Our study involves a large set of problem instances on ring networks with size up to 16 nodes (the largest SONET Ring). For each network size, we consider several problem instances. For each problem instance, the traffic demand matrix  $T = [t_{sd}]$  is generated by drawing the (integer) traffic demands (in units of lightpaths) uniformly at random in the interval  $[0, T_{max}]$ .

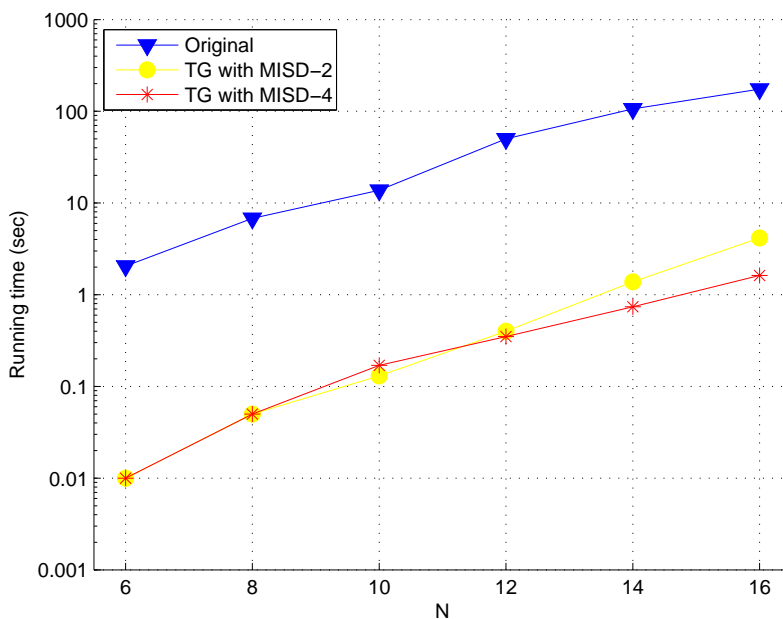


Figure 6.1: CPU time comparison vs. N,  $\alpha = 0.2$

Each data point in the figures we present in this section represents the average of 10 random problem instances for the given topology and value of parameters  $T_{max}$ .

In Figure 6.1, 6.2 and 6.3 we plot the running time comparison among the original traffic grooming ILP, ILP with MISD-2 RWA approach and ILP with MISD-4 RWA approach, with the increasing size of ring networks. We choose  $\alpha$  value as 0.2 in Figure 6.1, to represent considering minimizing power electronically switched traffic as the main objective,  $\alpha = 0.8$  in Figure 6.3 as to represent considering minimizing the number of lightpaths established as the main objective, and  $\alpha = 0.5$  as to represent considering the two objectives equally weighted.

As we can see, in all three situations, ILP with MISD approaches achieve around two orders of magnitude decrease in running time. Particularly, ILP with MISD-4 approach performs well in large networks, which it can solve the largest SONET ring (16 nodes) network within 2 CPU seconds in all cases. As a result, the new formulation makes it possible to solve network sizes of practical size fast enough to allow network designers and operators to perform extensive “what-if” analysis so as to investigate large numbers of scenarios regarding forecast demands.

Figure 6.4 compares running times of the original ILP, ILP with MISD approaches, with different traffic load, using the 16 node ring network. We assign the random different traffic instances by setting  $T_{max}$ . As we can see in the figure, again, the new approaches achieve two orders of magnitude decrease in running time, consistently with various traffic loads.

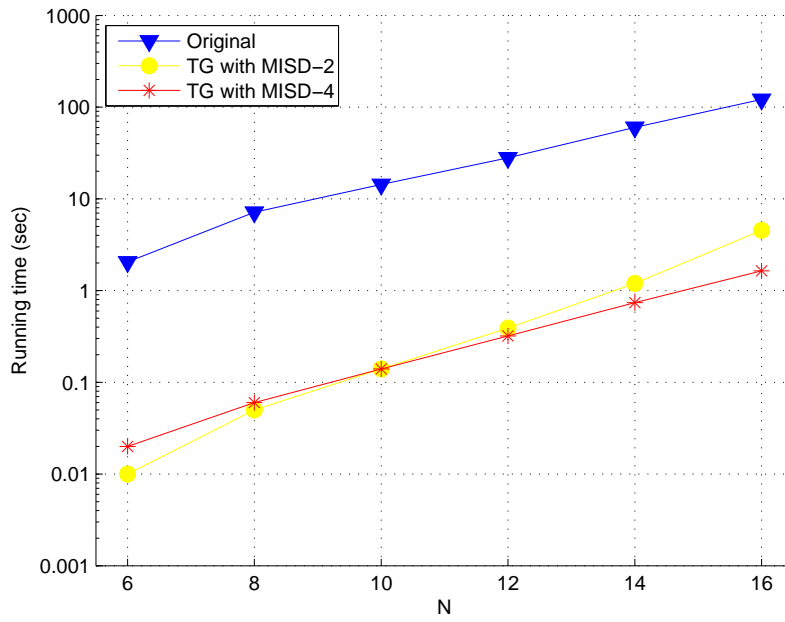


Figure 6.2: CPU time comparison vs. N,  $\alpha = 0.5$

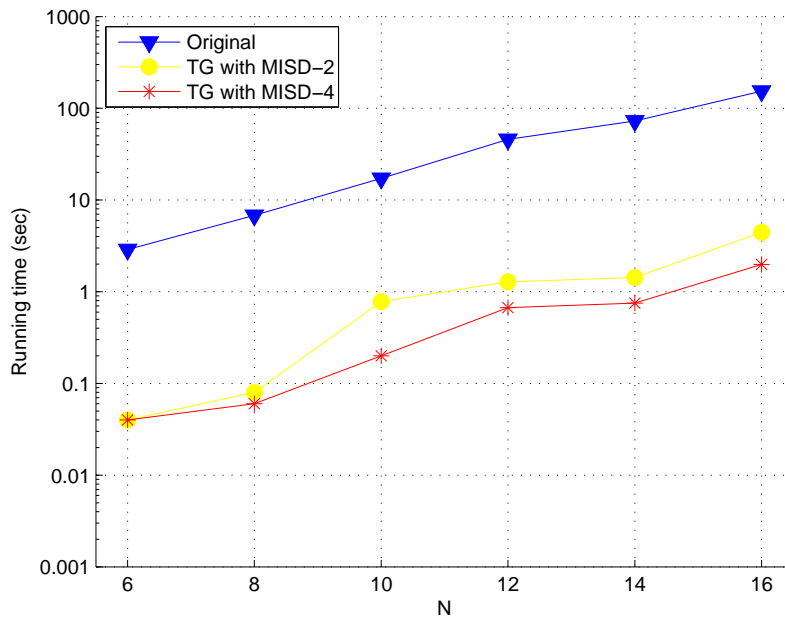


Figure 6.3: CPU time comparison vs. N,  $\alpha = 0.8$

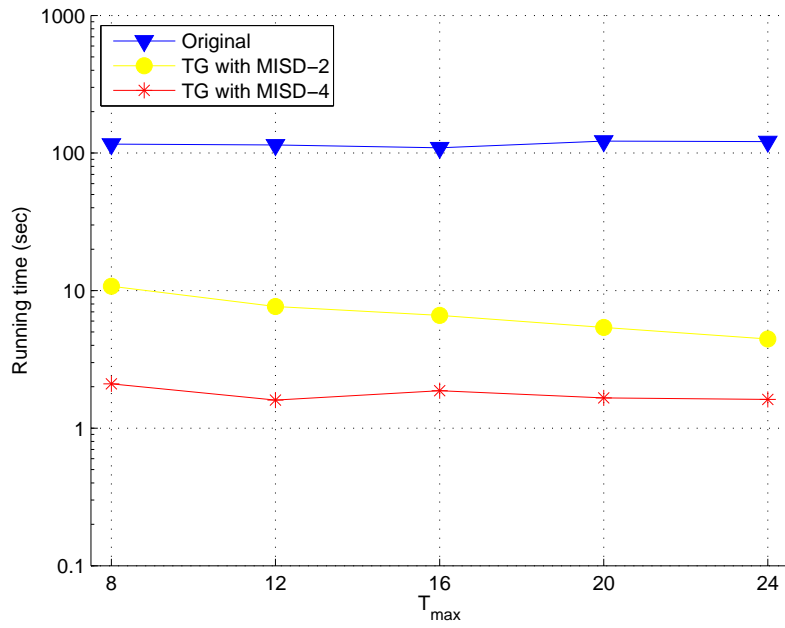


Figure 6.4: CPU time comparison vs.  $T_{max}$  at  $N = 16$

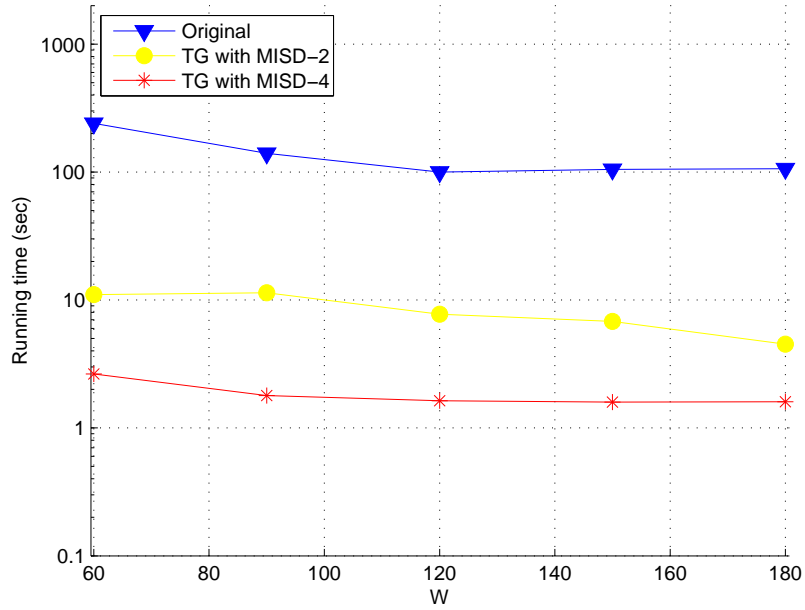


Figure 6.5: CPU time comparison vs.  $W$  at  $N = 16$

In the other hand, Figure 6.5 compares running times of the original ILP, ILP with MISD approaches, with different number of wavelengths available. In this figure, we select again the 16 node ring network and fix  $T_{max} = 20$ . Similar result as the above figure, the new approaches still achieve two orders of magnitude decrease in running time, consistently with various number of wavelengths available.

From a practical perspective, new approach with MISD-4 make it possible to solve traffic grooming optimally for maximum-size (16-node) SONET rings with the combined objective in only 2 seconds; importantly, the running times are not sensitive to the traffic load and number of wavelength available.

## 6.5 Concluding Remarks

We have presented a new approach to solve the traffic grooming problem with MIS decomposition in ring networks optimally, that scales well and enables network designers and operators to carry out extensive “what-if” analysis.



## Chapter 7

# Conclusion and Future Work

As a core problem in optical network, RWA problem is extensively studied with many existing approaches. However, conventional formulations are challenged with scalability issue due to the large network size and large number of wavelengths supported on a single fiber nowadays. We have developed three new, fast ILP formulations that improved the performance of all three existing formulations greatly, and extended our result to traffic grooming problem. The contributions include 1) speeding up the running time of all existing approaches by 2-3 orders of magnitude and make it possible to solve mesh network topologies representative of backbone and regional networks in a very reasonable time; 2) making it possible to speed up several optical network design problems that includes RWA as a subproblem, such as traffic grooming, survivability design and traffic scheduling; 3) characterizing the performance of heuristics on large networks and develop new efficient heuristics.

We now consider the following possible directions in the future work.

- **Advanced Technique in Speeding up Traffic Grooming in Mesh** In the previous chapter, we incorporate MISD formulation for RWA with traffic grooming ILPs, and speed up the traffic grooming solving in ring networks. We may further study on how to improve optimal traffic grooming in mesh networks. One possible direction is using technique similar to the link selection algorithm introduced in Chapter 5. As we mentioned earlier, the efficient link selection algorithm is applicable not only to the link-based formulation of the RWA problem, but also to ILPs for any problems that use multicommodity flow equations as their core constraints. In fact, the general ILPs of the traffic grooming problem are indeed based on multicommodity flow equation, so we can extend the link selection algorithm technique to traffic grooming in mesh networks.
- **Further Improve MIS-based and Path-based Formulation to RWA** We believe that we still have room to push MIS-based and path-based formulation to solve the RWA

problem. First, since path-based formulation is mathematically equivalent to MIS-based formulation and we received a lot of benefits by decomposing the graph and MIS, it is attractive to study the decomposition approach for path formulation to see if we can get the similar benefits as those in MIS decomposition. Second, MIS decomposition works well in ring networks, but not in mesh networks due to the enormous number of MIS generated by the mesh topologies. Hence, we are interested in assigning weight to MIS and select only those with top weights as variables in the formulation, so as to reduce the problem size. Our preliminary work for this direction uses path importance and traffic demands as criteria to assign weights and simulation results is encouraging, but we need to further study how to select the MIS with high weights efficiently.

- **Impairment-aware RWA Problem.** In the practical case, the incorporation of physical layer impairment in translucent and transparent network design and operations makes the previously well-studied (RWA) problem less practical. ILP formulations is an optimal approach to solve impairment-aware RWA problem, by modeling the physical impairment factors as parameters and including them in the formulation. The impairment-aware constraints introduced one more factor to consider in the optimization of the RWA problem, which makes the ILP formulation even harder to solve. Hence, the existing approaches have a big scalability issue. This problem has strong practical urge to solve and it is also intellectually interesting. We plan to study the problem as a longer term goal and extend the successful experience in our previous work on reducing the problem size of ILP formulations to the impairment-aware RWA problem. The characteristics and influence of impairment factors in the formulation need to be further studied, but at least both the symmetric solution technique stated in Chapter 4 and link selection technique introduced in Chapter 5 should be able to extended well to impairment-aware RWA problems.

## REFERENCES

- [1] D. Banerjee and B. Mukherjee. A practical approach for routing and wavelength assignment in large wavelength-routed optical networks. *IEEE JSAC*, 14(5):903–908, June 1996.
- [2] B. Chen, G. Rouskas, and R. Dutta. On hierarchical traffic grooming in WDM networks. *IEEE/ACM Trans. Netw.*, 16(5):1226–1238, Oct. 2008.
- [3] E. Chen and T. Bates. Current practice of implementing symmetric routing and load sharing in the multi-provider Internet. IETF Draft <draft-ietf-idr-symm-multi-prov-01.txt>, June 1995.
- [4] I. Chlamtac, A. Ganz, and G. Karmi. Lightpath communications: An approach to high bandwidth optical WANs. *IEEE Transactions on Communications*, 40(7):1171–1182, July 1992.
- [5] K. Christodoulopoulos, K. Manoudakis, and E. Varvarigos. Comparison of routing and wavelength assignment algorithms in WDM networks. In *Proceedings of IEEE GLOBECOM*, December 2008.
- [6] K. Christodoulopoulos, K. Manousakis, and E. A. Varvarigos. Offline routing and wavelength assignment in transparent WDM networks. *IEEE/ACM Trans. Netw.*, 18(5):1557–1570, Oct. 2010.
- [7] R. Dutta, A. E. Kamal, and G. N. Rouskas, editors. *Traffic Grooming in Optical Networks: Foundations, Techniques, and Frontiers*. Springer, 2008.
- [8] R. Dutta and G. N. Rouskas. A survey of virtual topology design algorithms for wavelength routed optical networks. *Optical Networks*, 1(1):73–89, January 2000.
- [9] R. Dutta and G. N. Rouskas. Traffic grooming in WDM networks: Past and future. *IEEE Network*, 16(6):46–56, November/December 2002.
- [10] T. Eilam-Tzoref. The disjoint shortest paths problem. *Discrete Applied Mathematics*, 85:113–138, October 1998.
- [11] D. Eppstein. Finding the  $k$  shortest paths. *SIAM Journal on Computing*, 28(2):652–673, 1998.
- [12] W.D. Grover and D.P. Onguetou. A new approach to node-failure protection with span-protecting  $p$ -cycles. *ICTON 2009*, June 2009.
- [13] F. Guerriero and R. Musmanno. Label correction methods to solve multicriteria shortest path problems. *Journal of Optimization Theory and Applications*, 111(3):589–613, December 2001.
- [14] B. Jaumard, C. Meyer, and B. Thiongane. ILP formulations and optimal solutions for the RWA problem. *IEEE GLOBECOM'04*, volume 3, pages 1918–1924, November 29–December 3 2004.

- [15] B. Jaumard, C. Meyer, and B. Thiongane. Comparison of ILP formulations for the RWA problem. *Optical Switching and Networking*, 3-4:157–172, 2007.
- [16] B. Jaumard, C. Meyer, and B. Thiongane. On column generation formulations for the RWA problem. *Discrete Applied Mathematics*, 157(6):1291–1308, March 2009.
- [17] W. John, M. Dusi, and kc claffy. Estimating routing symmetry on single links by passive flow measurements. *IWCMC'10*, Caen, France, 2010.
- [18] R. M. Krishnaswamy and K. N. Sivarajan. Algorithms for routing and wavelength assignment based on solutions of LP-relaxations. *IEEE Communication Letters*, 5(10):435–437, October 2001.
- [19] J. Kuri, N. Puech, M. Gagnaire, E. Dotaro, and R. Douville. A review of routing and wavelength assignment of scheduled lightpath demands. *IEEE JSAC*, 21(8):1231–1240, October 2003.
- [20] T. Lee, K. Lee, and S. Park. Optimal routing and wavelength assignment in WDM ring networks. *IEEE JSAC*, 18(10):2146–2154, October 2000.
- [21] A. Mehrotra and M.A. Trick. A column generation approach for graph coloring. *INFORMS Journal on Computing*, 8(4):344–354, Fall 1996.
- [22] M. O’Mahony, D. Simeonidou, A. Yu, and J. Zhou. The design of the European optical network. *JLT*, 13(5):726–733, May 1995.
- [23] A. E. Ozdaglar and D. P. Bertsekas. Routing and wavelength assignment in optical networks. *IEEE/ACM Trans. Netw.*, 11(2):259–272, Apr. 2003.
- [24] S. Ramamurthy and B. Mukherjee. Survivable WDM mesh networks, part I – protection. *INFOCOM '99*, pages 744–751, March 1999.
- [25] S. Ramamurthy, L. Sahasrabudde, and B. Mukherjee. Survivable WDM mesh networks. *JLT*, 21(4):870–883, April 2003.
- [26] R. Ramaswami and K. Sivarajan. Routing and wavelength assignment in all-optical networks. *IEEE/ACM Trans. Netw.*, 3(5):489–500, Oct. 1995.
- [27] M. Saad and Z. Luo. On the routing and wavelength assignment in multifiber WDM networks. *IEEE JSAC*, 22(9):1708–1717, 2004.
- [28] J. M. Simmons. *Optical Network Design and Planning*. Springer, 2008.
- [29] H. Siregar, H. Takagi, and Y. Zhang. Efficient routing and wavelength assignment in wavelength-routed optical networks. *Proc. 7th Asia-Pacific Network Oper. and Mgmt Symposium*, pages 116–127, Oct. 2003.
- [30] W. Su and G. Sasaki. Scheduling periodic transfers with flexibility. In *Proceedings of 41st Allerton Conference*, October 2003.

- [31] B. Mukherjee *et al.* Some principles for designing a wide-area WDM optical network. *IEEE/ACM Trans. Netw.*, 4(5):684–696, Oct. 1996.
- [32] E. Yetginer, Z. Liu, and G. N. Rouskas. Fast exact ILP decompositions for ring RWA. *Journal of Optical Communications and Networking*, vol. 3, no. 7, 577–586, July 2011.
- [33] H. Zang, J. P. Jue, and B. Mukherjee. A review of routing and wavelength assignment approaches for wavelength-routed optical WDM networks. *Optical Networks*, 1(1):47–60, January 2000.
- [34] K. Zhu and B. Mukherjee. Traffic grooming in an optical WDM mesh network. *IEEE JSAC*, 20(1):122–133, Jan 2002.
- [35] ILOG CPLEX 9.0 User’s Manual. Oct 2003.
- [36] Dhritiman Banerjee and Biswanath Mukherjee. A practical approach for routing and wavelength assignment in large wavelength-routed optical networks. *IEEE Journal on Selected Areas in Communications*, 14(5):903–908, 1996.
- [37] A. W. Brander and Mark C. Sinclair. A comparative study of  $k$ -shortest path algorithms. In *Proc. 11th UK Performance Engineering Worksh. for Computer and Telecommunications Systems*, September 1995.
- [38] B. Chen, G. N. Rouskas, and R. Dutta. On hierarchical traffic grooming in WDM networks. *IEEE/ACM Transactions on Networking*, 16(5):1226–1238, October 2008.
- [39] I. Chlamtac, A. Ganz, and G. Karmi. Lightpath communications: An approach to high bandwidth optical wans. *IEEE Transactions on Communications*, 40(7):1171–1182, July 1992.
- [40] R. Dutta, A. E. Kamal, and G. N. Rouskas. *Traffic Grooming in Optical Networks: Foundations, Techniques, and Frontiers*. Springer, 2008.
- [41] R. Dutta and G. Rouskas. Traffic grooming in wdm networks: Past and future. *IEEE Netw.*, 16(6):46–56, Nove./Dec. 2002.
- [42] Rudra Dutta and George N. Rouskas. A survey of virtual topology design algorithms for wavelength routed optical networks. *Optical Networks Magazine*, 1(1):73–89, Jan 2000.
- [43] David Eppstein. Finding the  $k$  shortest paths. *SIAM J. Comput*, 28(2):652–673, 1998.
- [44] Brigitte Jaumard, Christophe Meyer, and B. Thiongane. Comparison of ILP formulations for the RWA problem. *Optical Switching and Networking*, 4(3-4):157–172, 2007.
- [45] Konstantinos Manousakis Konstantinos Christodouloupoulos and Emmanouel (Manos) Varvarigos. Offline routing and wavelength assignment in transparent wdm networks. *IEEE/ACM TRANSACTIONS ON NETWORKING*, 18(5):1557–1570, 2010.
- [46] R. M. Krishnaswamy and K. N. Sivarajan. Algorithms for routing and wavelength assignment based on solutions of lp-relaxations. *Discrete Applied Mathematics*, 157(6):1291–1308, Mar. 2009.

- [47] Rajesh M. Krishnaswamy and Kumar N. Sivarajan. Design of logical topologies: A linear formulation for wavelength routed optical networks with no wavelength changers. In *INFOCOM*, pages 919–927, 1998.
- [48] J. Kuri, N. Puech, M. Gagnaire, E. Dotaro, and R. Douville. A review of routing and wavelength assignment of scheduled lightpath demands. *IEEE Journal Selected Areas in Communications*, 21(8):1231–1240, Oct. 2003.
- [49] S. Ramamurthy and B. Mukherjee. Survivable wdm mesh networks, part i protection. In *Proceedings of INFOCOM 99*, pages 744–751, Mar. 1999.
- [50] S. Ramamurthy, L. Sahasrabudde, and B. Mukherjee. Survivable wdm mesh networks. *Journal of Lightwave Technology*, 21(4):870–883, Apr. 2003.
- [51] R. Ramaswami and K. Sivarajan. Routing and wavelength assignment in all-optical networks. *IEEE/ACM Trans. Netw.*, 3(5):489–500, Oct. 1995.
- [52] George N. Rouskas. *Wiley Encyclopedia of Telecommunications*. John Wiley and Sons, 2001.
- [53] Thomas E. Stern and Krishna Bala. *Multiwavelength optical networks : a layered approach*. Addison-Wesley, 1999.
- [54] W. Su and G. Sasaki. Scheduling periodic transfers with flexibility. In *Proceedings of 41st Allerton Conference*, Oct. 2003.
- [55] D. M. Topkis. A  $k$  shortest path algorithm for adaptive routing in communications networks. *IEEE Trans. on Communications*, 36(7):855–859, July 1988.
- [56] Emre Yetginer, Zeyu Liu, and George N. Rouskas. Rwa in wdm rings: An efficient formulation based on maximal independent set decomposition. In *The 17th IEEE Workshop on Local and Metropolitan Area Networks (IEEE LANMAN 2010)*, May 5-7, 2010, Long Branch, New Jersey.
- [57] H. Zang, J. P. Jue, and B. Mukherjee. A review of routing and wavelength assignment approaches for wavelength-routed optical wdm networks. *Optical Networks*, 1(1):47–60, January, 2000.
- [58] K. Zhu and B. Mukherjee. Traffic grooming in optical wdm mesh networks. *IEEE J. Sel. Areas Commun.*, 20(1):122–133, Jan. 2002.
- [59] B. Chen, G. N. Rouskas, and R. Dutta. On hierarchical traffic grooming in WDM networks. *IEEE/ACM Transactions on Networking*, 16(5):1226–1238, October 2008.
- [60] A.L. Chiu and E.H. Modiano. Traffic grooming algorithms for reducing electronic multiplexing costs in WDM ring networks. *IEEE/OSA Journal of Lightwave Technology*, 18(1):2–12, jan 2000.
- [61] Milind Dawande, Rakesh Gupta, Sanjeewa Naranpanawe, and Chelliah Sriskandarajah. A traffic-grooming algorithm in wavelength-routed optical networks. *INFORMS Journal on Computing*, 19(4):565 – 574, 2007.

- [62] R. Dutta and G.N. Rouskas. On optimal traffic grooming in wdm rings. *IEEE Journal on Selected Areas in Communications*, 20(1):110 –121, jan 2002.
- [63] R. Dutta and G.N. Rouskas. Traffic grooming in WDM networks: past and future. *IEEE Network*, 16(6):46 – 56, nov/dec 2002.
- [64] Rudra Dutta, Shu Huang, and George N. Rouskas. Traffic grooming in path, star, and tree networks: Complexity bounds and algorithms, April 2006.
- [65] F. Farahmand, Xiaodong Huang, and J.P. Iue. Efficient online traffic grooming algorithms in WDM mesh networks with drop-and-continue node architecture. In *Broadband Networks, 2004. BroadNets 2004. Proceedings. First International Conference on*, pages 180 – 189, oct. 2004.
- [66] Jian-Qiang Hu. Traffic grooming in wavelength-division-multiplexing ring networks: a linear programming solution. *J. Opt. Netw.*, 1(11):397–408, Nov 2002.
- [67] J.Q. Hu and B. Leida. Traffic grooming, routing, and wavelength assignment in optical WDM mesh networks. In *INFOCOM 2004. Twenty-third Annual Joint Conference of the IEEE Computer and Communications Societies*, volume 1, pages 4 vol. (xxxv+2866), march 2004.
- [68] Shu Huang and Rudra Dutta. Research problems in dynamic traffic grooming in optical networks. In *Proc. 1st Int. Workshop on Traffic Grooming, San Jose, CA*, April 2004.
- [69] V. R. Konda and T. Y. Chow. Algorithm for traffic grooming in optical networks to minimize the number of transceivers. *IEEE Workshop on High Performance Switching and Routing*, pages 218 – 221, 2001.
- [70] Xavier Muoz and Ignasi Sau. Traffic grooming in unidirectional WDM rings with bounded degree request graph. In Hajo Broersma, Thomas Erlebach, Tom Friedetzky, and Daniel Paulusma, editors, *Graph-Theoretic Concepts in Computer Science*, volume 5344 of *Lecture Notes in Computer Science*, pages 300–311. Springer Berlin / Heidelberg, 2008.
- [71] B. Vignac, B. Jaumard, and F. Vanderbeck. A hierarchical optimization approach to optical network design where traffic grooming and routing is solved by column generation.
- [72] W. Yao, G. Sahin, M. Li, and Byrav Ramamurthy. Analysis of multi-hop traffic grooming in WDM mesh networks. In *Broadband Networks, 2005. BroadNets 2005. 2nd International Conference on*, pages 165 – 174 Vol. 1, oct. 2005.
- [73] E. Yetginer, Z. Liu, and G.N. Rouskas. Fast exact ILP decompositions for ring RWA. *IEEE/OSA Journal of Optical Communications and Networking*, 3(7):577 –586, july 2011.
- [74] Emre Yetginer and George N Rouskas. Power efficient traffic grooming in optical WDM networks. *GLOBECOM 2009 2009 IEEE Global Telecommunications Conference*, 5:1–6, 2009.

- [75] Hongyue Zhu, Hui Zang, Keyao Zhu, and B. Mukherjee. Dynamic traffic grooming in WDM mesh networks using a novel graph model. In *Global Telecommunications Conference, 2002. GLOBECOM '02. IEEE*, volume 3, pages 2681 – 2685 vol.3, nov. 2002.
- [76] K. Zhu and B. Mukherjee. A review of traffic grooming in WDM optical networks: Architectures and challenges. *Optical Networks Magazine*, 4(2):55–64, March/April 2003.
- [77] Keyao Zhu and Biswanath Mukherjee. Traffic grooming in an optical WDM mesh network. *IEEE Journal on Selected Areas in Communications*, 20(1):122–133, 2002.



## APPENDIX

# Appendix A

## Exact MISD- $2^x$ formulation

To discuss the exact MISD- $2^x$  formulation, we have following notations. We define  $q_{k,r}$  as core sets in non-leaf subgraph  $G_p^{k,r}$  ( $k = ccw, ccw, r = 0, 1, \dots, 2^{x-1} - 1$ ), and define  $m_{k,r}$  as MISs in leaf subgraph  $G_p^{k,r}$  ( $k = ccw, ccw, r = 2^{x-1}, \dots, 2^x - 1$ ). To include the network topology in the formulation, we define  $X_{ij,k}^{q_{k,r}}$  as binary variable that indicates whether  $p_{ij,k} \in q_{k,r}$ , and define  $X_{ij,k}^{m_{k,r}}$  as binary variable that indicates whether  $p_{ij,k} \in m_{k,r}$ . We also let  $M_{k,r}^{q_{k,r}}$  be the set of MISs in leaf subgraph  $G_p^{k,r}$  that corresponds to core set  $q_{k,r}$ , and let  $Q_{k,r}^{q_{k,r}}$  be the set of core sets in non-leaf subgraph  $G_p^{k,r}$  that corresponds to core set  $q_{k,r}$ .

Then, let us define the following sets of decision variables:

- $V_{q_{k,r}}$ : number of wavelengths assigned to core set  $q_{k,r}$
- $V_{m_{k,r}}$ : number of wavelengths assigned to MIS  $m_{k,r}$

With notations above, MISD- $2^x$  formulation is written as:

$$\text{Minimize : } W_{total}$$

Subject to:

$$\sum_k b_{ij,k} = t_{ij}, \quad \forall i, j \in V \quad (\text{A.1})$$

$$b_{ij,k} \leq \sum_{q_{k,1} \in Q_{k,1}} V_{q_{k,1}} X_{ij,k}^{q_{k,1}} \quad \forall p_{ij} \in G_p^{k,1}, \quad k = 0, 1 \quad (\text{A.2})$$

$$b_{ij,k} \leq \sum_{q_{k,1} \in Q_{k,1}} \sum_{q_{k,r} \in Q_{k,r}^{q_{k,1}}} V_{q_{k,r}} X_{ij,k}^{q_{k,r}} \quad \forall p_{ij} \in G_p^{k,r}, \quad k = 0, 1 \quad r = 2, 3 \quad (\text{A.3})$$

... ..

$$b_{ij,k} \leq \sum_{q_{k,1} \in Q_{k,r_1}} \sum_{q_{k,r_2} \in Q_{k,r_2}^{q_{k,1}}} \dots \sum_{q_{k,r_{s-1}} \in Q_{k,r_{s-1}}^{q_{k,r_{s-2}}}} \sum_{m_{k,r_s} \in M_{k,r_s}^{q_{k,r_{s-1}}}} V_{m_{k,r_s}} X_{ij,k}^{m_{k,r_s}}$$

$$\forall p_{ij,k} \in G_p^{k,r_s}, \quad s = x, \quad 2^{x-1} \leq r_s \leq 2^x - 1, \quad r_{s-1} = \lfloor \frac{r_s}{2} \rfloor, \quad r_{s-2} = \lfloor \frac{r_{s-1}}{2} \rfloor, \dots, \quad r_1 = \lfloor \frac{r_2}{2} \rfloor = 1, \quad k = 0, 1 \quad (\text{A.4})$$

$$\sum_{q_{k,r} \in Q_{k,r}^{q_{k,1}}} V_{q_{k,r}} = V_{q_{k,1}} \quad k = 0, 1 \quad r = 2, 3 \quad (\text{A.5})$$

... ..

$$\sum_{m_{k,r_s} \in M_{k,r_s}^{q_{k,r_{s-1}}}} V_{m_{k,r_s}} = V_{q_{k,r_{s-1}}} \quad s = x, \quad 2^{x-1} \leq r_s \leq 2^x - 1, \quad r_{s-1} = \lfloor \frac{r_s}{2} \rfloor \quad k = 0, 1 \quad (\text{A.6})$$

$$W_{total} \geq \sum_{q \in Q_k} v_q^{k,0}, \quad k = 0, 1 \quad (\text{A.7})$$

$$b_{ij,k}, \quad v_q^{k,0}, \quad v_{q,m}^{k,r} : \text{ integer} \quad (\text{A.8})$$

Expression (A.2)-(A.4) are represented as expression (3.12) (3.13) in Section 3.3, making sure that sufficient number of wavelengths are assigned to each path. Specifically, (A.2) takes care of paths in top level subgraph, (A.3) takes care of paths in second level subgraphs, ..., (A.4) takes care of paths in leaf subgraphs. Expression (A.5) (A.6) are represented as expression (3.3) in Section 3.3, used to keep consistency between wavelength assignment in different subgraphs.